

---

## **Chapter 2**

### **Carbohydrate derivative diphosphite ligands in asymmetric catalysis**

#### **2.1 Introduction**

**2.1.1** Carbohydrate derivative ligands in asymmetric catalyst

**2.1.2** Hydroformylation reaction

**2.1.3** Hydrogenation reaction

#### **2.2 Results and discussion**

**2.2.1** Synthesis of diphosphite ligands with carbohydrate backbone

**2.2.2** Synthesis of rhodium complexes  $[\text{Rh}(\text{cod})(\text{L})]\text{BF}_4$

**2.2.3** Hydroformylation of styrene and related prochiral olefins

**2.2.4** High pressure NMR study

**2.2.5** Rhodium-catalysed hydrogenation of methyl acetamidoacrylate

#### **2.3 Conclusions**

#### **2.4 Experimental section**

#### **2.5 References**

---

---

**Abstract.** *The synthesis of new modular diphosphite chiral ligands with C<sub>2</sub>-symmetry and carbohydrate backbone **74-76** is reported. Rhodium complexes [Rh(cod)(L)]BF<sub>4</sub> (L: **74-76**) have also been synthesised. The application of this new series of diphosphite ligands in asymmetric rhodium-catalysed hydroformylation of prochiral olefins provides high regioselectivities and moderate enantioselectivities. The application in rhodium-catalysed hydrogenation of methyl acetamidoacrylate with rhodium complexes provides low activities and low enantioselectivities. In both processes the asymmetric induction strongly depends on the structure of the ligand, behaviour that had been previously observed in diphosphinite ligands with the same carbohydrate backbone.*

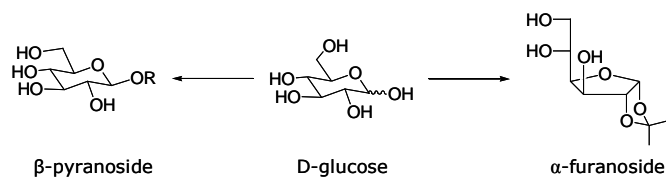
---

## 2.1 Introduction

### 2.1.1 Carbohydrate derivative ligands in asymmetric catalysts

In enantioselective homogeneous metal catalysis the design of new ligands is, perhaps, the most crucial step to achieve highest levels of reactivity and selectivity. One of the simplest ways of obtaining chiral ligands is to transform or derivatize natural chiral compounds, thus making optical-resolution procedures unnecessary. In recent decades, carbohydrates have been widely used as chiral synthons for the synthesis of enantiomerically pure compounds.<sup>[1]</sup> A variety of structures can be obtained from carbohydrates, mainly pyranoses and furanoses, through well-established procedures (Scheme 2.1). Because hydroxyl groups are present, phosphinite, phosphonite, and phosphite functional groups are easily introduced so that they can be used as ligands in metal-catalysed reactions.<sup>[2, 3]</sup> Carbohydrate derivative ligands have been used in a wide range of catalytic asymmetric reactions with excellent results. This kind of ligands have many advantages: they are readily available, they are highly functionalised, and they have several stereogenic centers. These properties make it possible to synthesise a series of chiral ligands -the electronic and steric factors of which can be systematically varied by introducing different functionalities. These series can be screened in the search for high activities and selectivities in many catalytic reactions. One of the limitations of the ligands prepared from the chiral pool is that only one enantiomer is accessible. However, this limitation can be partially overcome by using the so-called pseudo-enantiomer ligands.<sup>[4-6]</sup>

Because of the presence of hydroxyl groups in the carbohydrate skeleton, phosphinite, phosphonite and phosphite ligands are the most common ligands synthesised from carbohydrates. However, ligands containing other phosphorus moieties, such as phosphines and phosphoramidites, or other donor atoms such as sulfur or nitrogen, have also been reported. All these ligands were synthesised from various sugars including xylose, glucose, galactose, mannitol and trehalose among others.<sup>[4-6]</sup>



**Scheme 2.1.** Pyranoside and furanoside structures obtained from D-glucose

The first chiral ligands derived from carbohydrates were reported in the 1970s by Sinou and Descotes<sup>[7]</sup> who synthesised monophosphines **1** and **2** and diphosphine **3** (Figure 2.1) from D-xylose and D-glucose. They were all tested in asymmetric rhodium-catalysed hydrogenation, they obtained an enantiomeric excess of 85% with Rh/**3** catalytic system in the hydrogenation of  $\alpha$ -acetamidocinnamic and  $\alpha$ -actamidoacrylic acids. In the same year, Cullen<sup>[8]</sup> and Thompson<sup>[9]</sup> reported the first diphosphinite derived from glucose with a pyranoid skeleton **4**, and Thompson described the first diphosphinite derived from xylose with a furanoid skeleton **5** (Figure 2.1). They also studied the application of these ligands in asymmetric hydrogenation and their work led to a new family of ligands, which turned out to be highly efficient for chiral induction in several metal-catalysed processes.

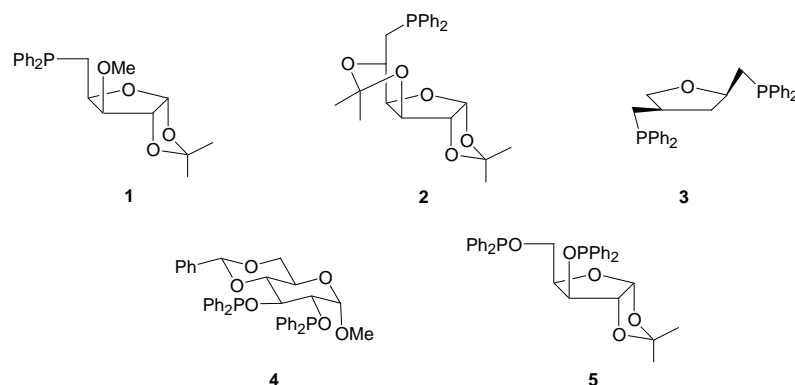


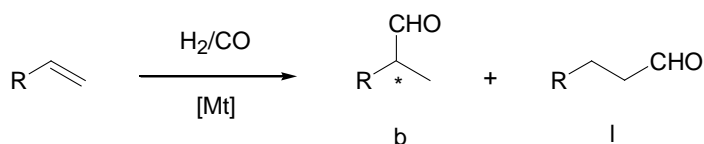
**Figure 2.1.** First chiral ligands prepared from carbohydrates

Ligands derived from carbohydrates have been applied to many homogeneous catalytic reactions. Asymmetric hydrogenation of different substrates, C=C or C=N double bonds, is the most studied reaction with this sort of ligands, mainly

bidentate phosphorus ligands. Asymmetric hydroformylation, allylic substitution and 1,4 addition reactions have also been widely studied with carbohydrate derivative ligands. The use of these ligands in such other asymmetric reactions as asymmetric 1,2 addition, the Heck reaction, hydroboration, hydrosilylation or cyclopropanation, has also been reported.<sup>[4-6]</sup>

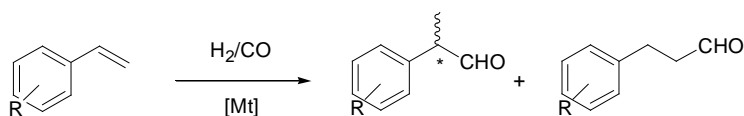
### 2.1.2 Hydroformylation reaction

Hydroformylation is an important and extensively studied process for the functionalization of carbon-carbon bonds. In this process, alkenes are converted into aldehydes by reaction with CO/H<sub>2</sub> via the addition of a formyl group to the double carbon-carbon bond (Scheme 2.2).<sup>[10-16]</sup>



**Scheme 2.2.** Hydroformylation reaction

The regioselectivity of the reaction is the ratio between the branched (b) and linear (l) aldehydes. Linear aldehydes are the desired products in the hydroformylation of long chain alkenes, because they make it possible to synthesise alcohols, which are used as intermediates for detergents and plasticizers.<sup>[10]</sup>



**Scheme 2.3.** Asymmetric hydroformylation of vinylarenes

In the asymmetric hydroformylation, however, the branched aldehydes are the product of interest.<sup>[11-13]</sup> Chiral aldehydes are important intermediates for the preparation of fine chemicals, such as flavours, fragrances, pharmaceuticals and agrochemicals.<sup>[11, 17, 18]</sup> Considerable attention has been paid to the

hydroformylation of vinylarenes (Scheme 2.3): the branched aldehyde (*S*)-2-phenylpropanal is of great interest because it is the key step in a straightforward route to synthesising enantiomerically pure non-steroidal anti-inflammatory drugs (Figure 2.2).

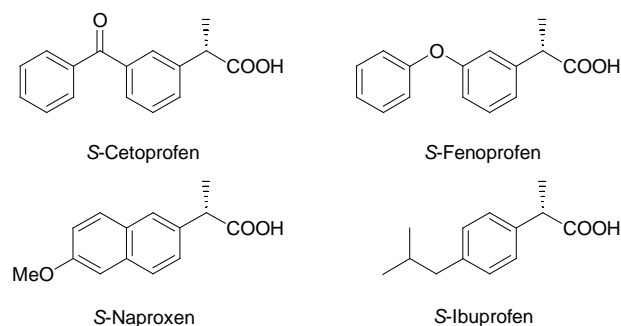


**Figure 2.2.** Enantiomerically anti-inflammatory drugs produced via asymmetric hydroformylation

## Mechanism

The accepted mechanism of the hydroformylation reaction of olefins is illustrated in Figure 2.3. It was proposed by Heck<sup>[19-21]</sup> and it corresponds to Wilkinson's so-called dissociative mechanism.<sup>[22-24]</sup>

The starting material,  $[\text{RhHCO}(\text{PPh}_3)_3]$  **6**, under CO pressure forms the complexes **7ee** and **7ea**, the ligands of which are coordinated in equatorial-equatorial position (**ee**) or in equatorial-axial position (**ea**).

The dissociation of one equatorial ligand (L or CO) leads to the square planar complexes **8c** and **8t**, with phosphines in *cis* (c) or *trans* (t). The association of ethene give complexes **9**, which undergo a migratory insertion to give square-planar alkyl complexes **10**. Complex **10** can undergo  $\beta$ -hydride elimination which leads to isomerisation when alkenes higher than ethene are used, or it can react with CO to form trigonal bipyramidal complexes **11**. Thus, under low CO pressure more isomerisation may be expected. At low temperatures (<70°C) and a sufficiently high CO pressure (>10 bar), the insertion reaction is usually irreversible

and so the regioselectivity of the hydroformylation of  $\alpha$ -alkenes is determined at this point also. Acyl complexes **12** are formed by a second migratory insertion in complexes **11**. The acyl complexes can react with CO to give saturated acyl intermediates **13**, which have been observed spectroscopically, or they can react with  $H_2$  to give the aldehyde and intermediates **8**. The reaction with  $H_2$  involves an oxidative addition and a reductive elimination. Dirhodium species such as **14** are formed at low hydrogen and high rhodium concentrations and can be regenerated as active species with  $H_2$ .<sup>[25, 26]</sup>

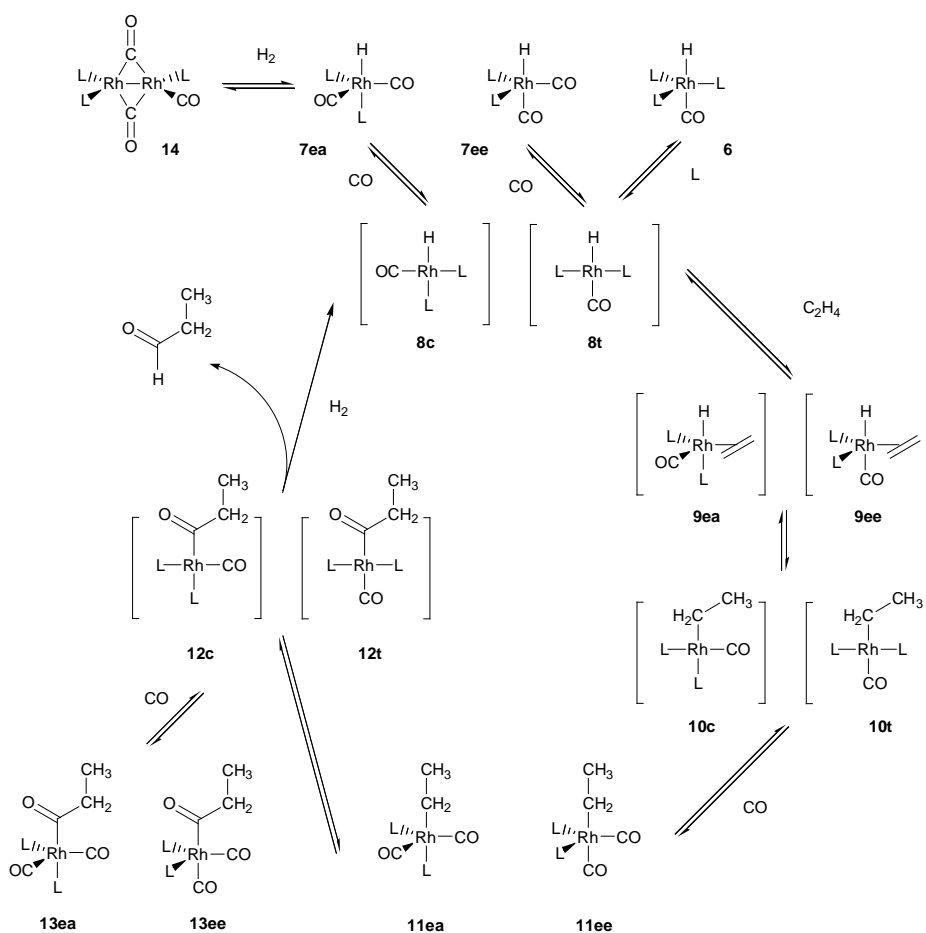


**Figure 2.3.** Simplified mechanism for the hydroformylation of ethene (L:  $PPh_3$ )<sup>[14]</sup>

Ever since the hydroformylation reaction was discovered in 1938 by Otto Roelen,<sup>[27, 28]</sup> who used cobalt carbonyl as catalyst, the process has been evolving even the asymmetric version. In the 1970s transition metal complexes based on rhodium and platinum were used as catalysts in asymmetric hydroformylation. The Pt/diphosphine catalyst yielded high enantioselectivities, but low chemo- and regioselectivities,<sup>[29, 30]</sup> while the Rh/diphosphine catalyst provided high activities and regioselectivities, but low enantioselectivities.<sup>[31]</sup>

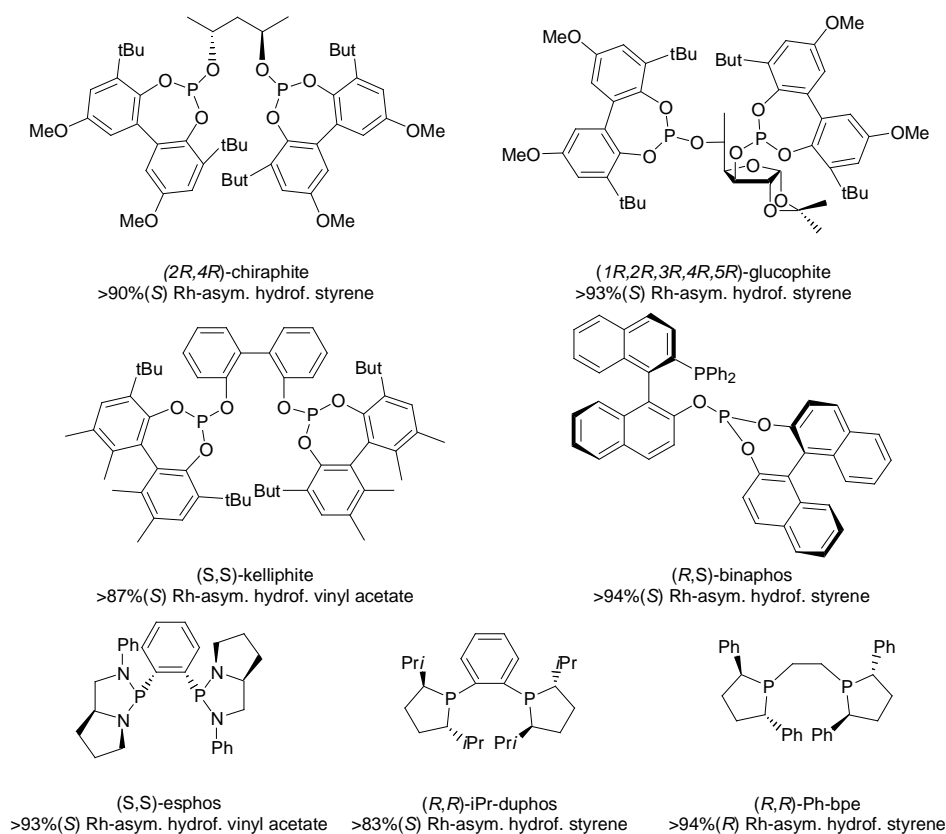


**Figure 2.4.** Chiral ligands that have been successfully applied in asymmetric hydroformylation reactions

In the last decade, Rh/diphosphite and Rh/phosphine-phosphite catalysts have shown high activities, regioselectivities and enantioselectivities. Results have been best with diphosphite ligands such as (*2R,4R*)-chiraphite,<sup>[32, 33]</sup> glucophite,<sup>[34-36]</sup> and



(*S,S*)-kelliphite,<sup>[37, 38]</sup> and phosphine-phosphite ligands, (*R,S*)-binaphos and related ligands.<sup>[39, 40]</sup> Recently, such other ligands as diazaphospholidine, (*S,S*)-esphos,<sup>[41, 42]</sup> and phospholanes, (*R,R*)-Me-duphos and (*R,R*)-iPr-bpe,<sup>[43]</sup> have been successfully applied to rhodium-catalysed asymmetric hydroformylation showing high enantioselectivities in various substrates (see Figure 2.4).

### 2.1.2.1 Diphosphite ligands in asymmetric hydroformylation

#### **Chiral diphosphite ligands with $C_2$ -symmetry**

The first reports on asymmetric hydroformylation using diphosphite ligands revealed no asymmetric induction.<sup>[44]</sup> Takaya and co-workers, in 1992, reported enantioselectivities up to 50% in the asymmetric hydroformylation of vinyl acetate using chiral diphosphite ligands with a binaphthyl backbone.<sup>[45]</sup> In the same year, enantioselectivities up to 90% in the asymmetric hydroformylation of various alkenes were patented by Babin and Whiteker at Union Carbide, with diphosphite ligands **21a-c** derived from (*2R,4R*)-pentane-2,4-diol (Figure 2.5).<sup>[32]</sup> The results showed that bulky substituents at the *ortho*-positions of the biphenyl moieties (**21a,b**) led to better regio- and enantioselectivities than when there were no substituents (**21c**). The presence of methoxy groups in the *para*-positions of the biphenyl moieties **21b** always produced better enantioselectivities than those with *tert*-butyl groups in *para*-position **21a**.

Optically pure diols are useful building blocks for the synthesis of chiral diphosphite ligands. Ligands **15c**, **16c** and **17a,c** (Figure 2.5) were synthesised from commercially available optically pure 1,2 and 1,4 diols. These ligands were used in the asymmetric hydroformylation of styrene in mild conditions and the regioselectivities were high (>95%) and enantioselectivities low (20% ee) with the most bulky diphosphite **17c**. The less bulky and more flexible diphosphites hardly produced enantioselectivity.<sup>[46]</sup>

van Leeuwen and co-workers studied how the length of the bridge of diphosphites **18a**, **19a-b**, **20a-b**, **21a-c** and **23b** affected in the hydroformylation reaction (Figure 2.5).<sup>[47]</sup> They also observed that bulky substituents at the *ortho*-positions of

the biphenyl moieties were necessary for obtaining better enantioselectivities, and the methoxy groups in *para*-positions of the biphenyl moieties enhanced the enantioselectivity (Table 2.1, entries 6 vs. 7). Because bulky substituents in the biphenyl moieties significantly affect the catalyst performance, they synthesised ligands based on 2,4-pentanediol **21** where the steric hindrance increased when bulky substituents **21d-m** were introduced.<sup>[33, 48]</sup> Bulky groups Si(*t*-Bu)(CH<sub>3</sub>)<sub>2</sub> and Si(CH<sub>2</sub>CH<sub>3</sub>)<sub>3</sub> did not improve the enantiomeric excess. The steric bulk in the *ortho*-positions was optimal with the trimethylsilyl substituent **21d** (Table 2.1, entry 10).

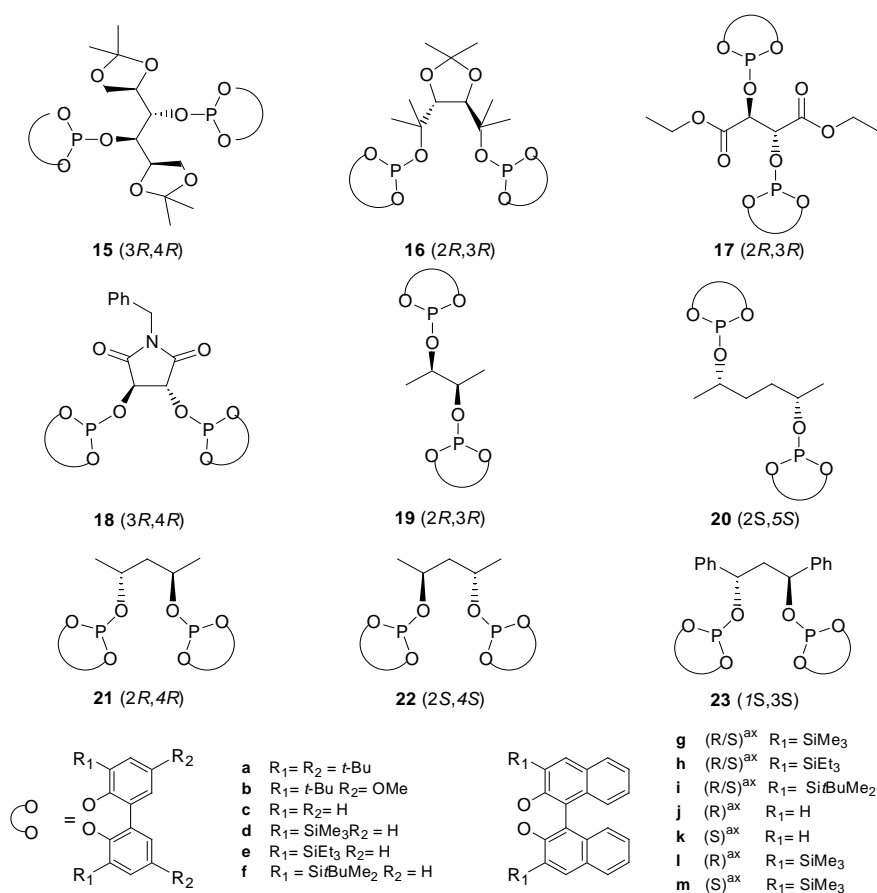


**Figure 2.5.** Chiral diphosphate ligands with C<sub>2</sub>-symmetry

They found an interesting connection between the enantiomeric excess and the structure of the diphosphite. Enantiomeric excesses are highest for the backbones of the diphosphites based on (2*R*,4*R*)-pentane-2,4-diol, **21** and **23** (Table 2.1, entries 7 and 14), which form eight-membered rings in the catalyst. The enantioselectivities were low for the diphosphites based on (2*S*,5*S*)-hexane-2,5-diol **20**, which form nine-membered rings in the catalyst (Table 2.1, entry 5), and moderate for the backbones of the diphosphites based on (2*R*,3*R*)-butane-2,3-diol, **19**, which form seven-membered rings when coordinates to the rhodium (Table 2.1, entry 2). In most cases, when the ligands are based on (*R,R*) diols the (*S*)-aldehyde is predominantly formed. If the configuration is inverted at the chiral carbon atoms, C-2 and C-5 in the (2*S*,5*S*)-hexane-2,5-diol, the (*R*)-aldehyde is predominantly formed.

**Table 2.1.** Hydroformylation of styrene with chiral rhodium diphosphite catalysts<sup>[33, 47, 48]</sup>

Entry	Diphosphite	T (°C)	TOF <sup>b</sup>	% Conversion <sup>c</sup>	% 2-phenyl propanal	% ee
<b>1</b>	<b>19a</b>	40	66	74	93	19 ( <i>S</i> )
<b>2</b>	<b>19b</b>	40	177 <sup>d</sup>	99	92	25 ( <i>S</i> )
<b>3</b>	<b>19b</b>	25	31	40	93	34 ( <i>S</i> )
<b>4</b>	<b>20a</b>	40	19	26	93	1 ( <i>R</i> )
<b>5</b>	<b>20b</b>	40	19	26	92	7 ( <i>R</i> )
<b>6</b>	<b>21a</b>	40	113	89	96	50 ( <i>S</i> )
<b>7</b>	<b>21b</b>	40	207 <sup>d</sup>	98	94	67 ( <i>S</i> )
<b>8</b>	<b>21c</b>	40	117	81	80	11 ( <i>R</i> )
<b>9</b>	<b>21d</b>	40	45	21	89	67 ( <i>S</i> )
<b>10</b>	<b>21d<sup>e</sup></b>	25	9	26 <sup>d</sup>	93	87 ( <i>S</i> )
<b>11</b>	<b>21g</b>	25	14	20	91	47 ( <i>S</i> )
<b>12</b>	<b>21m<sup>e</sup></b>	25	17	38	88	69 ( <i>S</i> )
<b>13</b>	<b>23b</b>	40	165	99	90	47 ( <i>S</i> )
<b>14</b>	<b>23b</b>	25	40	45	95	62 ( <i>S</i> )

styrene: 13.3 mmol, CO/H<sub>2</sub>=10 bar, styrene:Rh=421:1, P:Rh=2.5:1 <sup>b</sup>mol/molRh.h determined after 2h of reaction by GC, <sup>c</sup>of styrene after 5h., <sup>d</sup> after 1h of reaction, <sup>e</sup> styrene:Rh=1000:1, P:Rh=2.2:1 TOF mol/molRh.h determined after 1h of reaction by GC, conversion of styrene after 24 h.

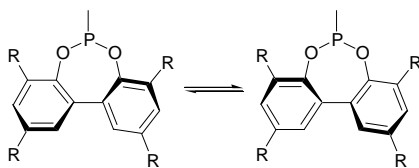


**Figure 2.6.** Atropisomerism in biphenyl moieties

Diphosphite ligands containing biphenyl moieties have a low energy barrier for interconversion in atropisomers, which could lead to the formation of several diastereomers (Figure 2.6). However, the rotation around the biphenyl axis of the diphosphite ligands containing bulky substituents in the biphenyl moieties is hindered. In the rhodium system with diphosphite ligands **21** it was observed that introducing chiral binaphthyl moieties instead of bulky substituted biphenyl led to similar results (Table 2.1, entries 7, 9 and 12). This indicated that the biphenyl moiety adopted one preferable configuration when coordinates to the rhodium.<sup>[14, 33]</sup>

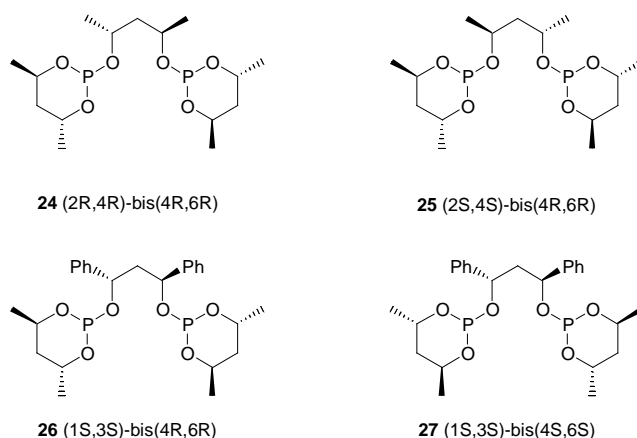


**Figure 2.7.** Diphosphite chiral ligands

Bakos et al. prepared ligands **24** to **27** (Figure 2.7).<sup>[49, 50]</sup> These ligands led to active rhodium systems, and are considerably affected by chiral cooperativity between the stereocenters. Enantioselectivities were no higher than 24%.<sup>[49]</sup> Ligands **28-31** (Figure 2.8) based on binaphthol were used in rhodium asymmetric

hydroformylation. These ligands have shown good regioselectivities in 2-phenylpropanal (up to 87%) and low-to-moderate enantioselectivities (up to 37% ee).<sup>[50, 51]</sup>

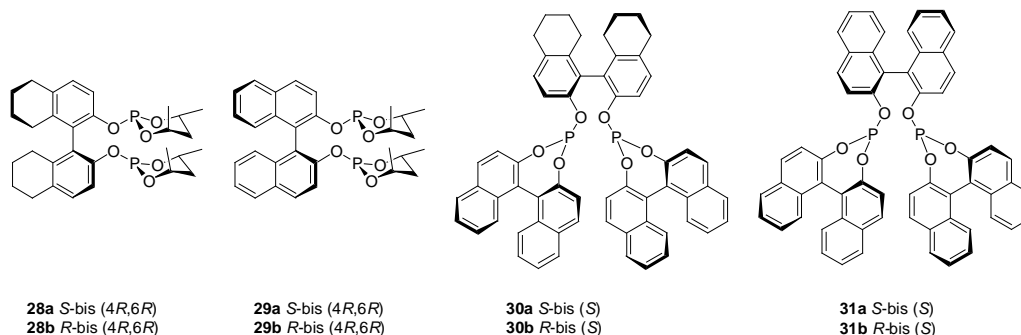


**Figure 2.8.** Diphosphite ligands based on binaphthol

Chiral diphosphite ligand **32** (Figure 2.9) which contains a spiro backbone in the bridge and forms a complex with an eight-membered ring, has also been used in the rhodium-catalysed asymmetric hydroformylation of styrene and related vinyl arenes. Regioselectivities were high and enantioselectivities moderate to good enantioselectivities (up to 70%).<sup>[52]</sup> Bayón et al.<sup>[53]</sup> reported the first example of chiral macrocyclic diphosphite ligands **33** (Figure 2.9). They provided good enantioselectivities (up to 76%), but moderate regioselectivities to the branched aldehyde (up to 83%)

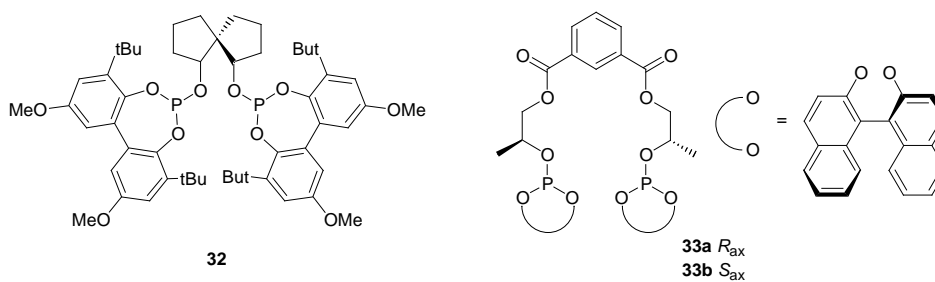


**Figure 2.9.** Diphosphite chiral ligands

Recently, the rhodium-catalysed hydroformylation of allyl cyanide and vinyl acetate with (*S,S*)-kelliphite **34** provided high enantioselectivities, up to 75% and 87%, respectively.<sup>[37, 38]</sup>

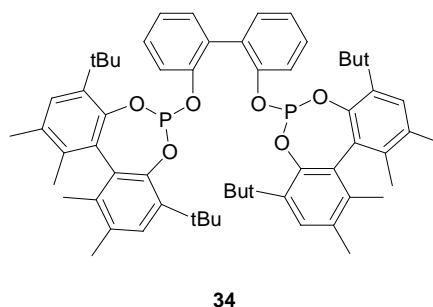


**Figure 2.10.** (*S,S*)-kelliphite diphosphite chiral ligand

### **Chiral diphosphite ligands derived from carbohydrates**

Phosphite functional groups can be easily introduced into carbohydrate backbones because of the presence of hydroxyl groups. The first report in this field, by van Leeuwen et al. in 1995,<sup>[54]</sup> showed the potential of this type of backbone (providing enantioselectivities up to 65% in rhodium-catalysed hydroformylation of styrene). In 1998, Selke and co-workers tested a series of diphosphite ligands **35** (Figure 2.11), with a  $\beta$ -D-glucopyranoside backbone, in the rhodium-catalysed asymmetric hydroformylation of vinyl acetate, allyl acetate and *p*-methoxystyrene.<sup>[55]</sup> In general, regioselectivities in branched product were good (>90%) and enantioselectivities were low to moderate (up to 36%).

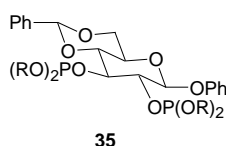


**Figure 2.11.** Diphosphite ligands with  $\beta$ -D-glucopyranoside backbone

Tunable furanoside diphosphite ligands **36-41** (Figure 2.12) derived from carbohydrates have been developed in our group, which have been successfully applied in rhodium-catalysed asymmetric hydroformylation.<sup>[34-36, 56]</sup> They have

shown excellent enantioselectivities (up to 93%) and regioselectivities (up to 98%) under mild conditions (Table 2.2). It has been found that a) a methyl substituents must be present in C-5 enantioselectivities are to be high (Table 2.2, entries 1 and 2 vs. entries 4 and 10), b) the enantioselectivity is influenced by a cooperative effect between stereocenters C-3 and C-5: ligands **38** and **41** provide better enantioselectivities than ligands **39** and **40** (Table 2.2, entries 4 and 10 vs. entries 6 and 8), c) the absolute configuration of the product is governed by the configuration of the stereogenic center C-3: ligands **36**, **38** and **40** gave (*S*)-2-phenylpropanal and ligands **37**, **39** and **41** gave (*R*)-2-phenylpropanal (Table 2.2, entries 1, 4 and 8 vs. entries 2, 6 and 10) and d) the substituents of the biphenyl moieties have an influence: when methoxy or trimethylsilyl groups are present enantioselectivities were better (Table 2.2, entries 3, 4 and 12).

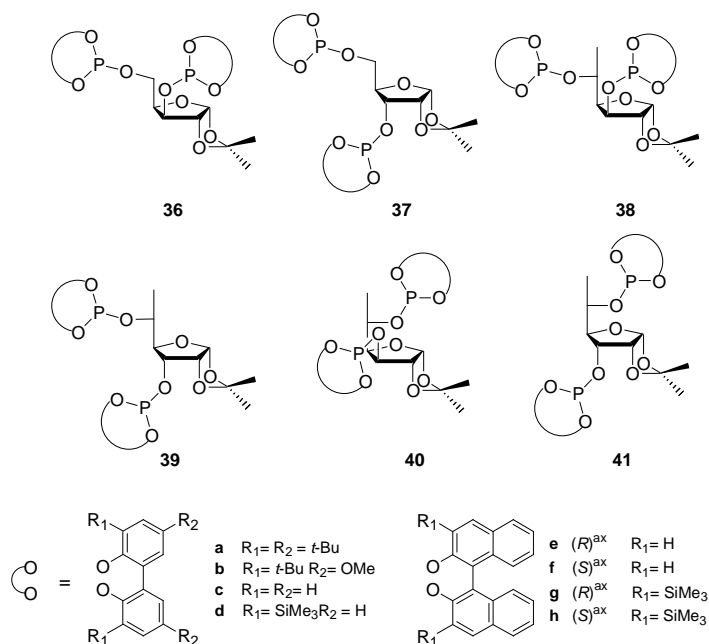


**Figure 2.12.** Tunable furanoside diphosphite ligands derived from carbohydrates

In summary, diphosphite ligands **36-41** derived from carbohydrates provided excellent regio- and enantioselectivities in the asymmetric hydroformylation of vinyl arenes, and gave one of the best enantioselectivities in this reaction. Recently,

good enantioselectivities and excellent regioselectivities have been achieved in the rhodium-catalysed asymmetric hydroformylation of 2,5- and 2,3-dihydrofuran using diphosphite ligands **36a** and **38a**. When diphosphite ligand **38a** was used in both substrates enantioselectivities were high (up to 75%).<sup>[57]</sup>

**Table 2.2.** Hydroformylation of styrene with chiral rhodium diphosphite **36-41**<sup>a[34-36, 56]</sup>

Entry	Ligand	TOF <sup>b</sup>	% 2-phenyl propanal <sup>c</sup>	% ee
1	<b>36b</b>	5	97	60 (S)
2	<b>37b</b>	5	97	61 (R)
3	<b>38a</b>	19	98.4	74 (S)
4	<b>38b</b>	18	98.6	90 (S)
5	<b>39a</b>	14	97.1	46 (R)
6	<b>39b</b>	13	97.2	58 (R)
7	<b>40a</b>	15	97.4	52 (S)
8	<b>40b</b>	12	97.6	64 (S)
9	<b>41a</b>	16	98.7	76 (R)
10	<b>41b</b>	17	98.3	89 (R)
11	<b>39d</b>	10	98.1	62 (R)
12	<b>38d</b>	11	98.8	93 (S)

<sup>a</sup> [Rh(acac)(CO)<sub>2</sub>]=0.0135 mmol; ligand/Rh=1.1; substrate/Rh=1000; Toluene=15 mL; PH<sub>2</sub>=CO =10 bar; T =20 °C; PCO/PH<sub>2</sub> =0.5. <sup>b</sup> TOF in mol styreneXmol Rh<sup>-1</sup>x h<sup>-1</sup> determined after 1 h reaction time. <sup>c</sup> Regioselectivity for 2-phenylpropanal.

### 2.1.2.2 Phosphine-phosphite ligands in asymmetric hydroformylation

#### *Binaphos and related ligands*

The first report on asymmetric hydroformylation using phosphine-phosphite ligands was by Takaya and co-workers in 1993.<sup>[58]</sup> They developed the (*R,S*)-Binaphos ligand **42** (Figure 2.13) in order to combine the high enantioselectivity obtained with diphosphines such as BINAP in asymmetric hydrogenation, with the apparently efficient coordination of the phosphite moiety. (*R,S*)-Binaphos ligand **42** (Figure 2.13) provided higher enantioselectivities (up to 95%) than other *C*<sub>2</sub>-symmetry diphosphine or diphosphite ligands in asymmetric hydroformylation of a wide variety of substrates. They have reported a wide range of structural variations (Figure 2.13).<sup>[39, 59-61]</sup> They observed that: a) the configuration of the binaphthyl bridge governs the sense of the enantioselectivity, b) the enantioselectivities are



enhanced when the configuration of the binaphthyl moieties are opposite and c) the substituents of the aryl groups also positively affect the enantioselectivity (see Figure 2.13).

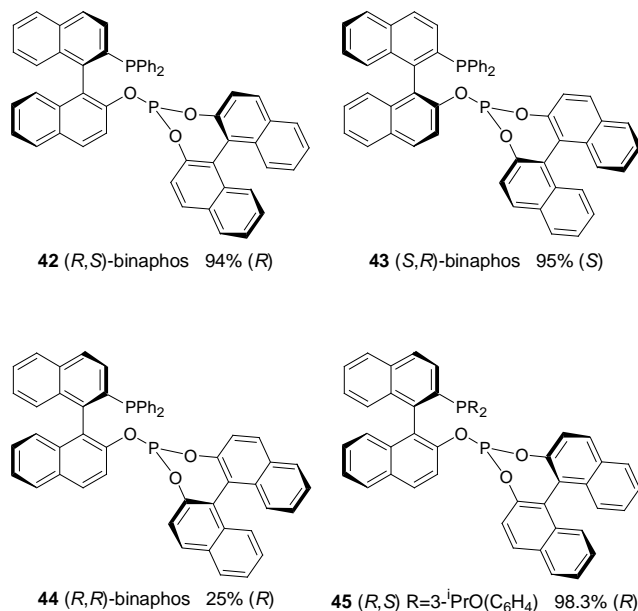


**Figure 2.13.** Binaphos and related ligands. Enantioselectivities obtained in asymmetric hydroformylation of styrene.

### Other phosphine-phosphite ligands

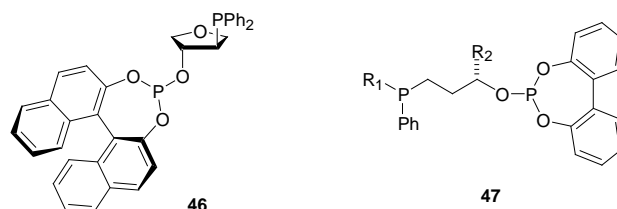


**Figure 2.14.** Chiral phosphine-phosphite ligands

Börner et al.<sup>[62]</sup> developed a series of phosphine-phosphite ligands with furanoside backbones. They observed enantioselectivities up to 40% in the rhodium-catalysed

asymmetric hydroformylation of vinyl acetate with ligand **46** (Figure 2.14). van Leuween et al. [63] reported a series of phosphine-phosphite ligands **47** (Figure 2.14), and obtained enantioselectivities up to 62% in the rhodium-catalysed asymmetric hydroformylation of styrene.

Our group [64] has also developed a series of phosphine-phosphite ligands. These ligands, with carbohydrate backbone **48** (Figure 2.15), showed low-to-moderate enantioselectivities in the rhodium-catalysed asymmetric hydroformylation of styrene (up to 49%).

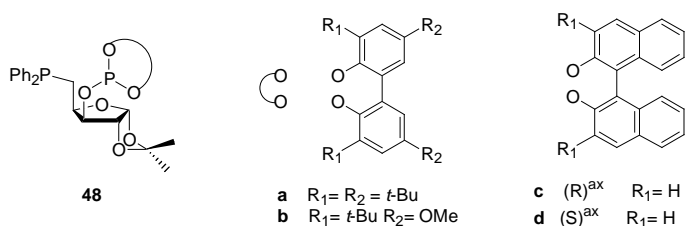


**Figure 2.15.** Phosphine-phosphite ligands with furanoside backbone

### 2.1.2.3 Characterisation of $[\text{RhH}(\text{CO})_2(\text{L})]$ intermediates. Structure versus stability and enantioselectivity.

The solution structures of the trigonal bipyramidal  $[\text{RhH}(\text{CO})_2(\text{L})]$  (L: bidentate ligand) complexes, which are the resting states in the hydroformylation reaction, have been widely studied. [14] The species are generally formed from the  $[\text{Rh}(\text{acac})(\text{CO})_2]$  complex by adding one equivalent of bidentate ligand, under syngas pressure. The complexes are generally assumed to have a trigonal bipyramidal structure with two possible isomeric structures: the ligand coordinated in an equatorial-equatorial (**ee**) or an equatorial-axial (**ea**) fashion (Figure 2.16).

The structure can be elucidated by high pressure IR and NMR data.  $^{31}\text{P}$  and  $^1\text{H}$  NMR spectroscopy combined with IR studies establish a relation between the results from catalysis, the coordination mode of the diphosphites to the rhodium and the stability of these species. In the carbonyl region of the infrared spectrum the vibrations of the **ee** and **ea** complex can be easily distinguished. The **ee** complexes

show absorptions around 2015 and 2075  $\text{cm}^{-1}$ , whereas the **ea** complexes show absorptions around 1990 and 2030  $\text{cm}^{-1}$ , when diphosphite ligands are analysed. The  $^{31}\text{P}$  NMR gives additional information. In the complexes with **ee** coordination, the phosphorus atoms coordinated in the equatorial plane, have small phosphorus to hydrogen coupling constants ( $<10\text{Hz}$ ), whereas the coupling constant of a *trans* coordinated phosphite, **ea** complex, has a large phosphorus to hydrogen coupling constant of 180-200 Hz. The phosphorus to phosphorus coupling constants are much larger for the **ee** (around 250 Hz) than for the **ea** complex (usually 70 Hz).<sup>[14]</sup>

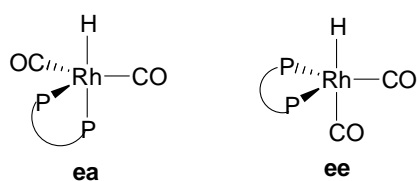


**Figure 2.16.** Equatorial-equatorial (**ee**) and equatorial-axial (**ea**) rhodium hydride dicarbonyl diphosphite

Several studies have observed that the phosphorus atoms of the **ee** and **ea** complexes show fluxional behaviour at room temperature, which can be halted at low temperatures. It has been suggested that the exchange process of the phosphorus donor atoms of the **ee** and **ea** complexes proceeds by the low energy rearrangement mechanism described by Meakin (Figure 2.17).<sup>[65, 66]</sup>

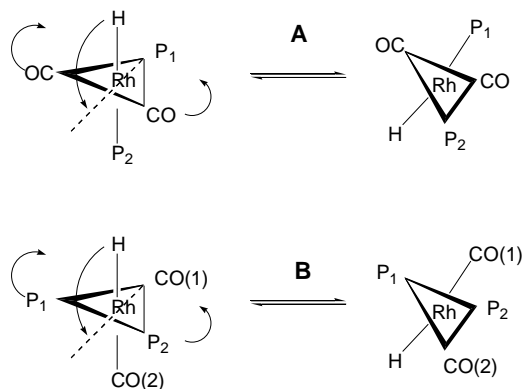


**Figure 2.17.** A: equatorial-axial phosphorus exchange.  
B: equatorial-equatorial phosphorus exchange.<sup>[65, 66]</sup>

A simultaneous bending motion of the hydride and carbonyl ligands takes place in the hydridorhodium diphosphite complexes with **ea** coordination (Figure 2.17A). However, for **ee** coordinated diphosphite complexes a motion of the hydride and the equatorial phosphite function is responsible for the exchange (Figure 2.17B). The latter process is expected to be more difficult than the former, which explains the higher fluxionality of the **ea** coordinating complexes.

van Leuween and co-workers<sup>[47, 48]</sup> established a correlation between the structure of the ligand, the coordination mode in the trigonal bipyramidal hydridorhodium diphosphite complexes and the selectivity of the process. They observed that seven-membered chelate rings (ligands **19a-b**, Figure 2.5) generally give equatorial-axial coordination, while eight- and nine-membered chelate rings (ligands **21a-b** and **20a-b**, respectively, Figure 2.5) preferably coordinate bis-equatorially to rhodium. The highest enantiomeric excesses were observed with relatively stable complexes of **21a-b** and **23b**, which form eight-membered rings and coordinate bis-equatorial to rhodium. Ligand **20a-b**, which forms nine-membered rings coordinated in **ee** fashion formed rather unstable complexes giving lower enantiomeric excesses than ligands **21** and **23**. The enantiomeric excess were lowest with ligands **19a-b**, which coordinated in a **ea** fashion in the more fluxional  $[\text{RhH}(\text{CO})_2(\text{L})]$  complexes. However, ligand **18a**, which forms a seven-membered ring, coordinated in **ee** fashion, when an **ea** coordination was expected. This could be due to the rigid tartarimide backbone of the diphosphite.

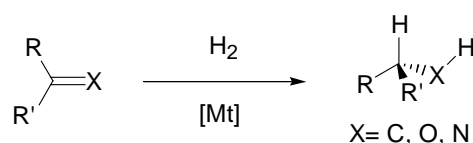
Our group has also used high pressure IR spectroscopy and NMR techniques to characterize the rhodium complexes formed under hydroformylation conditions with diphosphites **36-41** (Figure 2.12).<sup>[35, 36]</sup> It has been observed that enantioselectivities were generally highest with ligands with a strong **ee** coordination preference, while an equilibrium of species with **ee** and **ea** coordination modes considerably reduced the enantiomeric excess.

The study of Binaphos **42** ligand (which shows enantioselectivities up to 90% in the hydroformylation reaction) under hydroformylation conditions revealed that Binaphos coordinates in an equatorial-axial mode with the phosphite moiety in axial position.<sup>[39, 67]</sup> However, correlations have been made between the  $[\text{RhH}(\text{CO})_2(\text{L})]$

complex structure and the selectivity of the hydroformylation reaction, they are not always straightforward.

### 2.1.3 Hydrogenation reaction

Metal-catalysed asymmetric hydrogenation to reduce prochiral olefins, ketones and imines using molecular hydrogen is one of the most efficient asymmetric catalytic methods for synthesising chiral compounds (Scheme 2.4). This process has been widely used in stereoselective organic synthesis and some processes have found industrial applications.<sup>[13, 68, 69]</sup>



**Scheme 2.4.** Asymmetric hydrogenation of prochiral compounds

The asymmetric hydrogenation of ketones makes it possible to synthesise chiral secondary alcohols; ruthenium is the most widely used metal source, followed in lesser extent by rhodium. The asymmetric hydrogenation of C=N double bonds allows to obtain chiral amines; rhodium and ruthenium are the most studied metal sources, but the most of the recent effort has focused on iridium. The hydrogenation of carbon-carbon bonds is widely used: for example, the hydrogenation of  $\alpha$ -dehydroaminoacid derivatives and enamides make it possible to synthesise aminoacids and amines, which are useful intermediates for the pharmaceutical and agrochemical industries. The hydrogenation of  $\alpha$ -dehydroaminoacid derivatives is a typical reaction for testing new chiral ligands.<sup>[13, 68, 69]</sup>

#### **Mechanism**

The mechanism for the rhodium-catalysed hydrogenation of methyl- $\alpha$ -acetamidocinnamate, depicted in Figure 2.18, was proposed by Landis and Halpern.<sup>[70]</sup> The catalytic cycle consists on two coupled diastereoisomeric manifolds.

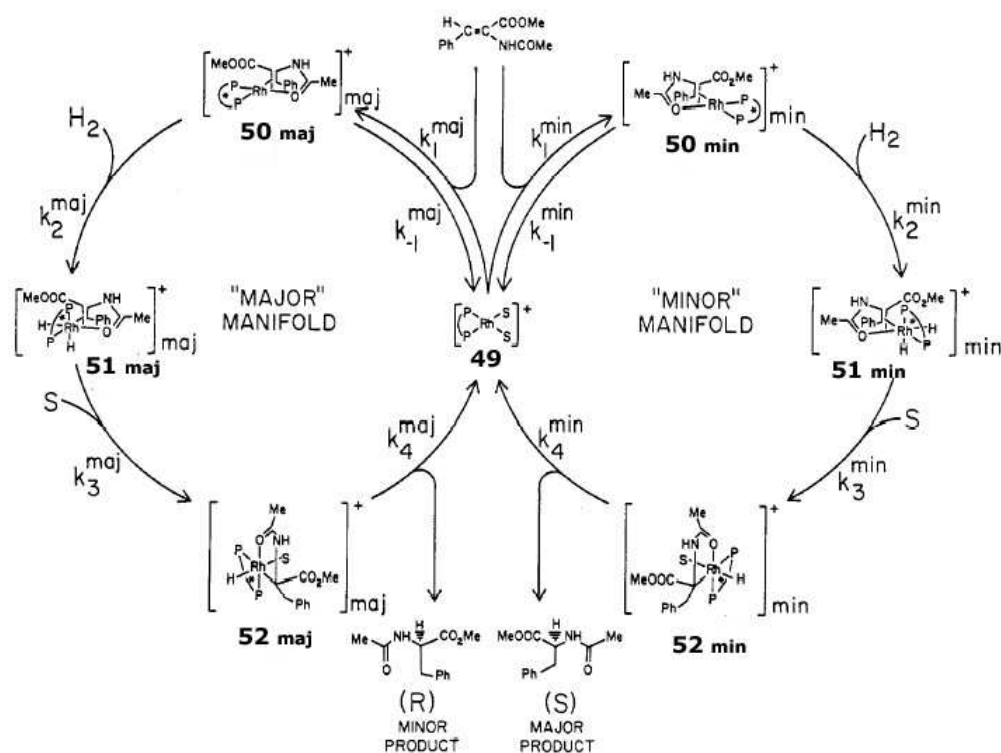


**Figure 2.18.** Mechanistic scheme for the  $[\text{Rh}(\text{dipamp})]^+$ -catalysed hydrogenation of methyl- $\alpha$ -acetamidocinnamate<sup>[70]</sup>

The square planar Rh(I) complex **49** containing the coordinated diposphine and two molecules of solvent is the starting species of the catalytic cycle. Next, the substrate displaces the two molecules of solvent to form two diastereoisomeric adducts, **50maj** and **50min**, where the substrate is coordinated as a bidentate ligand. The irreversible oxidative addition of hydrogen gives the octahedral *cis*-dihydridorhodium complexes **51**. The insertion of the olefin into one of the Rh-H bonds produces the two diastereomeric alkyl complexes **52**. Next, by reductive elimination, the enantiomeric forms of the product are formed and the catalytic active species **49** regenerated. It is accepted that the oxidative addition of hydrogen is the rate- and enantioselective determining step. The reactivity of the minor diastereomer **50min** is much higher than that of the major diastereomer **50maj**, so the minor isomer becomes the determining product.

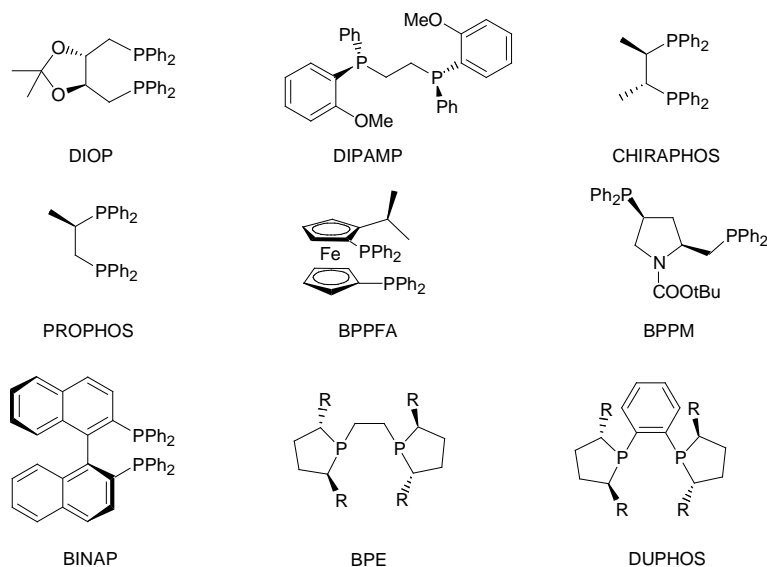


**Figure 2.19.** Chiral ligands that have been successfully applied in asymmetric hydrogenation reactions<sup>[71]</sup>

The first contributions to asymmetric hydrogenation were made by Knowles<sup>[72]</sup> and Horner,<sup>[73]</sup> who replaced the triphenyl phosphine of Wilkinson's catalyst,  $[\text{RhCl}(\text{PPh}_3)_3]$ ,<sup>[74]</sup> with chiral monophosphines. Later Kagan<sup>[75]</sup> reported the diphosphine ligand DIOP (Figure 2.19), which was successfully applied in asymmetric hydrogenation. Knowles<sup>[76-78]</sup> reported the use of the diphosphine ligand DIPAMP ((1*R*,2*R*)-(-)-Bis[(2-methoxyphenyl)phenylphosphino]ethane) (Figure 2.19) in this reaction, and because of its high catalytic efficiency was employed in the industrial production of L-Dopa. Since then, a thousand other successful chiral diphosphorus ligands have been developed: for example Chiraphos and Propfos developed by Bonisch, Kumada's ferrocene ligand BPPFA and Achiwa's BPPM, among others (Figure 2.19).<sup>[71]</sup> In the 1980s Noyori and co-workers reported the Ru/BINAP ((1,1'-Binaphthalene-2,2'-diyl)bis(diphenylphosphine)) catalyst, which is efficient catalyst for hydrogenation of various substrates.<sup>[79, 80]</sup> In the past decade such phosphorus ligands as DUPHOS and BPE developed by Burk and co-workers, showed efficient catalytic properties for the asymmetric hydrogenation of various substrates.<sup>[81, 82]</sup>

Nowadays, many chiral ligands, mainly phosphorus donor ligands have been successfully applied to asymmetric hydrogenation.<sup>[13, 68, 69, 71]</sup> Carbohydrate derivative ligands have also been successfully applied in this reaction.<sup>[4-6]</sup>

### 2.1.3.1 Carbohydrate derivative ligands in asymmetric hydrogenation reaction

#### Diphosphine ligands

Diphosphine ligands derived from carbohydrates are mainly related to DIOP and DUPHOS ligands. Ligands **53** and **54**<sup>[83-85]</sup> (Figure 2.20) increased the rigidity of the seven-member chelate ring in the DIOP ligand by introducing methyl groups in the  $\alpha$  positions of the phosphine groups, and ligands **55** and **56**<sup>[86]</sup> by introducing a conformationally rigid 1,4-dioxane backbone. These ligands led to high enantioselectivities (>99%) in the rhodium-catalysed hydrogenation of aryl enamides.

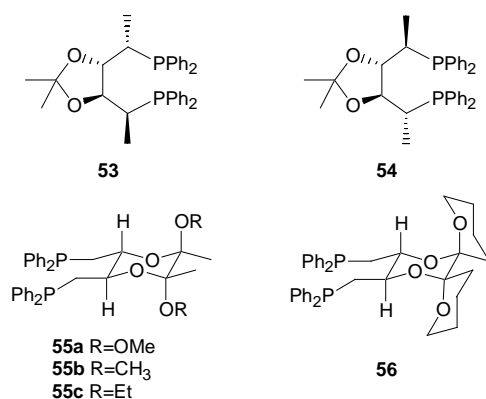


**Figure 2.20.** Diphosphine ligands related to DIOP

Ligands related to DUPHOS and BPE are mainly derived from D-mannitol (Figure 2.21). Diphospholanes **57**, **58a-c** and **59**, developed by Holz and co-workers<sup>[87]</sup> and Zhang and co-workers,<sup>[88-90]</sup> which introduced various substituents in  $\alpha$  and  $\beta$  positions, provided high enantioselectivities (between 93-99%). Rieger and co-workers<sup>[91]</sup> studied the effect of the substituents in the  $\alpha$  position, **58b-f**. The



results showed that methyl and ethyl substituents led to best results. Diphospholanes **60** and **61** (Figure 2.21) have also been applied to the rhodium-catalysed asymmetric hydrogenation of various substrates and enantioselectivities have been high (up to 99%).<sup>[92]</sup> Other ligands with phospholane moieties derived from D-mannitol **62** were applied in the rhodium-catalysed asymmetric hydrogenation of several itaconates leading to enantioselectivities between 80 to 95%.<sup>[93]</sup>

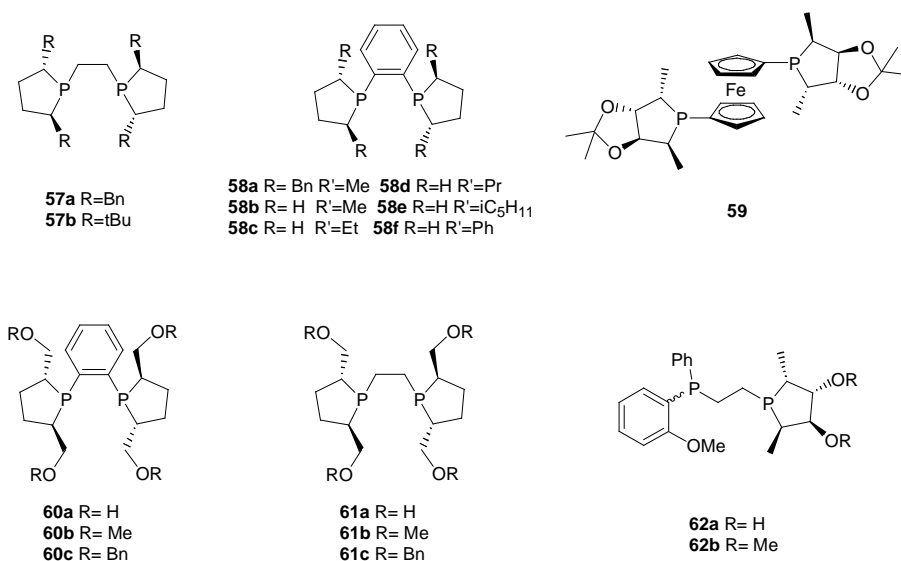


**Figure 2.21.** Diphosphine ligands

Recently, our group prepared diphosphines **63-65** with a furanoside backbone (Figure 2.22).<sup>[94]</sup> These ligands showed high enantioselectivities in the rhodium-catalysed asymmetric hydrogenation of  $\alpha$ ,  $\beta$ -unsaturated carboxylic acids.

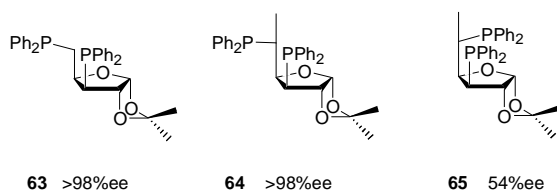


**Figure 2.22.** Diphosphine ligands with furanoside backbone

The introduction of a methyl group in the C-5 position (ligands **64** and **65** vs. ligand **63**) increases activity and its configuration has a strong influence on the enantioselectivity. While catalysts based on ligand **64** showed high enantioselectivities (98% ee), ligand **65**, with a different configuration in this stereocenter, showed a lower enantioselectivity (54% ee) (see Figure 2.22).

### Diphosphinite ligands

As has been mentioned above, the first chiral ligands derived from carbohydrates with phosphinite moieties were reported by Cullen<sup>[8]</sup>, Thompson<sup>[9]</sup>, Selke<sup>[95]</sup> and Descotes.<sup>[96]</sup> Cullen and Thompson synthesised a ligand derived from glucose with a pyranoid skeleton **4**, and Thompson described the first diphosphinite derived from xylose with a furanoid skeleton **5** (Figure 2.1). The ligands with a pyranoside backbone were applied in the asymmetric hydrogenation of dehydroamino acid derivatives.

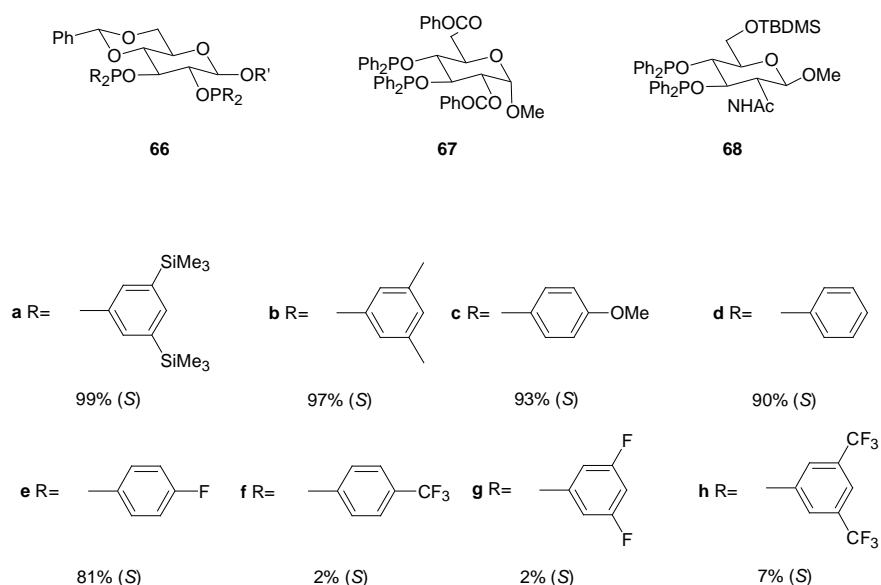


**Figure 2.23.** Diphosphinite ligands with pyranoside backbone. Enantioselectivities in the hydrogenation of methyl  $\alpha$ -acetamidocinnamate

Ligand series **66** showed enantioselectivities above 96%. Selke and co-workers<sup>[95, 97-99]</sup> studied the effect of the substituents R' (R' = Me, Ph, Bn; R = Ph) (see Figure 2.23), while RajanBabu and co-workers studied the electronic and steric effects of the substituents of the phenyl groups by introducing various diphosphinite groups in the same backbone (R' = Ph, see Figure 2.23).<sup>[100-102]</sup> In all cases, the (*S*)-enantiomer of the hydrogenated product was obtained and the enantioselectivity was strongly influenced by the substituents of the phenyl groups. The electron-rich diphosphinite ligands increased the enantioselectivities, whereas the electron-deficient ligands decreased them. The same group prepared ligands **67** and **68**, which can be considered as pseudo-enantiomers of ligand **66**.<sup>[100-102]</sup> These ligands provided the (*R*)-enantiomer of the hydrogenated product, while ligand **66** provided the (*S*)-enantiomer, and showing that the electron-rich diphosphinite enhanced the enantioselectivity.

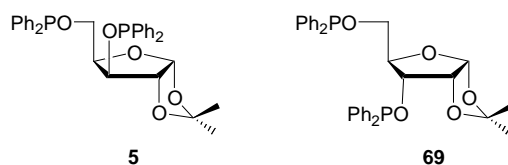


**Figure 2.24.** Diphosphinite ligands with furanoside backbone.

Our group<sup>[103]</sup> synthesised diphosphinite ligand **69**. Its configuration in carbon 3 is different to that previously described for diphosphinite ligand **5** by Thompson (Figure 2.24).<sup>[9]</sup> The use of these ligands, **69** and **5**, in rhodium- and iridium-catalysed hydrogenation showed that the results are strongly influenced by the metal and the ligand used. Ligand **5** showed better results with iridium-based catalysis (>78% ee) and ligand **69** with rhodium-based catalysis (>81% ee). These diphosphinite ligands, **5** and **69**, have also been used in a variety of catalytic reactions, asymmetric Rh-hydroformylation<sup>[104]</sup>, asymmetric Cu-1,4 addition<sup>[105]</sup> and asymmetric Pd-allylic alkylation<sup>[106]</sup>, and enantioselectivities have been low to moderate.

Recently, diphosphinites **70a-d** and **71a-d** (Figure 2.25) have been prepared from D-glucosamine and D-glucitol.<sup>[107]</sup> These new series of diphosphinite ligands with

$C_2$ -symmetry were used in the rhodium-catalysed hydrogenation of methyl acetamidoacrylate, methyl acetamidocinnamate and dimethyl itaconate. Catalytic systems containing the ligand **70b** afforded the best results with enantioselectivities of 93% in the hydrogenation of methyl acetamidoacrylate. Ligand **72**, which does not contain substituents at positions 2 and 5 of the tetrahydrofuran ring only gave a 22% of enantioselectivity. This indicates that the stereogenic centers which are not directly bonded to the coordinating atoms have a strong influence on the selectivity. Substituents X in **70** and **71** (Figure 2.25) also affect the stereoselectivity. The enantioselectivities were lower for the dimethyl itaconate than for the other substrates but the configuration of the major enantiomer, when ligands **70a** and **71a** were used, unexpectedly seems to be determined by the configuration of substituents at carbons 2 and 5.

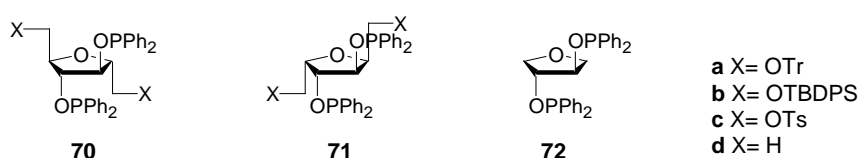


**Figure 2.25.** Diphosphinite ligands developed by our group

### Diphosphite ligands

Diphosphite ligands have been successfully used in the asymmetric hydrogenation of prochiral olefins. The first application of these ligands in this reaction was reported by Reetz and co-workers with ligands **73** derived from D-mannitol. These ligands were applied in the rhodium-catalysed hydrogenation of prochiral olefins providing high enantioselectivities (up to 98%).<sup>[108]</sup>

Tunable diphosphite chiral ligands **36-41** (Figure 2.12, see above), which have been applied successfully in the hydroformylation reaction of vinyl arenes, were used as ligands in rhodium-catalysed asymmetric hydrogenation. They were developed in our group,<sup>[35, 56, 109]</sup> and showed high enantioselectivities (>99%). The enantiomeric excesses were strongly influenced by the configuration of the ligands, which was also the case in the hydroformylation reaction.

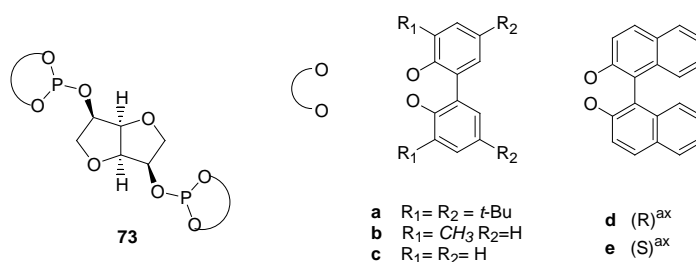


**Figure 2.26.**  $C_2$ -symmetry diphosphite chiral ligands developed by Reetz

## Objective

The carbohydrate derivative ligands synthesised in our group have been successfully applied in several asymmetric catalytic reactions. We emphasise the results obtained in the asymmetric hydroformylation of vinyl arenes with  $C_1$ -symmetry diphosphites derived from carbohydrates, **36-41** (Figure 2.12, see above), which are one of the best reported in the literature.<sup>[34-36, 56]</sup> The application of these ligands to the asymmetric hydrogenation of prochiral olefins also led to excellent results.<sup>[35, 56, 109]</sup>

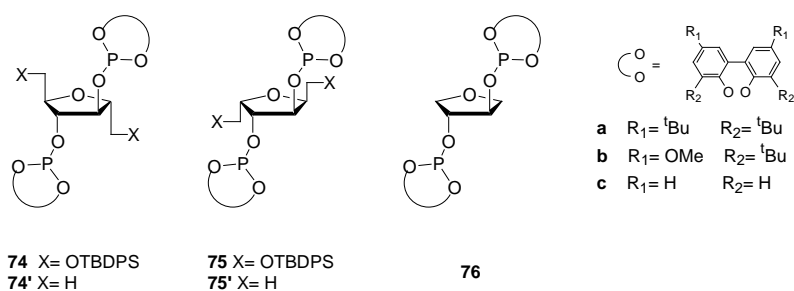


**Figure 2.27.** New series of  $C_2$ -symmetry diphosphite ligands **74-76**

Since it has been shown that additional stereocenters in ligands **70, 71** (Figure 2.25) lead to a considerably higher enantioselectivity in the hydrogenation of enamidoesters in comparison than the reference compound **72**, and given that, until now, the diphosphites derived from 1,2-diols provided moderate enantiomeric

excess in the asymmetric hydroformylation of styrene, we decided to synthesise a new series of  $C_2$ -symmetry diphosphite ligands, **74-76** (Figure 2.27), with the same backbone as the previously reported diphosphinites **70** and **71** (see Figure 2.25) in order to test whether a similar effect was also produced in the hydroformylation reaction with a rhodium-diphosphite catalytic system.<sup>[107]</sup>

These diphosphites can also be modified by changing the substituents of the phosphorus moieties, the nature of the substituents and the configuration at positions 2 and 5. We shall use these ligands to synthesise their rhodium cationic complexes. This new series of chiral ligands **74-76** will be applied in the rhodium-asymmetric hydroformylation reaction of vinyl arenes. We also report the application of the rhodium cationic complexes that contain chiral ligands **74-76** in the hydrogenation of methyl acetamidoacrylate.

## 2.2 Results and discussion

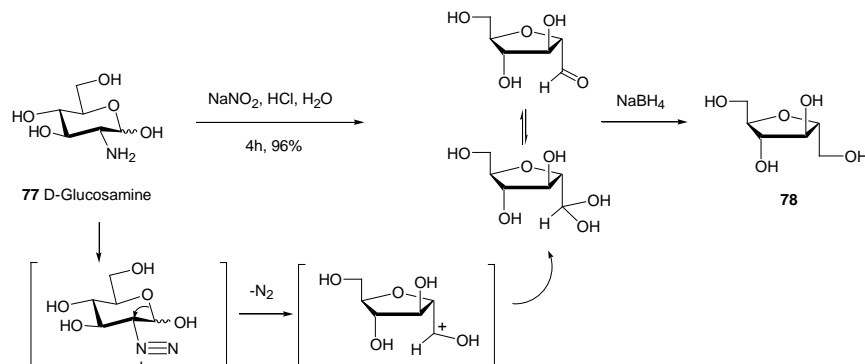
### 2.2.1 Synthesis of diphosphite ligands with carbohydrate backbone

#### 2.2.1.1 Synthesis of 2,5-anhydro-D-mannitol derivative ligands **74a-c** and **74'a,b**

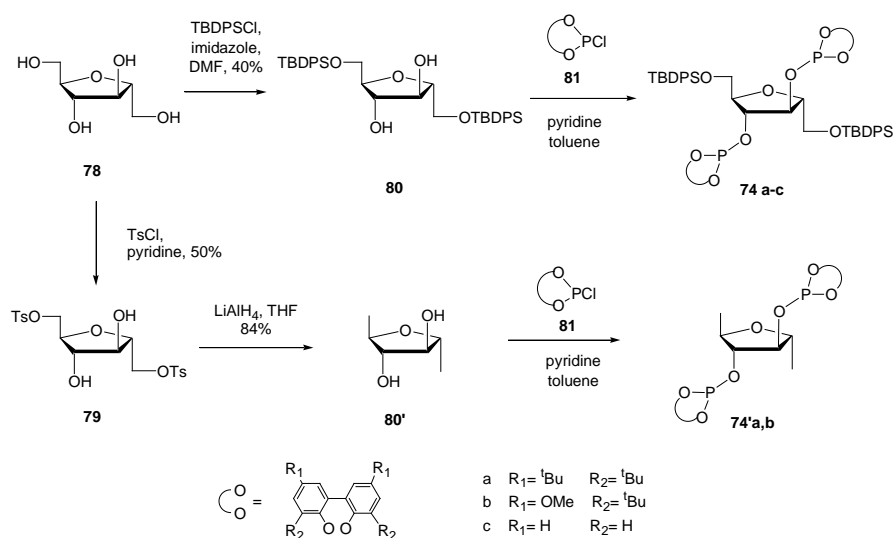
Phosphorus ligands **74** and **74'** can be prepared from 2,5-anhydro-D-mannitol (**78**), which in turn can be prepared from D-glucosamine (**77**) in a straightforward manner (Scheme 2.5). Treating **77** with sodium nitrite gives the diazonium salt which undergoes a ring contraction reaction to give the tetrahydrofuran aldehyde derivative. This aldehyde is in equilibrium with its hydrate. The reduction of the aldehyde/hydrate mixture with sodium borohydride provides tetrol **78** in 82% yield (Scheme 2.5).<sup>[110-112]</sup>

To study the effect of the groups at positions 2 and 5 we prepared the diols **80** and **80'** from the tetrol **78** (Scheme 2.6). The primary alcohols in **78** were protected by reaction with *tert*-butyldiphenylchlorosilane (TBDPSCI) to afford the diol **80**. To obtain the diol **80'** with a methyl group at positions 2 and 5, the primary alcohols of

**78** were selectively ditosylated<sup>[113]</sup> to give diol **79**, which was then treated with LiAlH<sub>4</sub> to afford compound **80'** (Scheme 2.6).<sup>[113]</sup>



**Scheme 2.5.** Synthesis of 2,5-anhydro-D-mannitol **78**

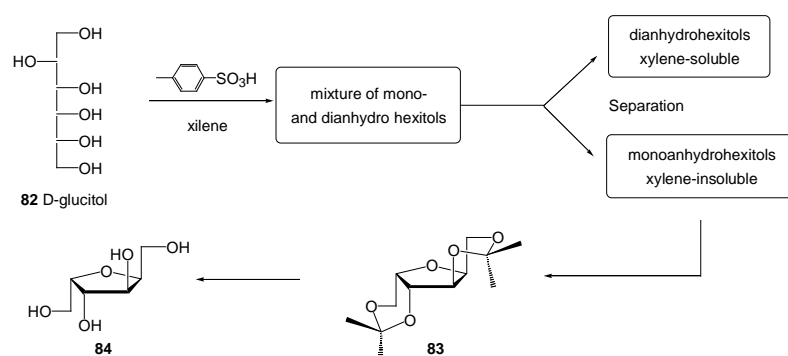


**Scheme 2.6.** Synthesis of 2,5-anhydro-D-mannitol derivative ligands **74a-c** and **74'a, b**

The diols **80** were treated with the corresponding phosphorochloridite **81**, which had been previously synthesised by standard procedures,<sup>[46, 114]</sup> to give the corresponding diphosphites **74a-c** and **74'a,b** in moderate to good yields (31-72%) (Scheme 2.6).

### 2.2.1.2 Synthesis of 2,5-anhydro-L-idoitol derivative ligands **75a,b** and **75'a,b**

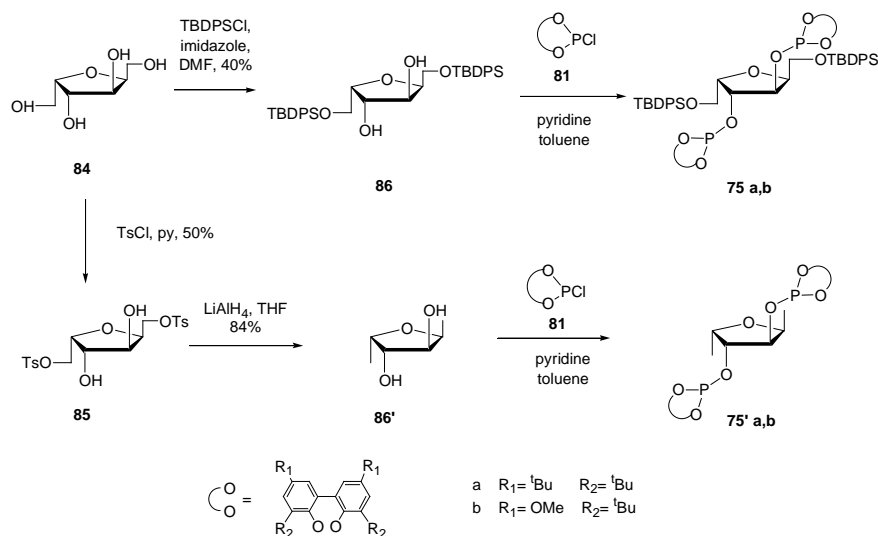
To study the effect of the configuration of carbons 2 and 5, ligands **75** and **75'** were prepared from 2,5-anhydro-L-idoitol **84**. Tetrol **84** was obtained from D-glucitol **82** following a reported procedure (Scheme 2.7).<sup>[115, 116]</sup> The yield was only 5%, similar to previously reported yields, but this procedure allows **84** to be easily obtained from a very accessible nonexpensive starting material in a multigram scale.



**Scheme 2.7.** Synthesis of 2,5-anhydro-L-idoitol **84**

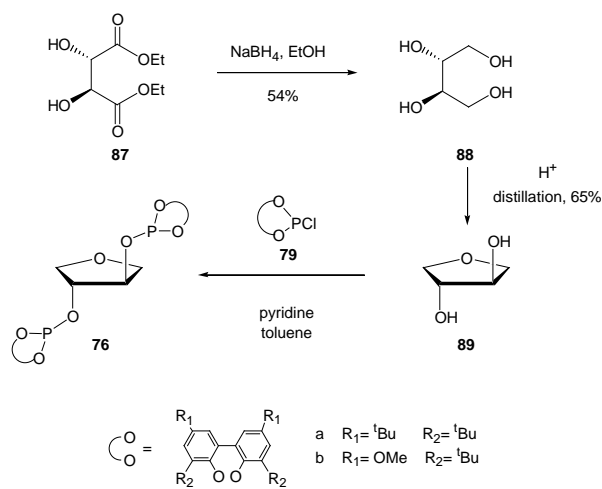
We also prepared diols **86** and **86'** (Scheme 2.8) in a similar way to **80** and **80'**. The diols **86** were then treated with the corresponding phosphorochloridite **81**, synthesised *in situ* by standard procedures,<sup>[46, 114]</sup> to give the corresponding diphosphites **75a,b** and **75'a,b** in moderate to good yields (32-92%) (Scheme 2.8).





**Scheme 2.8.** Synthesis of 2,5-anhydro-L-iditol derivative ligands **75a, b** and **75'a, b**

### 2.2.1.3 Synthesis of (3*R*,4*R*)-3,4-dihydroxytetrahydrofuran derivative ligands **76a, b**



**Scheme 2.9.** Synthesis of (3*R*,4*R*)-3,4-dihydroxytetrahydrofuran derivative ligands **76a, b**

In order to compare the effect of the stereocenters 2 and 5, we prepared the diphosphite ligands **76a, b** which do not contain substituents in these positions. They were synthesised from diol (3*R*, 4*R*)-3,4-dihydroxytetrahydrofuran.<sup>[117]</sup> The diol **89** was prepared from (2*S*,3*S*)-diethyl tartrate in two steps. The reaction of **87** with NaBH<sub>4</sub> affords tetrol **88**, which was distilled in the presence of catalytic amounts of *p*-toluenesulfonic acid to afford **89** in moderate yields. The treatment of **89** with phosphorochloridite **81**, synthesised *in situ* by standard procedures,<sup>[46, 114]</sup> gives the corresponding diphosphites **76a,b** in moderate to good yields (29-75%) (Scheme 2.9).

### 2.2.1.4 Structural elucidation of diphosphites 74-76

The structure of diphosphite ligands **74-76** was determined by one-dimensional <sup>1</sup>H, <sup>13</sup>C and <sup>31</sup>P NMR. The signals were unequivocally assigned by the bidimensional techniques COSY and HSQC. We also determined the crystal structure of diphosphite ligand **74a** by X-ray diffraction.

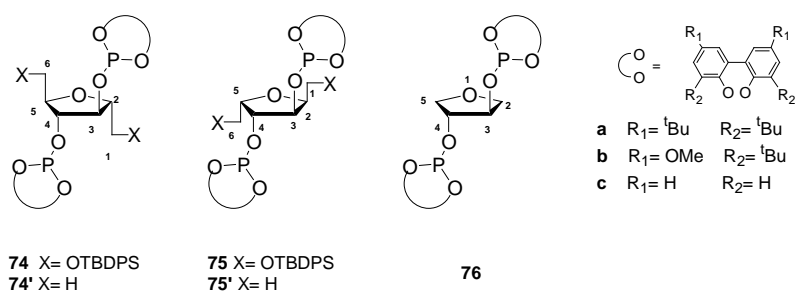


**Figure 2.28.** C<sub>2</sub>-symmetry diphosphite ligands derived from carbohydrates

Ligands **74a-c**, **74'a, b**, **75a, b**, **75'a, b** and **76a, b**, as well as their alcohol precursors, showed simple <sup>1</sup>H and <sup>13</sup>C NMR spectra, characteristic of compounds with a C<sub>2</sub>-symmetry.

The <sup>31</sup>P{<sup>1</sup>H} NMR spectrum of ligands **74-76** showed only one signal between 140 and 147 ppm, characteristic of a phosphite function. The <sup>1</sup>H NMR spectra of ligands **74-76** showed signals corresponding to the second order protons H2/H5 and H3/H4

so coupling constants cannot be directly measured in the spectra. These second order spectra are derived from the existence of protons that are chemically but not magnetically equivalent, which give rise to spin systems  $AA'BB'X_2X'_2$  for compounds **74-75** and  $AA'BB'X_3X'_3$  for compounds **74'-75'**.

The  $^1\text{H}$  NMR spectra of ligands **74-76** showed three different regions. We observed the aromatic protons between 6.58 and 7.83 ppm, the methynic and methylenic protons bonded to oxygen and the methyl protons of the methoxy groups (for **b** ligands) at lower chemical shifts (3.38-5.20 ppm), and finally the signals of the protons of the *tert*-butyl and methyl groups in the area between 1.46 and 1.06 ppm.

In the  $^1\text{H}$  NMR spectra of ligands **74** and **75**, with OTBDPS groups, we observed four signals corresponding to methynic and methylenic protons. H1/H6, H1'/H6' appeared in the range 3.38 to 3.67 ppm for ligands **74** and between 3.79-3.98 ppm for ligands **75**. Protons H2/H5 appeared around 4.0 ppm for ligands **74** and around 4.4 ppm for ligands **75**. Protons H3/H4 appeared near 5.1 ppm in ligands **74** and **75**.

The  $^1\text{H}$  NMR spectra of ligands **74'** and **75'**, with methyl substituents in carbons 2 and 5, showed two signals between 4.07 and 4.70 ppm corresponding to methynic protons. Protons H2/H5 appeared at 4.07 and 4.31 for ligands **74'** and at 4.12 and 4.26 for ligands **75'**. Protons H3/H4 appeared at 4.56 and 4.65 for ligands **74'** and at 4.63 and 4.73 for ligands **75'**. The methyl substituents in carbons 2 and 5, appeared as a doublet with chemical shifts of 1.09 to 1.29 ppm and coupling constants between 6.2-6.6 Hz.

The  $^1\text{H}$  NMR spectra for ligand **76** presents three signals in the same area corresponding to protons H2/H5, H2'/H5' and H3/H4. The methylenic protons H2/H5 and H2'/H5' appeared in the range 3.84 to 3.96 ppm while the methynic protons H3/H4 appeared around 4.8 ppm (see Table 2.3).

The  $^{13}\text{C}$  NMR spectrum of ligands **74-76** showed aromatic carbons in the range 155-122 ppm, the signal of *tert*-butyl groups appeared at 35-31 ppm and the

methoxy groups of ligands **b** showed chemical shifts around 55 ppm. The  $^{13}\text{C}$  NMR spectrum of ligands **74** and **75** showed chemical shifts around 63 ppm for C1, while C2 appeared in the range 79.7 to 82.9 ppm and C3 in the range 79.9 to 79.5 ppm. For ligands **74'** and **75'** C1 appeared in the range 14.3 to 18.5 ppm, while C2 showed chemical shifts between 75.2 and 79.9 ppm and C3 between 80.0 and 85.4 ppm. Ligands **76** showed to signals in this area, C2 appeared around 72 ppm and C3 at 79.1 ppm (Table 2.4).

**Table 2.3.**  $^1\text{H}$  and  $^{31}\text{P}\{^1\text{H}\}$  NMR ( $\text{CDCl}_3$ ) chemical shifts of compounds **74–76**

Diphosphite	Ph	H <sub>1</sub>	H <sub>1'</sub>	H <sub>2</sub>	H <sub>3</sub>	CH <sub>3</sub>	OCH <sub>3</sub>	C(CH <sub>3</sub> ) <sub>3</sub>	<sup>31</sup> P
<b>74a</b>	7.64– 7.00	3.60	3.38	3.96	5.20	0.93	-	1.43-1.20	143.85
<b>74b</b>	7.65– 6.58	3.67	3.53	4.05	5.14	0.98	3.81, 3.74	1.42, 1.35	144.54
<b>74c</b>	7.66– 7.06	3.76	3.72	4.14	5.16	0.99	-	-	146.70
<b>74'a</b>	7.41, 7.15	1.06	-	4.07	4.56	-	-	1.46-1.33	143.03
<b>74'b</b>	7.08– 6.82	1.29	-	4.31	4.65	-	3.90	1.55, 1.53	142.45
<b>75a</b>	7.65– 7.17	3.85	3.79	4.30	4.56	0.96	-	1.45–1.28	147.47
<b>75b</b>	7.83– 6.85	3.98	3.98	4.47	5.14	0.94	4.00, 3.96	-	146.72
<b>75'a</b>	7.42, 7.16	1.09	-	4.12	4.63	-	-	1.46–1.33	146.95
<b>75'b</b>	6.96, 6.68	1.16	-	4.26	4.70	-	3.79, 3.77	1.42, 1.40	146.07
<b>76a</b>	7.42, 7.16	-	-	3.84, 3.69 <sup>a</sup>	4.82	-	-	1.46–1.34	141.50
<b>76b</b>	7.00, 6.74	-	-	3.96, 3.85 <sup>a</sup>	4.85	-	3.83	1.47, 1.43	140.97

<sup>a</sup> ppm chemical shift of H<sub>2'</sub>.

**Table 2.4.**  $^{13}\text{C}\{^1\text{H}\}$  NMR ( $\text{CDCl}_3$ ) chemical shifts of compounds **74–76**

Diphosphite	Ph	C <sub>1</sub>	C <sub>2</sub>	C <sub>3</sub>	OCH <sub>3</sub>	C(CH <sub>3</sub> ) <sub>3</sub>	C(CH <sub>3</sub> ) <sub>3</sub>
<b>74a</b>	146.3– 124.1	62.5	82.5	79.5	-	35.4– 34.5, 19.2	31.6–31.3, 26.8
<b>74b</b>	155.5– 112.6	62.6	82.9	79.6	55.5, 55.4	35.7–35.6, 19.5	31.5–31.3, 27.5
<b>74c</b>	146.7– 121.3	63.1	83.4	79.9	-	19.5	27.0
<b>74'a</b>	146.5– 124.2	18.5	79.5	85.4	-	35.4–34.6	31.5–31.1
<b>74'b</b>	155.6– 112.7	18.3	79.9	85.4	55.5, 55.4	35.3	31.0, 30,8
<b>75a</b>	146.5– 124.1	62.9	79.7	77.8	-	35.4–34.6, 19.2	31.5–31.1, 26.8
<b>75b</b>	156.0– 112.9	62.7	80.0	77.7	55.5, 55.4	35.3, 35.3, 19.2	31.2, 31.0, 26.1
<b>75'a</b>	146.5– 124.1	14.3	75.2	80.0	-	35.4–34.6	31.5–31.2
<b>75'b</b>	155.6– 112.8	15.0	75.2	80.2	55.5, 55.4	35.4– 5.3	31.0
<b>76a</b>	146.6– 124.2	-	72.3	79.1	-	35.4–34.6	31.5–31.1
<b>76b</b>	155.6– 112.8	-	72.3	79.1	55.5, 55.5	35.3, 35.2	30.9, 30.9

Monocrystals of **74a** suitable for X-ray diffraction were obtained by slow diffusion of hexane into a  $\text{CH}_2\text{Cl}_2$  solution of the ligand. The structure of **74a** was unambiguously revealed by single crystal X-ray diffraction. The ligand crystallizes as a solvate with two molecules of *n*-hexane in the elementary cell. The central five-membered ring O1-C1-C2-C3-C4 has a twisted conformation. The measured compound crystallizes as a racemic twin (74:16).

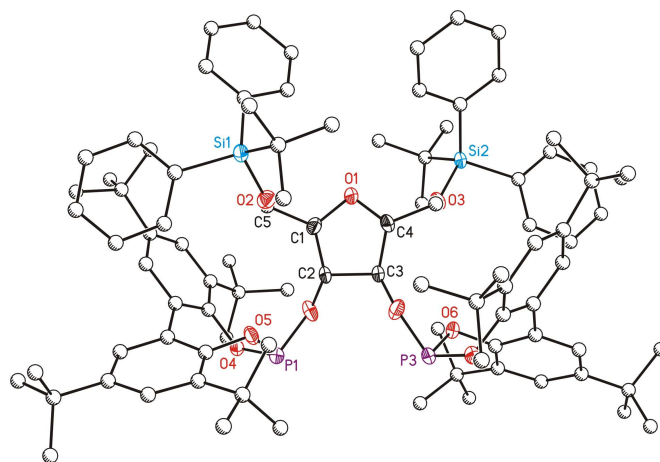


**Figure 2.29.** Structure model (ellipsoids at 50 % probability level) of ligand **74a**. Counterions, solvates and hydrogen atoms have been omitted for the sake of clarity. Selected bond distances and angles are given in Tables 1 and 2 of the appendix.

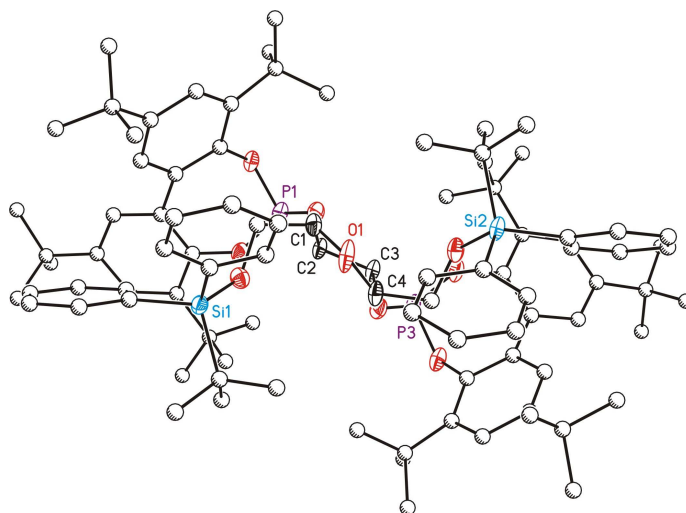
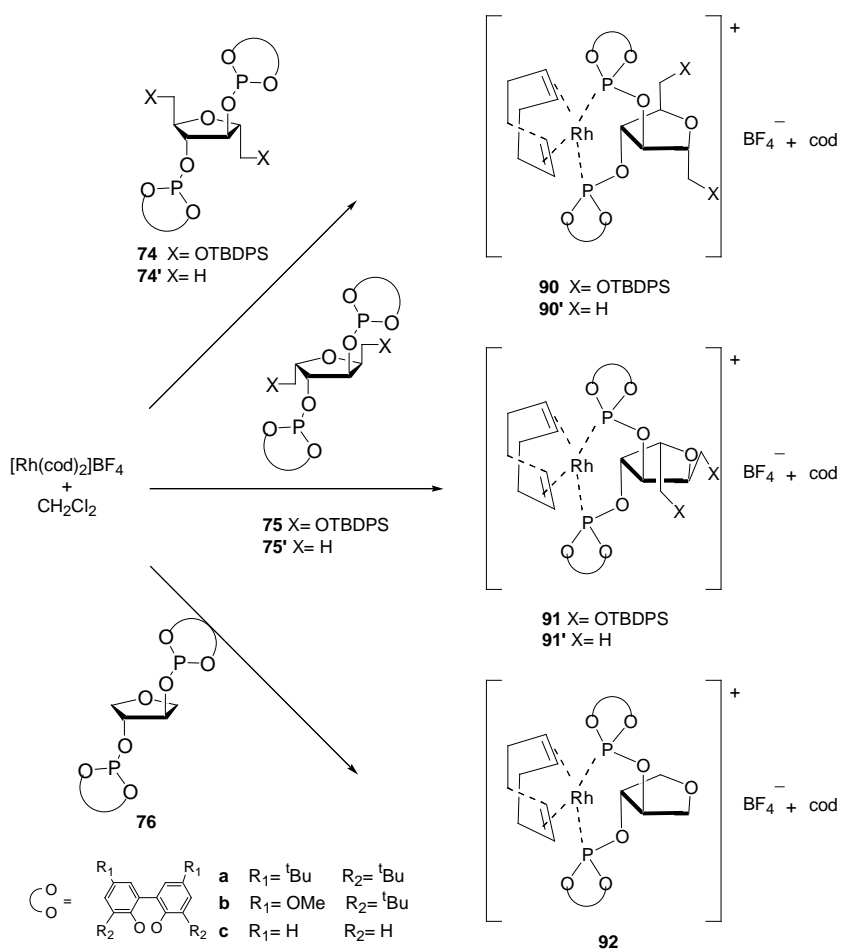


**Figure 2.30.** Structure model showing a lateral view of the molecule **74a**.

## 2.2.2 Synthesis of rhodium complexes

### 2.2.2.1 Synthesis of rhodium complexes $[\text{Rh}(\text{cod})(\text{L})]\text{BF}_4$

Rhodium complexes  $[\text{Rh}(\text{cod})(\text{L})]\text{BF}_4$ , L: diphosphite ligand, **90-92** were prepared by reacting  $[\text{Rh}(\text{cod})_2]\text{BF}_4$  with ligands **74a-c**, **74'a-b**, **75a**, **75'a** and **76a,b**, respectively. All complexes were isolated as coloured solids and were stable in air (Scheme 2.10).



**Scheme 2.10.** Synthesis of cationic rhodium complexes

### 2.2.2.2 Structural elucidation of rhodium complexes [Rh(cod)(L)]BF<sub>4</sub>

The structure of the rhodium complexes **90-92** was elucidated by NMR spectroscopic techniques. Tables 2.5 and 2.6 summarise the <sup>1</sup>H, <sup>13</sup>C and <sup>31</sup>P NMR data. The signals were unequivocally assigned by the bidimensional techniques COSY and HSQC. We also determined the crystal structure of rhodium complexes **90a** and **91'a** by X-ray diffraction.

**Table 2.5.** <sup>1</sup>H and <sup>31</sup>P{<sup>1</sup>H} NMR (CDCl<sub>3</sub>) chemical shifts of complexes **90-92**

Rh	Ph	H <sub>1</sub>	H <sub>1'</sub>	H <sub>2</sub>	H <sub>3</sub>	CH <sub>3</sub>	OCH <sub>3</sub>	C(CH <sub>3</sub> ) <sub>3</sub>	CH	CH <sub>2</sub>	<sup>31</sup> P
<b>90a</b>	7.62– 6.87	3.52	2.82	3.73	5.69	0.89	-	1.65– 1.14	5.88, 4.92	2.34– 2.00	129.35
<b>90b</b>	7.51– 6.54	3.59	3.10	3.87	5.72	0.98	3.93, 3.66	1.71, 1.47	5.81, 4.96	2.45– 2.05	129.85
<b>90c</b>	7.54– 7.18	3.85	3.57	4.12	5.68	0.95	-	-	5.68	2.50– 2.09	136.71
<b>90'a</b>	7.60, 7.06	0.84	-	3.84	5.78	-	-	1.76– 1.32	4.87	2.32– 1.94	128.38
<b>90'b</b>	7.22– 6.71	1.03	-	3.96	5.98	-	3.97, 3.92	1.84, 1.57	5.85, 5.00	2.44– 2.05	128.65
<b>91a</b>	7.51– 7.13	3.44	3.44	3.89	4.66	0.96	-	1.51– 1.25	5.67, 5.34	2.36– 2.05	126.62
<b>91'a</b>	7.58, 7.09	0.86	-	4.13	5.49	-	-	1.76– 1.34	5.85, 5.00	2.34– 2.01	127.97
<b>92a</b>	7.61, 7.08	-	-	4.13, 3.72 <sup>a</sup>	5.51	-	-	1.75– 1.36	5.51, 4.65	2.21, 2.07	127.85
<b>92b</b>	7.13, 6.62	-	-	4.07, 3.66 <sup>a</sup>	5.53	-	3.87, 3.83	1.71, 1.48	5.64, 4.80	2.26– 1.82	129.36

<sup>a</sup> ppm chemical shift of H<sub>2</sub>.

The NMR spectra of the complexes at 25 °C show that they have C<sub>2</sub>-symmetry in solution. In the <sup>31</sup>P{<sup>1</sup>H} NMR spectrum, only one signal appeared between 127 and 136 ppm (*J*<sub>P-Rh</sub> = 253–256 Hz). The chemical shift and coupling constant values are



in agreement with those observed for structurally related cationic diphosphite rhodium complexes.<sup>[56]</sup> The chemical shifts of the <sup>1</sup>H NMR and <sup>13</sup>C NMR (Table 2.5 and 2.6, respectively) were similar to those of the free ligands, and 1,5-cyclooctadiene showed two groups of signals between 4.65 and 5.88 ppm, and between 1.94 and 2.34 ppm for the methynic groups and methylenic groups, respectively.

The mononuclearity of the complexes was confirmed by MALDI spectra, which in all cases showed molecular ions corresponding to the cation [Rh(cod)(L)]<sup>+</sup> (L= **74a-b**, **74'a-b**, **75a**, **75'a** and **76a,b**).

**Table 2.6.** <sup>13</sup>C{<sup>1</sup>H} NMR (CDCl<sub>3</sub>) chemical shifts of complexes **90–92**

Rh	Ph	C <sub>1</sub>	C <sub>2</sub>	C <sub>3</sub>	OCH <sub>3</sub>	C(CH <sub>3</sub> ) <sub>3</sub>	C(CH <sub>3</sub> ) <sub>3</sub>	CH	CH <sub>2</sub>
<b>90a</b>	149.4–125.2	60.7	78.6	77.4	-	36.0–34.6, 19.4	32.9–31.1, 26.8	112.9, 103.5	30.6, 29.7
<b>90b</b>	157.2–113.8	61.2	76.6	77.2	56.0, 55.4	36.1, 35.6, 19.4	32.9, 31.6, 26.7	112.8, 103.7	31.1, 29.4
<b>90c</b>	148.0–121.4	62.3	79.1	80.1	-	19.3	26.8	110.8, 110.1	30.4, 29.8
<b>90'a</b>	149.4–125.4	17.9	72.6	84.2	-	35.8–34.8	32.6–31.3	112.4, 103.6	30.6, 29.6
<b>90'b</b>	157.1–114.1	18.1	72.7	85.3	55.9, 55.7	35.8, 35.5	32.4, 31.5	112.2, 103.2	30.8, 29.6
<b>91a</b>	149.6–125.4	63.1	80.9	74.7	-	35.6–34.8, 19.2	32.3–31.4, 26.8	112.8, 103.4	30.3, 29.7
<b>91'a</b>	149.2–125.3	16.1	71.0	81.5	-	35.8–34.7	32.4–31.3	111.8, 104.2	30.1, 29.6
<b>92a</b>	149.7–125.6	-	67.9	80.1	-	35.8–34.7	32.7–31.3	112.6, 103.2	30.5, 29.5
<b>92b</b>	157.3–114.2	-	68.1	80.3	56.2, 55.3	36.1, 35.7	32.7, 31.6	113.6, 103.8	30.8, 30.1

Monocrystals of the complexes  $[\text{Rh}(\text{cod})(\mathbf{74a})]\text{BF}_4$  (**90a**) and  $[\text{Rh}(\text{cod})(\mathbf{75'a})]\text{BF}_4$  (**91'a**), suitable for X-ray diffraction, were obtained by slow diffusion of hexane into a  $\text{CH}_2\text{Cl}_2$  solution of the complex.

Compound  $[\text{Rh}(\text{cod})(\mathbf{74a})]\text{BF}_4$ , **90a**, crystallizes as a cation together with a  $\text{BF}_4^-$  anion (Figure 2.31 and 2.32), a disordered water molecule and two disordered positions of dichloromethane. The rhodium atom is coordinated in a slightly distorted square planar geometry with a mean deviation from the plane of 0.101 Å. The distances between the metal atom and the centers of the double bonds at the cyclooctadiene rings are A: 2.169 Å and 2.183 Å. The five-membered ring C1-C2-O3-C3-C4 has a twisted conformation. The measured compound crystallizes in a pure chiral structure.

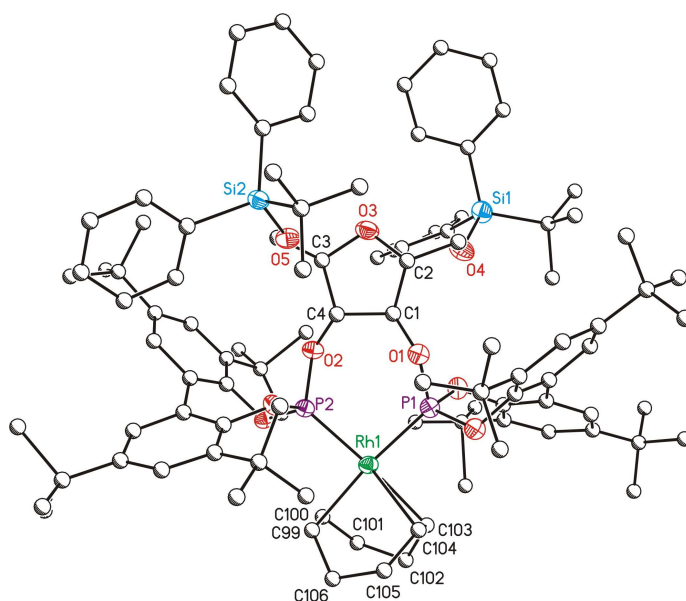


**Figure 2.31.** Structure model (ellipsoids at 50 % probability level) of  $[\text{Rh}(\text{cod})(\mathbf{74a})]\text{BF}_4$ , **90a**. Counterions, solvates and hydrogen atoms have been omitted for the sake of clarity. Selected bond distances and angles are given in Tables 3 and 4 of the appendix.

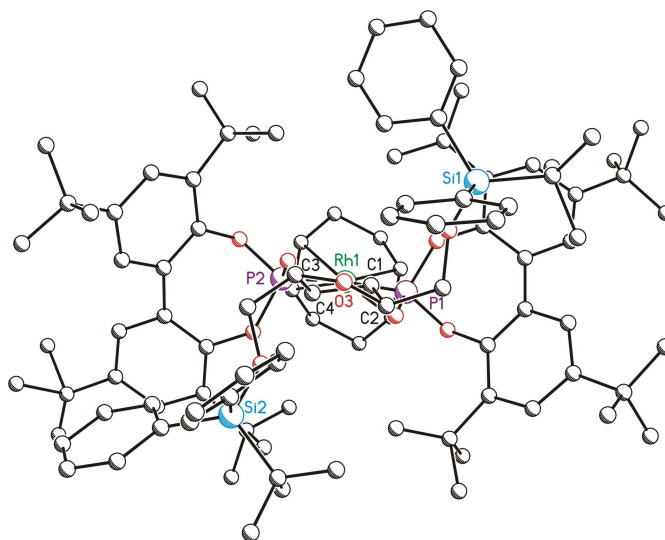


**Figure 2.32.** Structure model showing a lateral view of the complex  $[\text{Rh}(\text{cod})(\mathbf{74a})]\text{BF}_4$ , **90a**.

Compound  $[\text{Rh}(\text{cod})(\mathbf{75'a})]\text{BF}_4$  (**91'a**) crystallizes with two independent cations in the elementary cell (Figure 2.33 to 2.36). The crystal cell also contains two anions of  $\text{BF}_4^-$  and four disordered positions of dichloromethane molecules. The independently obtained cationic structures have different conformations. In molecule A, the five-membered ring C1-C2-O1-C3-C4 has a twisted conformation and in molecule B the same ring has an envelope conformation. The seven-membered ring formed by the metal atom also shows different folding in molecules A and B. For molecule B, the folding of this seven-membered ring is more pronounced. In both molecules the rhodium atom is coordinated in a slightly distorted square planar geometry. In molecule A, the mean deviation from the plane is 0.041 Å and in molecule B the mean deviation from plane is 0.081 Å. The distances between the metal atom and the centers of the double bonds at the cyclooctadiene rings are in molecule A: 2.221 Å and 2.196 Å and in molecule B: 2.254 Å and 2.259 Å. The measured compound crystallizes in a pure chiral structure.

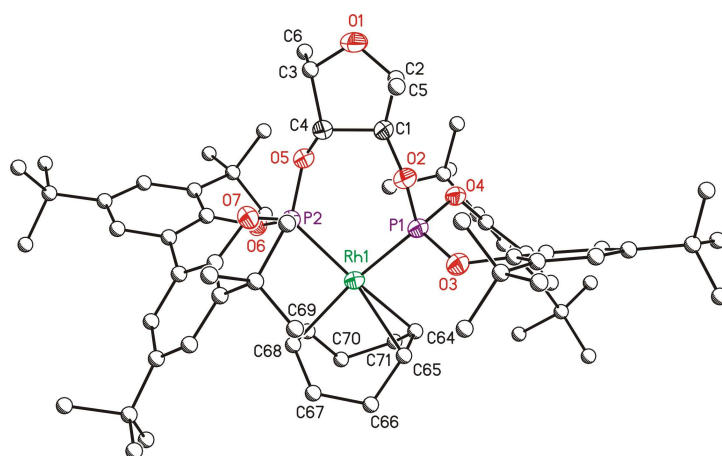


**Figure 2.33.** Structure model (ellipsoids at 50 % probability level) of  $[\text{Rh}(\text{cod})(\mathbf{75}'\mathbf{a})]\text{BF}_4$ , **91'a**, molecule A. Counterions, solvates and hydrogen atoms have been omitted for the sake of clarity. Selected bond distances and angles are given in Tables 5 and 6 of the appendix.

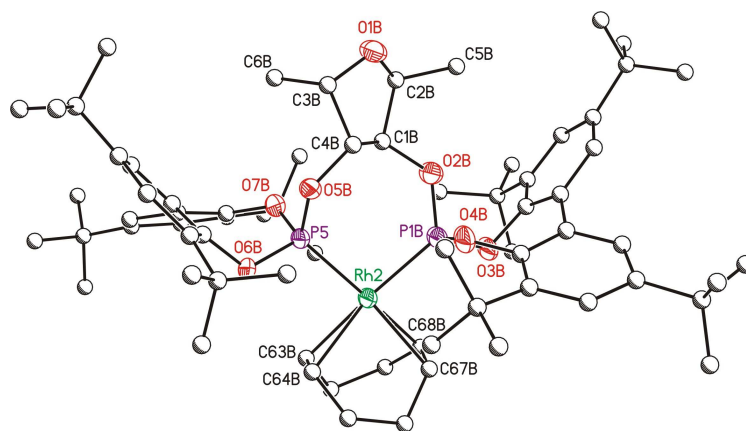


**Figure 2.34.** Structure model (ellipsoids at 50 % probability level) of  $[\text{Rh}(\text{cod})(\mathbf{75}'\mathbf{a})]\text{BF}_4$ , **91'a**, molecule B. Counterions, solvates and hydrogen atoms have been omitted for the sake of clarity. Selected bond distances and angles are given in Tables 5 and 6 of the appendix.

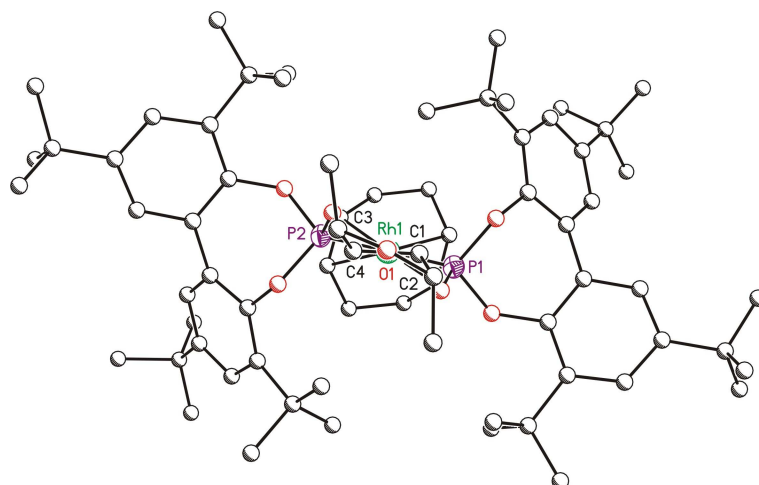


**Figure 2.35.** Structure model showing a lateral view of the  $[\text{Rh}(\text{cod})(\mathbf{75}'\mathbf{a})]\text{BF}_4$ ,  $\mathbf{91}'\mathbf{a}$ , molecule A.

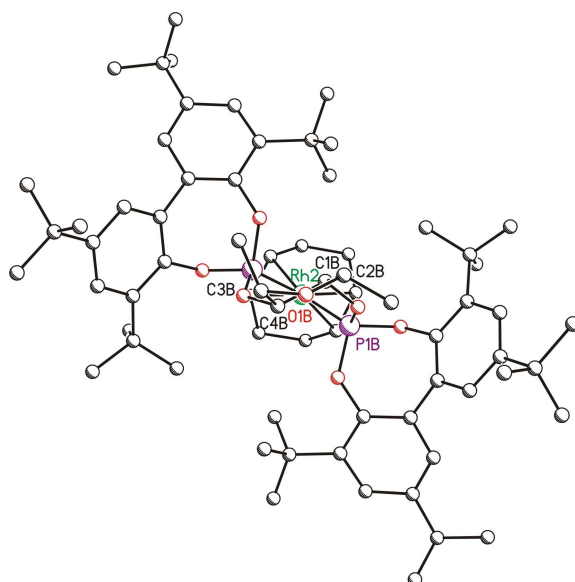


**Figure 2.36.** Structure model showing a lateral view of the  $[\text{Rh}(\text{cod})(\mathbf{75}'\mathbf{a})]\text{BF}_4$ ,  $\mathbf{91}'\mathbf{a}$ , molecule B.

Although there are not many X-ray structures of rhodium complexes with carbohydrate ligands, the rhodium distances are similar to those of the previously described X-ray structure of rhodium-diphosphinite complex, **71d** (Figure 2.25), where diphosphinite ligand has the same furanoside backbone.<sup>[107]</sup>

### 2.2.3 Hydroformylation of styrene and related prochiral olefin

The chiral diphosphites **74-76** were used in the rhodium-catalysed asymmetric hydroformylation of styrene. The catalyst was prepared *in situ* by adding first the diphosphite ligand to a solution of  $[\text{Rh}(\text{acac})(\text{CO})_2]$  (acac=acetylacetonate), and then the substrate. The results of the asymmetric hydroformylation of styrene are given in Tables 2.7 and 2.8. Neither hydrogenated nor polymerised products were observed. The effects of different reaction parameters were investigated for catalytic precursors containing diphosphite ligands **74** to **76**. The reaction parameters were in the range 60°C to 25°C of temperature, 20 bar ( $\text{CO}/\text{H}_2=1/1$ ) to 30 bar ( $\text{CO}/\text{H}_2=1/2$ ) of pressure and a rhodium/ligand ratio between 1/1 to 1/4.

We optimised the conditions with ligands **74a-c** and **74'a,b** (Table 2.7). We observed that when the Rh/L ratio was 1:2 the enantioselectivity increased and the activity decreased (Table 2.7, entry 3 vs entry 4, entries 7 and 9 vs 8 and 11, entries 14-15 vs 16-17, and entry 18 vs 19). This is because at low Rh/L ratios  $[\text{RhH}(\text{CO})_4]$  is formed, which is a highly active achiral hydroformylation catalyst.<sup>[14]</sup> A rhodium/ligand ratio of 1/4 did not enhance the regioselectivity or the enantioselectivity (Table 2.7, entries 11-12).

The effect of the partial pressure of hydrogen was also studied. We observe no improvement in the activity, the regioselectivity or the enantioselectivity when the hydrogen pressure was increased to 20 bar ( $P_{\text{CO}/\text{H}_2}=1/2$ ) (Table 2.7, entries 4-5 and 9-10). The fact that the activity did not increase when the partial pressure of  $\text{H}_2$  was increased suggests that the rate determining step is not the hydrogenolysis but the alkene coordination.

Lower temperatures led to a decrease in the activities (Table 2.7, entries 7 vs. 11 or 16 vs. 17), thus we needed 48 hours at 25°C of temperature to have comparable conversions than the obtained at 40°C for 15 hours. In some cases a slight increase in the enantioselectivities (Table 2.7, entries 2 to 4) was also observed.

**Table 2.7.** Styrene hydroformylation with diphosphites **74-76**<sup>a</sup>

Entry	L	Rh/L	t (h)	T (°C)	% conversion <sup>b</sup>	% regioselec. <sup>c</sup>	%ee
1	<b>74a</b>	1/1	15	60	99	78	20 (S)
2	<b>74a</b>	1/2	15	40	57	96	41 (S)
3	<b>74a</b>	1/1	48	25	>99	93	20 (S)
4	<b>74a</b>	1/2	48	25	77	97	46 (S)
5	<b>74a</b> <sup>d</sup>	1/2	48	25	85	97	42 (S)
6	<b>74b</b>	1/1	15	60	99	79	24 (S)
7	<b>74b</b>	1/1	15	40	99	88	28 (S)
8	<b>74b</b>	1/2	15	40	64	93	30 (S)
9	<b>74b</b>	1/1	48	25	>99	95	30 (S)
10	<b>74b</b> <sup>d</sup>	1/1	48	25	99	94	25 (S)
11	<b>74b</b>	1/2	48	25	97	93	39 (S)
12	<b>74b</b>	1/4	48	25	61	95	37 (S)
13	<b>74c</b>	1/1	15	60	99	79	0
14	<b>74'a</b>	1/1	15	40	99	93	4 (R)
15	<b>74'a</b>	1/1	48	25	98	95	4 (R)
16	<b>74'a</b>	1/2	15	40	98	93	14 (R)
17	<b>74'a</b>	1/2	48	25	96	97	12 (R)
18	<b>74'b</b>	1/1	15	40	98	92	5 (R)
19	<b>74'b</b>	1/2	15	40	98	94	19 (R)

<sup>a</sup>Substrate/Rh=200, styrene 2.7 mmol, [Rh(acac)(CO)<sub>2</sub>] 0.0135mmol P=20 bar, 15 ml toluene P<sub>CO</sub>/H<sub>2</sub>=1 <sup>b</sup> % conv. Styrene determined by G.C. <sup>c</sup> % 2-fenylpropanal <sup>d</sup> P<sub>CO</sub>= 10 P<sub>H<sub>2</sub></sub>=20

For comparative purposes, the rest of the ligands were tested under conditions that gave the optimum compromise between enantioselectivities and reaction rates; that is a ligand to rhodium ratio of 2, a total pressure of 20 bar of synthesis gas with a P<sub>CO</sub>/P<sub>H<sub>2</sub></sub> ratio of 1 and a temperature of 40 °C. The results are given in Table 2.8.

The comparison of the different catalysts that incorporate ligands derived from mannitol **74**, iditol **75** and dihydroxytetrahydrofuran **76**, showed that those that contain ligands **74a,b** and **75a,b** have slightly higher activity than those containing the reference ligands **76a,b** (Table 2.8, entries 1, 2 and 5, 6 vs. 9, 10). More

curious and difficult to explain are the results obtained with the catalytic systems Rh/**74'a, b**, which are much more actives, and Rh/**75'a,b**, which are the least actives (Table 2.8, entries 3, 4 and 7, 8). Ligands **74'a,b** and **75'a,b** have a methyl group at positions 2 and 5 of the tetrahydrofuran backbone, and are less crowded than ligands **74a,b** and **75a,b**, which have a OTBDPS group, but more hindered than ligands **76a,b** which have no substituents at these positions. In all cases, the regioselectivity in the branched aldehyde was higher than 90%, and in several cases it was higher than 95%. This values are in agreement with those obtained with diphosphite ligands containing biphenyl moieties. <sup>[14, 16, 56]</sup>

**Table 2.8.** Styrene hydroformylation with diphosphite **74-76**<sup>a</sup>

Entry	L	% conversion <sup>b</sup>	% regioselect. <sup>c</sup>	%ee
1	<b>74a</b>	57	96	41 (S)
2	<b>74b</b>	64	93	30 (S)
3	<b>74'a</b>	98	93	14 (R)
4	<b>74'b</b>	98	94	19 (R)
5	<b>75a</b>	57	95	22 (R)
6	<b>75b</b>	40	98	43 (R)
7	<b>75'a</b>	33	96	17 (S)
8	<b>75'b</b>	25	94	18 (S)
9	<b>76a</b>	43	>99	26 (R)
10	<b>76b</b>	38	94	34 (R)

<sup>a</sup>Substrate/Rh=200, Rh/L=0.5, styrene 2.7 mmol, [Rh(acac)(CO)<sub>2</sub>] 0.0135mmol, P=20 bar, 15 ml toluene Pco/H<sub>2</sub>=1, temp=40°C, reaction time: 15 hours <sup>b</sup> % conv. Styrene determined by G.C. <sup>c</sup> % 2-fenylpropanal <sup>d</sup> Pco= 10 PH<sub>2</sub>=20

If we compare the results obtained with ligands **74a** and **74b** with **74c** (Table 2.7, entries 1, 6 and 13) we observe that they have similar the activities and regioselectivities but no enantioselectivity was observed with ligand **74c**. This indicates that bulky substituents need to be in the *ortho*-positions of the biphenyl moieties if asymmetric induction is to be obtained. This behaviour was also observed in other diphosphite ligands with the same biphenyl moieties. <sup>[14, 16, 56]</sup> Introducing a methoxy group into ligands **74-76** (ligands **b**) at the *para*-positions



of biphenyl moieties increased the enantioselectivity. Nevertheless, the activity for ligands **74b-76b** was slightly lower than for the corresponding **74a-76a** (see for instance Table 2.8, entries 5 vs. 6). Similar behaviour has also been observed in other carbohydrate derivative diphosphite ligands.<sup>[14, 16, 56]</sup> Ligands **74a, b** are an exception, since when ligand **74b** was used the activity was higher and the enantioselectivity lower than with ligand **74a**.

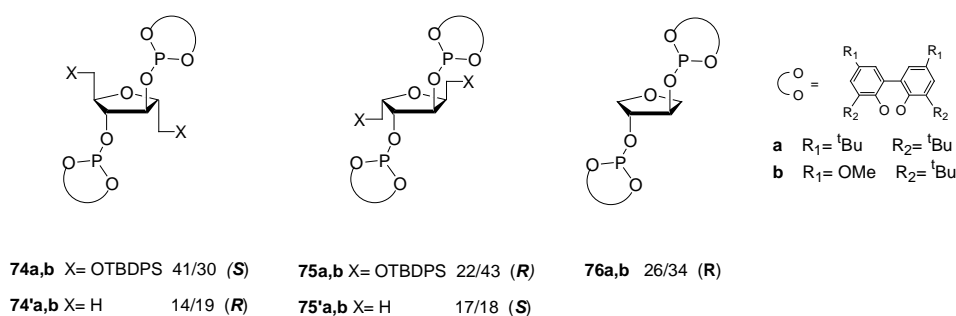


**Figure 2.37.** Values of enantioselectivity and configuration of the major enantiomer obtained in the hydroformylation of styrene using Rh/**74-76** catalytic systems

In general the enantiomeric excess obtained with ligands **74-76** was always moderate and the absolute values obtained with the catalytic systems Rh/**74a,b-75a,b** were in the same range as those obtained with Rh/**76a,b**. However, we observed that the configuration of the stereocenters at positions 2,5 of the tetrahydrofuran backbone and the substituents of these positions had a strong effect on the sense of the asymmetric induction (Table 2.8).

In general, as has been mentioned above, the enantioselectivities were higher when the bulky substituents in the chains were at positions 2 and 5. This is the case of ligands **74a,b** and **75a,b** (where X= OTBDPS, Table 2.8, entries 1 and 6) (Figure 2.37), in comparison with ligands **76** (Table 2.8, entries 9 and 10). The enantioselectivities were poorest when ligands had a methyl group in positions 2 and 5, **74'a,b** and **75'a,b** (Table 2.8, entries 3, 4 and 7, 8, respectively). This tendency that has already been mentioned for ligands **74** and **74'**, is also observed in ligands **75** and **75'**.

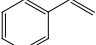
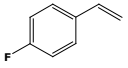
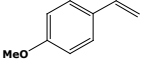
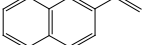
However, what is noteworthy is the fact that the configuration of the major enantiomer obtained is governed by both the substituents and the configuration of the remote stereocenters at positions 2 and 5 (Table 2.8, Figure 2.37). Thus, taking ligand **76**, which has no substituents at positions 2 and 5, as a reference ligand it can be observed that when **75** was used as the ligand the enantioselectivity increased slightly to afford the major enantiomer with the same configuration as **76**. Curiously, ligand **74**, which differs from **75** only in the configuration of the stereogenic centers at positions 2 and 5, preferentially gave the opposite enantiomer.

The behaviour of ligands **74'** and **75'** is also curious. From the point of view of the influence of the chains at positions 2,5, they would be expected to provide results intermediates between **74**, **75** and **76**. However, **75'** gave an enantiomeric excess lower than **75** and **76**, but preferentially afforded the opposite enantiomer. Similarly, **74'** also gave a lower enantioselectivity than **74**, and the opposite enantiomer was also the major one. Thus, the configuration of the major enantiomer is inverted by changing the group at positions 2 and 5, but more significantly because the effect is more important, when change the configuration at positions 2 and 5.

This behaviour has already been observed in the asymmetric hydrogenation reaction of enamidoesters with diphosphinite ligands **70-72** (Figure 2.25) which have a similar structure.<sup>[107]</sup> We are currently exploring the reasons for this behaviour, and although we have not yet an explanation for that, it can be suggested that the influence of the remote stereocenters on the sense of the chiral induction can be due to the influence of the chains at positions 2 and 5, in the conformation on the biphenyl moieties, which are ultimately responsible for the chirality transfer. It is known that the rotation around the biaryl axis of the diphosphite ligands containing bulky substituents in the biaryl moieties is hindered and that the biphenyl moiety preferentially adopts one configuration (see Figure 2.6).<sup>[14, 33]</sup>

Finally, we applied the diphosphite ligand **74a** in the rhodium-catalysed hydroformylation of various substituted vinyl arenes. The results are summarised in Table 2.9.

**Table 2.9.** Hydroformylation of different vinyl arenes with diphosphite **74a**<sup>a</sup>

Entry	Substrate	% conv <sup>b</sup>	% regiosec. <sup>c</sup>	%ee
1		57	96	41 ( <i>S</i> )
2		60	97	49 ( <i>S</i> )
3		34	96	60 ( <i>S</i> )
4		96	94	18 ( <i>S</i> )

<sup>a</sup>Substrate/Rh=200, Rh/L=0.5, substrate 2.7 mmol, [Rh(acac)(CO)<sub>2</sub>] 0.0135mmol P=20 bar, 15 ml toluene Pco/H<sub>2</sub>=1, temp=40°C, reaction time: 15 hours <sup>b</sup> % conv. substrate determined by G.C. <sup>c</sup> % branched aldehyde

The presence of a fluoro substituent in the *para*-position of the substrate (Table 2.9, entry 2) did not affect the activity or the regioselectivity. If we compare the results with those obtained in the hydroformylation of styrene (Table 2.9, entry 1), a slight increase in the enantioselectivity (41%ee (*S*) to 49%ee (*S*)) is observed. When a methoxy group is introduced in the *para*-position the enantioselectivity is enhanced to 60%ee (*S*) (Table 2.9, entry 3), but the activity is lower. Unexpectedly, the hydroformylation of 2-vinylnaphthalene with diphosphite **74a** evolved with high activity but very low enantioselectivity, 18%ee (*S*) (Table 2.9, entry 4). In all cases, the sense of the asymmetric induction was the same. We can conclude that introducing various substituents in the *para*-position of the substrate, which changes not only its electronic but also its steric properties, affects the conversion and the enantioselectivity. When a methoxy group is introduced in the *para*-position the activity decreases whereas the enantioselectivity is enhanced. The opposite behaviour is observed in the asymmetric hydroformylation of 2-vinylnaphthalene. The literature describes some examples in which the rhodium-catalysed hydroformylation of *p*-methoxystyrene provided higher enantioselectivities than other vinylarenes such as styrene, 2-vinylnaphthalene and

*p*-fluorostyrene.<sup>[104, 118, 119]</sup> However, the enantioselectivities obtained with the other ones depended on the ligand used and no correlation was found.

### 2.2.4 High pressure NMR study

The hydridorhodium diphosphite complexes  $[\text{RhH}(\text{CO})_2(\text{L})]$  (L: bidentate ligand) are generally considered as the resting state in the hydroformylation reaction.<sup>[32, 33, 39, 40]</sup> They are generally assumed to have a trigonal-bipyramidal structure. Two isomeric structures of these complexes, with a coordinated bidentate ligand, can be formed (Figure 2.38). The bidentate ligand can be coordinated in an equatorial-equatorial (**ee**) or in equatorial-axial (**ea**) fashion. The presence of only one active diastereoisomeric hydridorhodiumcarbonyl species with bidentate ligands is presumably the key of an efficient control of the chirality transfer.<sup>[14]</sup>

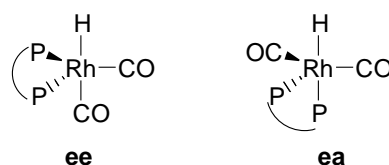
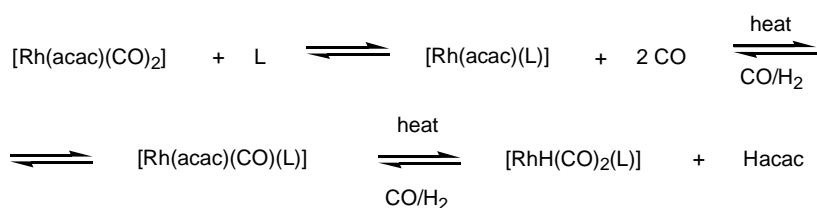


**Figure 2.38.** Equatorial-equatorial (**ee**) and equatorial-axial (**ea**)  $[\text{RhH}(\text{CO})_2(\text{L})]$  species.

In our previous study of the hydroformylation reaction with ligands **74-76** we used  $[\text{Rh}(\text{acac})(\text{CO})_2]$  as catalyst precursor. We therefore used the same compound as starting material in our study on the evolution of this precursor in the presence of diphosphite ligand under the reaction conditions. Under typical hydroformylation conditions,  $[\text{Rh}(\text{acac})(\text{L})]$  complexes transform to trigonal bipyramidal hydridorhodium diphosphites (Scheme 2.11). For this study we used high pressure-NMR spectroscopy.

$[\text{Rh}(\text{acac})(\text{L})]$  complexes were prepared by adding one equivalent of diphosphite ligand to the rhodium precursor  $[\text{Rh}(\text{acac})(\text{CO})_2]$ . For  $[\text{Rh}(\text{acac})(\text{L})]$  species chemical shifts around 140 ppm have been reported with rhodium-phosphorus coupling constants close to 300 Hz when L is a diphosphite.<sup>[47, 48]</sup> Intermediate

complexes  $[\text{Rh}(\text{acac})(\text{CO})(\text{L})]$  can also be formed under hydroformylation conditions. They have slightly lower chemical shifts than  $[\text{Rh}(\text{acac})(\text{L})]$  complexes with a rhodium-phosphorus coupling constants close to 290 Hz.<sup>[47, 48]</sup> Under typical hydroformylation conditions,  $[\text{Rh}(\text{acac})(\text{L})]$  complexes undergo transformation to trigonal bipyramidal hydridorhodium diphosphites in which the diphosphite ligand coordinates in an **ee** or **ea** fashion. The complexes with **ee** (equatorial-equatorial) coordination show small phosphorus-hydrogen coupling constants (<10Hz), whereas the coupling constant of a *trans* coordinated phosphite, **ea** (equatorial-axial) complex, shows a large phosphorus-hydrogen coupling constant of 180-200 Hz. The phosphorus-phosphorus coupling constants are much larger for the **ee** complex (around 250 Hz) than for the **ea** complex (usually 70 Hz).<sup>[14, 47, 48, 54]</sup>



**Scheme 2.11.** Formation of  $[\text{RhH}(\text{CO})_2(\text{L})]$  from  $[\text{Rh}(\text{acac})(\text{CO})_2]$  and diphosphite (L)

The initial solution of  $[\text{Rh}(\text{acac})(\text{CO})_2]$  and diphosphite ligand (**74-76**) in toluene- $d_8$  was analysed by  $^{31}\text{P}$  and  $^1\text{H}$  NMR. Then the NMR tube was pressurised with syngas (20 bar) and heated at 80°C for 30 minutes, hydroformylation conditions, and the spectra of  $^{31}\text{P}$  and  $^1\text{H}$  NMR were then recorded. Finally the NMR tube was shaken for 15 h at 80°C and the  $^{31}\text{P}$  and  $^1\text{H}$  NMR spectra were again recorded.

When ligands **74a** and **74b** were added to a solution of  $[\text{Rh}(\text{acac})(\text{CO})_2]$  in toluene- $d_8$ , the colour changed immediately and in  $^{31}\text{P}$  NMR spectrum showed the presence of a doublet assigned to  $[\text{Rh}(\text{acac})(\text{L})]$  (L=**74a**, **74b**) species (Figure 2.39a). After the NMR tube was pressurized and heated for 30 minutes, the presence of a new doublet in the  $^{31}\text{P}$  NMR spectrum indicated that a new species had formed (Figure 2.39b). Maintaining the solution under hydroformylation conditions the  $[\text{Rh}(\text{acac})(\text{L})]$  for 15 h, all species completely evolved to this new species (Figure

2.39c), which it was assigned to be  $[\text{RhH}(\text{CO})_2(\text{L})]$  on the basis of  $^{31}\text{P}$  and  $^1\text{H}$  spectrum (see later structural elucidation). No traces of intermediate species  $[\text{Rh}(\text{acac})(\text{CO})(\text{L})]$  or other species were detected.

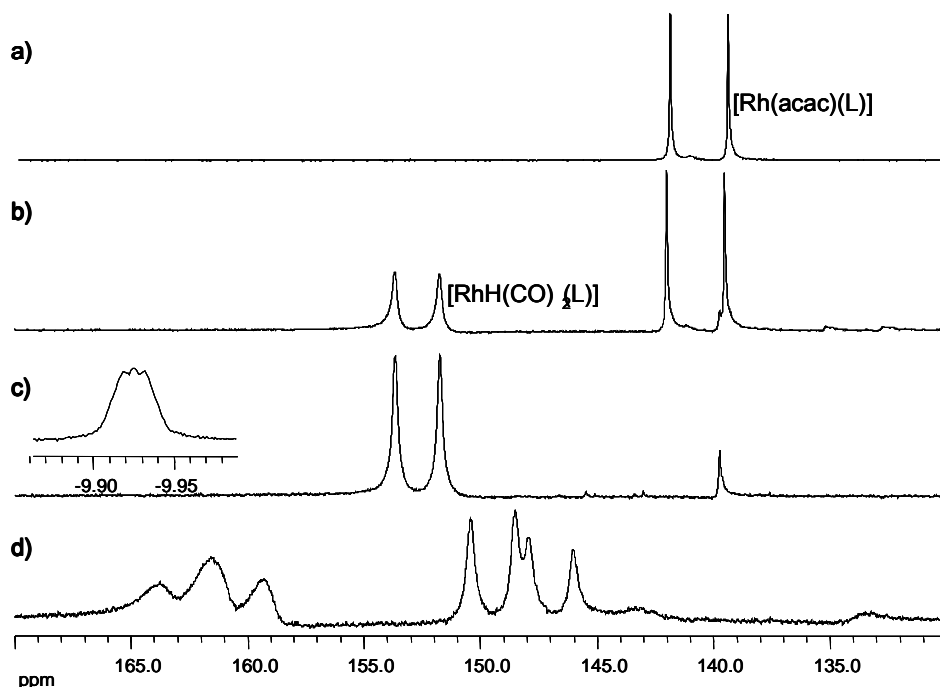


**Figure 2.39.**  $^1\text{H}$  and  $^{31}\text{P}\{^1\text{H}\}$  NMR spectra of the evolution of the precursor  $[\text{Rh}(\text{acac})(\text{CO})_2]$  in the presence of ligand **74a**, under hydroformylation conditions (80°C and 20 bar of syn gas) in toluene- $d_8$ . a)  $[\text{Rh}(\text{acac})(\text{74a})]$  at room temperature, b) after 30 minutes under hydroformylation conditions c) after 15 h under hydroformylation conditions, spectrums collected at room temperature and d) after 15 h under hydroformylation conditions, spectrum collected at  $-100^\circ\text{C}$ .

The study that started from  $[\text{Rh}(\text{acac})(\text{CO})_2]$  and used ligands **74'a**, **75a**, **75'a** and **76a** showed a different behaviour than for ligands **74a** and **74b** because intermediate species  $[\text{Rh}(\text{acac})(\text{CO})(\text{L})]$  were observed. As was observed for ligands **74a** and **74b**, when ligands **74'a**, **75'a** and **76a** were added to the solution of  $[\text{Rh}(\text{acac})(\text{CO})_2]$  in toluene- $d_8$  a fast change of colour and displacement of CO were observed and the  $^{31}\text{P}$  NMR spectrum also showed a doublet that was characteristic of the  $[\text{Rh}(\text{acac})(\text{L})]$  (L= **74'a**, **75'a** and **76a**) species (Figures 2.40a and 2.41a and b). However, in the case of diphosphite ligand **75a**, for which the displacements of CO and the change in colour were also observed, the  $^{31}\text{P}$  NMR

spectrum showed a mixture of  $[\text{Rh}(\text{acac})(\text{CO})(\text{L})]$ , where **75a** coordinated in a bidentate fashion, and traces of another complex where ligand was coordinated in a monodentate fashion (Figure 2.40a). The  $^{31}\text{P}\{^1\text{H}\}$  NMR chemical shifts (in ppm) and the coupling constants (in Hertz) of these species are summarised in Table 2.10.

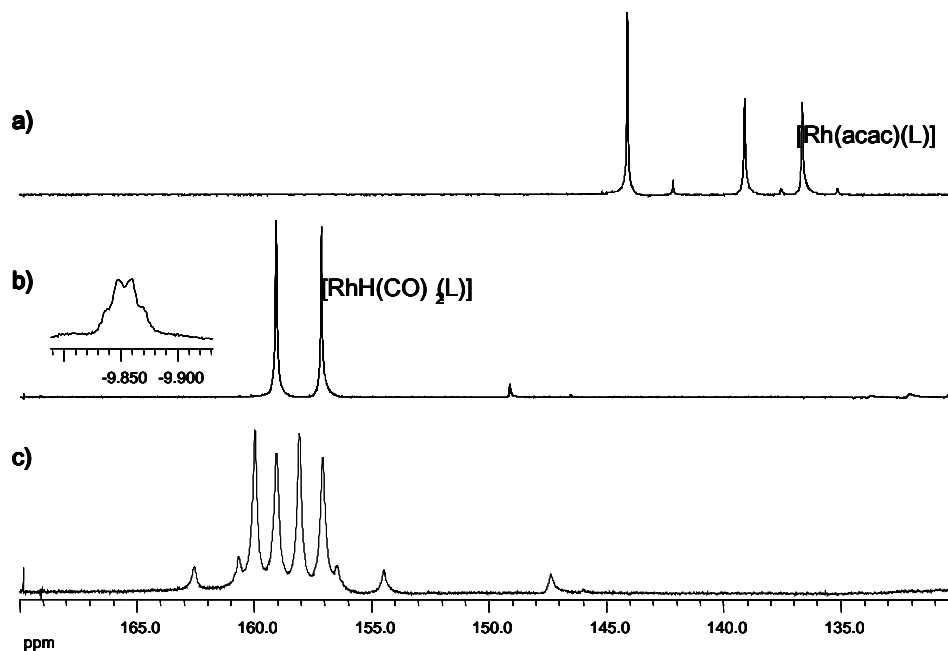


**Figure 2.40.**  $^1\text{H}$  and  $^{31}\text{P}\{^1\text{H}\}$  NMR spectra of the evolution of the precursor  $[\text{Rh}(\text{acac})(\text{CO})_2]$  in the presence of ligand **75a**, under hydroformylation conditions (80°C and 20 bar of syn gas) in toluene- $d_8$ . a)  $[\text{Rh}(\text{acac})(\text{75a})]$  at room temperature, b) after 15 h under hydroformylation conditions, spectrum collected at room temperature and c) after 15 h under hydroformylation conditions, spectrum collected at  $-80^\circ\text{C}$ .

After a reaction time of 15 hours and shaking at the desired temperature, the solution was analysed at room temperature. In all cases stable  $[\text{RhH}(\text{CO})_2(\text{L})]$  complexes were obtained exclusively, since a doublet was observed in  $^{31}\text{P}$  NMR around 155 ppm with a rhodium-phosphorus coupling constant near 230 Hz; small amounts of the phosphonate signal was observed around 10 ppm. In the  $^1\text{H}$  NMR spectrum we detected the signal for the hydride around  $-10$  ppm (Figures 2.39c, 2.40b and 2.41c).

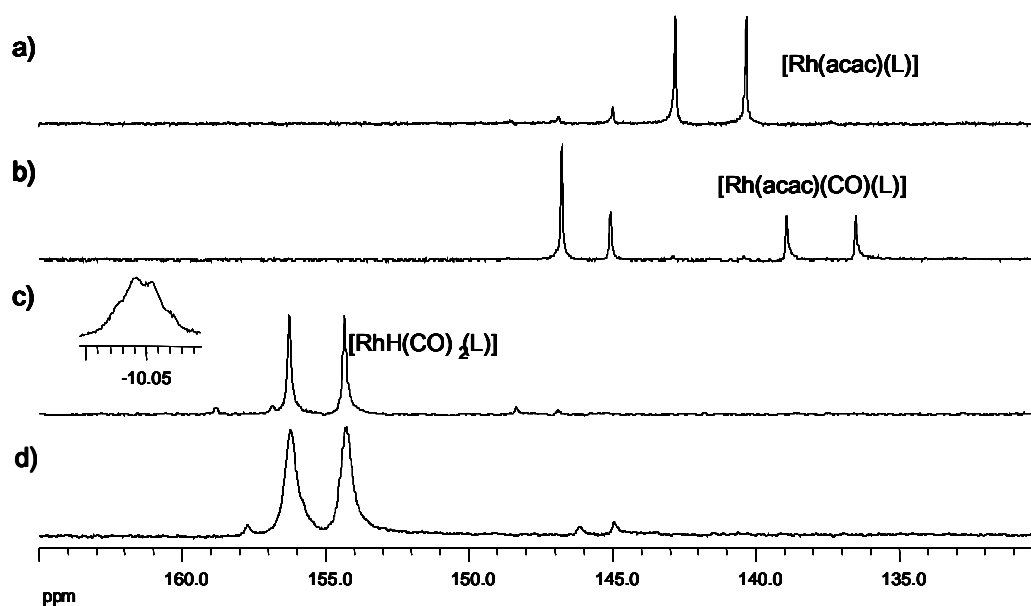


**Figure 2.41.**  $^1\text{H}$  and  $^{31}\text{P}\{^1\text{H}\}$  NMR spectra of the evolution of the precursor  $[\text{Rh}(\text{acac})(\text{CO})_2]$  in the presence of ligand **76a**, under hydroformylation conditions (80°C and 20 bar of syn gas) in toluene- $d_8$ . a)  $[\text{Rh}(\text{acac})(\text{76a})]$  at room temperature, b) after a short period of time under hydroformylation conditions, c) after 15 h under hydroformylation conditions, spectrum collected at room temperature and d) after 15 h under hydroformylation conditions, spectrum collected at  $-80^\circ\text{C}$ .

### Structural assignments

The  $^{31}\text{P}\{^1\text{H}\}$  NMR chemical shifts (in ppm) and the coupling constants (in Hertz) of complexes  $[\text{Rh}(\text{acac})(\text{L})]$  and  $[\text{Rh}(\text{acac})(\text{CO})(\text{L})]$  are summarised in Table 2.10. The  $[\text{Rh}(\text{acac})(\text{L})]$  complexes showed chemical shifts in the range 140 to 147 ppm with  $^1J_{\text{Rh-P}}$  coupling constants around 300 Hz. The bidentate  $[\text{Rh}(\text{acac})(\text{CO})(\text{L})]$  species showed doublets between 133.71 and 137.97 ppm with  $^1J_{\text{Rh-P}}$  coupling constants around 295 Hz; when the ligand coordinates in a monodentate fashion we detected a singlet between 141.72 and 146.76 ppm, near the signal of the free ligand, and a doublet between 135.47 and 137.76 ppm with  $^1J_{\text{Rh-P}}$  coupling constants around 295 Hz.



**Table 2.10.**  $^{31}\text{P}\{^1\text{H}\}$  NMR data for  $[\text{Rh}(\text{acac})(\text{L})]$  and  $[\text{Rh}(\text{acac})(\text{CO})(\text{L})]$  complexes<sup>a</sup>

Ligand	$[\text{Rh}(\text{acac})(\text{L})]^{\text{b}}$		$[\text{Rh}(\text{acac})(\text{CO})(\text{L})]^{\text{b}}$	
	$\delta(^{31}\text{P})^{\text{b}}$	$^1J_{\text{Rh-P}}^{\text{c}}$	$\delta(^{31}\text{P})^{\text{b}}$	$^1J_{\text{Rh-P}}^{\text{c}}$
<b>74a</b>	140.78 (d)	301.4	-	-
<b>74b</b>	141.29 (d)	300.3	-	-
<b>74'a</b>	141.14 (d)	299.5	133.71 (d) 141.72 (s), 135.47 (d)	296.3 293.9
<b>75a</b>	-	-	137.86 (d) 142.16 (s), 136.34 (d)	299.13 290.75
<b>75'a</b>	141.55 (d)	300.1	146.76 (s), 137.70 (d)	291.60
<b>76a</b>	147.12 (d)	294.1	137.97 (d) 143.82(s), 137.76 (d)	295.85 294.12

<sup>a</sup>Prepared in toluene- $d_8$  by adding 1.1 equivalents of ligand to  $[\text{Rh}(\text{acac})(\text{CO})_2]$  solution. <sup>b</sup> $^{31}\text{P}$  and  $^1\text{H}$  NMR spectra recorded in toluene- $d_8$  using High-pressure NMR. Chemicals shifts  $\delta$  in ppm multiplicity) <sup>c</sup> Coupling constants in Hz.

Table 2.11 shows selected data obtained for the  $[\text{RhH}(\text{CO})_2(\text{L})]$  (L:**74–76**) complexes, which showed somewhat broadened doublets at room temperature in the  $^{31}\text{P}\{^1\text{H}\}$  NMR spectra. These broad signals suggest a fluxional process on the NMR time scale.<sup>[33]</sup> The doublets appeared between 152.70 and 158.09 ppm showing a  $^1J_{\text{Rh-P}}$  coupling constants in the range 230.0 to 234.1 Hz. These large  $^1J_{\text{Rh-P}}$  coupling constants indicate that the ligands coordinate in an equatorial-equatorial fashion in the trigonal-bipyramidal hydridorhodiumcarbonyl species.<sup>[14, 47, 48, 54]</sup> In the  $^1\text{H}$  NMR spectrum we detected the signal for the hydride around  $-10$  ppm. The  $^1J_{\text{Rh-H}}$  coupling constants were in the range of 2.0 to 3.8 Hz and the  $^2J_{\text{P-H}}$  coupling constants were between 2.0 and 9.0 Hz. These small phosphorus-hydrogen coupling constants ( $<10\text{Hz}$ ) mean that the hydride signal appears as a quadruplet in most cases, except for the complex with ligand **74a** where the really small coupling constants revealed a broad signal, and for the complex with ligand **76a** where a double triplet was observed in the hydride region. This confirms the a *cis* relationship between the phosphorus and the hydrogen atom bonded to the rhodium. Large  $^1J_{\text{Rh-P}}$  coupling constants around 235 Hz, and small  $^2J_{\text{P-H}}$  coupling

constants have been reported for diphosphite ligands which coordinate in an equatorial-equatorial fashion in the hydridorhodium species.<sup>[14, 47, 48, 54]</sup>

**Table 2.11.** Selected <sup>1</sup>H and <sup>31</sup>P{<sup>1</sup>H} NMR data for [RhH(CO)<sub>2</sub>(L)] complexes<sup>a</sup>

Ligand	δ( <sup>31</sup> P) <sup>b</sup>	δ( <sup>1</sup> H) <sup>b</sup>	<sup>1</sup> J <sub>Rh-P</sub> <sup>c</sup>	<sup>1</sup> J <sub>Rh-H</sub> <sup>c</sup>	<sup>2</sup> J <sub>P-H</sub> <sup>c</sup>
<b>74a</b>	152.70 (d)	-9.93 (br t)	231.9	2.0	2.0
<b>74b</b>	155.33 (d)	-9.91 (q)	230.0	3.4	3.9
<b>74'a</b>	155.43 (d)	-10.14 (q)	231.6	2.7	3.8
<b>75a</b>	158.09 (d)	-9.85 (q)	233.6	2.9	3.1
<b>75'a</b>	155.27 (d)	-10.05 (q)	234.1	3.8	3.9
<b>76a</b>	156.40 (d)	-10.24 (dt)	232.6	3.4	9.0

<sup>a</sup>Prepared in toluene-d<sub>8</sub> by adding 1.1 equivalents of ligand to [Rh(acac)(CO)<sub>2</sub>] solution, 15 h. at 80°C and 20 bar of syn gas. <sup>b</sup><sup>31</sup>P and <sup>1</sup>H NMR spectra recorded in toluene-d<sub>8</sub> using High-pressure NMR. Chemicals shifts δ in ppm (multiplicity) <sup>c</sup> Coupling constants in Hz.

### Low temperature studies

As a consequence of the C<sub>2</sub>-symmetry, phosphorus atoms are equivalent in the free ligand. However, this is not the case in hydridorhodiumcarbonyl diphosphite complexes, because even when both phosphorus atoms are coordinated in an equatorial-equatorial fashion to the rhodium the complex has C<sub>1</sub>-symmetry. The fact that only one doublet is observed in the <sup>31</sup>P{<sup>1</sup>H} NMR spectrum, means that either the chemical shifts of both atoms accidentally coincide or that they exchange rapidly on the NMR time scale.<sup>[14, 47, 48, 54]</sup> We studied the hydridorhodiumcarbonyl species at low temperature under hydroformylation conditions. Table 2.12 summarizes selected <sup>1</sup>H and <sup>31</sup>P{<sup>1</sup>H} NMR data for [RhH(CO)<sub>2</sub>(L)] complexes at low temperature.

We detected that the behaviour of these species strongly depends on the structure of the diphosphite ligands. Complexes [RhH(CO)<sub>2</sub>(L)] where L: **74a**, **74b** and **74'a**, derived from 2,5-anhydro-D-mannitol, showed the same behaviour. When the

temperature decreased we observed line broadening in the  $^{31}\text{P}\{^1\text{H}\}$  NMR and in the hydride region of the  $^1\text{H}$  NMR. The signals of the  $^{31}\text{P}\{^1\text{H}\}$  NMR for complexes  $[\text{RhH}(\text{CO})_2(\text{L})]$ , where L: **74a** and **74'a**, were resolved at  $-100^\circ\text{C}$  (see Figure 2.39d). We observed two double doublets in the  $^{31}\text{P}\{^1\text{H}\}$  NMR spectrum: one signal appeared around 160 ppm, and the other around 150 ppm. The coupling constants,  $^1J_{\text{Rh-P1}}$  around 270 Hz and  $^1J_{\text{Rh-P2}}$  around 230 Hz, and  $^2J_{\text{P-P}}$  around 300 Hz, indicated that the ligand was coordinated in an equatorial-equatorial fashion to the complex. The hydride region in the  $^1\text{H}$  NMR spectrum was not resolved showing a line broadening at this temperature.

**Table 2.12.** Selected  $^1\text{H}$  and  $^{31}\text{P}\{^1\text{H}\}$  NMR data for  $[\text{RhH}(\text{CO})_2(\text{L})]$  complexes at low temperature<sup>a</sup>

Ligand	$\delta(^{31}\text{P})^b$		$^1J_{\text{Rh-P1}}^c$	$^1J_{\text{Rh-P2}}^c$	$^2J_{\text{P-P}}^c$	T/ $^\circ\text{C}$
<b>74a</b>	161.56 (dd)	148.21 (dd)	270.9	230.2	302.2	-100
<b>74b</b>	153.92 (broad)		Unresolved			-80
<b>74'a</b>	164.42 (dd)	153.62 (dd)	269.3	232.6	305.1	-100
<b>75a</b>	160.30 (dd)	156.75 (dd)	230.1	240.4	314.2	-80
<b>75'a</b>	157.49 (broad d)		238.6		-	-100
<b>76a</b>	158.68 (broad d)		233.5		-	-80

<sup>a</sup>Prepared in toluene- $d_8$  by adding 1.1 equivalents of ligand to  $[\text{Rh}(\text{acac})(\text{CO})_2]$  solution, 15 h. at  $80^\circ\text{C}$  and 20 bar of syn gas. <sup>b</sup> $^{31}\text{P}$  and  $^1\text{H}$  NMR spectra recorded in toluene  $d_8$  using High-pressure NMR. Chemicals shifts  $\delta$  in ppm (multiplicity) <sup>c</sup> Coupling constants in Hz.

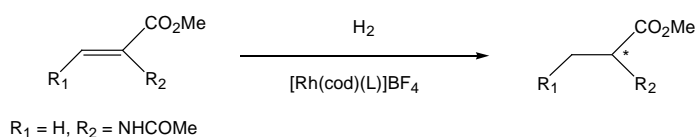
For the  $[\text{RhH}(\text{CO})_2(\mathbf{75a})]$  complex, where diphosphite ligand **75a** is derived from 2,5-anhydro-L-*iditol*, the decrease in the temperature also led to line broadening in the  $^{31}\text{P}\{^1\text{H}\}$  NMR and the hydride region on the  $^1\text{H}$  NMR. The  $^{31}\text{P}\{^1\text{H}\}$  NMR was resolved at  $-80^\circ\text{C}$ , we observed an eight-line spectrum for phosphorus atoms. These was due to an ABX system where  $^1J_{\text{Rh-P1}}$  and  $^1J_{\text{Rh-P2}}$  were very close, 230 and 240 Hz, and the signals appeared at 160.30 and 156.75 ppm with a phosphorus-phosphorus coupling constant of 314.2 Hz (see Figure 2.40c). These coupling constants indicated an equatorial-equatorial coordination mode.

In the variable temperature study of the hydridorhodiumdicarbonyl complexes with ligands **75'a** and **76a** we observed only a slight broadening of the doublet at  $-80^{\circ}\text{C}$  (Figure 2.41d). This indicates that the fluxional process at this temperature does not halt completely, which indicates a lower-energy-barrier in this process than the ligands **74a**, **74b**, **74'a** and **75a**.

These new carbohydrate derivative ligands **74-76** were expected to show an equatorial-axial coordination mode in the trigonal bipyramidal hydridorhodium dicarbonyl species since they form a seven-membered chelate ring when they coordinate to the rhodium, as usual as observed in ligands which form seven-membered rings coordinate mainly in **ea** fashion.<sup>[47, 48, 120]</sup> However, this is not the case for ligands **74-76**, which coordinate in an **ee** fashion (corroborated by large  $^1J_{\text{Rh-P}}$  and  $^2J_{\text{P-P}}$  coupling constants and small  $^2J_{\text{P-H}}$  coupling constants, observed in the NMR spectrum). This behaviour may be due to the rigidity of the ligands, and the presence of the tetrahydrofuran backbone could favour this coordination. A reported ligand derived from *N*-benzyltartarimide,<sup>[47]</sup> which forms a seven-membered ring when it coordinates to the rhodium and has a backbone composed by five-membered ring (diphosphite **18a**, see Figure 2.5), also coordinates in an equatorial-equatorial mode. Even when the ligands coordinated in an equatorial-equatorial mode, the enantioselectivities obtained with these ligands in asymmetric the hydroformylation reaction were moderate or low.<sup>[47]</sup>

### 2.2.5 Rhodium-catalysed hydrogenation of methyl acetamidoacrylate

In order to know how complexes  $[\text{Rh}(\text{cod})(\text{L})]\text{BF}_4$  **90-92** behave in asymmetric hydrogenation, we tested them as catalyst precursors in the hydrogenation of methyl acetamidoacrylate in a multireactor (Scheme 2.12). The results are summarised in Table 2.13.



**Scheme 2.12.** Hydrogenation of methyl acetamidoacrylate with  $[\text{Rh}(\text{cod})(\text{L})]\text{BF}_4$  catalytic system

Table 2.13 summarizes the results obtained in the hydrogenation of methyl acetamidoacrylate with [Rh(cod)(L)]BF<sub>4</sub> complexes **90-92** using dichloromethane or dichloromethane/methanol (2/1) as a solvent, rhodium/substrate ratio=100 at 10 bar of H<sub>2</sub> pressure and at room temperature. We also decided to use a mixture of dichloromethane and methanol as the solvent in order to improve the activity and selectivity of the system, since in Rh/diphosphite asymmetric hydrogenation it was observed that these solvents improve the results.<sup>[35, 56, 109]</sup>

**Table 2.13.** Hydrogenation of methyl acetamidoacrylate with [Rh(L)(cod)]BF<sub>4</sub> complexes **90-92**<sup>a</sup>

Entry	Ligand	solvent	conv. (%)	TOF (h <sup>-1</sup> )	% ee
1	<b>74a</b>	CH <sub>2</sub> Cl <sub>2</sub>	7	0.5	0
2	<b>74a</b> <sup>b</sup>	CH <sub>2</sub> Cl <sub>2</sub>	61	4.1	10 (R)
3	<b>74a</b>	CH <sub>2</sub> Cl <sub>2</sub> /CH <sub>3</sub> OH	41	2.7	45 (R)
4	<b>74b</b>	CH <sub>2</sub> Cl <sub>2</sub>	6	0.4	8 (R)
5	<b>74c</b>	CH <sub>2</sub> Cl <sub>2</sub>	>99	-	57 (R)
6	<b>74c</b>	CH <sub>2</sub> Cl <sub>2</sub> /CH <sub>3</sub> OH	21	1.4	0
7	<b>74'a</b>	CH <sub>2</sub> Cl <sub>2</sub>	21	1.4	16 (R)
8	<b>74'a</b> <sup>b</sup>	CH <sub>2</sub> Cl <sub>2</sub>	59	3.9	19 (R)
9	<b>74'a</b>	CH <sub>2</sub> Cl <sub>2</sub> /CH <sub>3</sub> OH	24	1.6	3 (R)
10	<b>74'b</b>	CH <sub>2</sub> Cl <sub>2</sub>	74	4.9	34 (R)
11	<b>74'b</b>	CH <sub>2</sub> Cl <sub>2</sub> /CH <sub>3</sub> OH	20	1.3	11 (R)
12	<b>75a</b>	CH <sub>2</sub> Cl <sub>2</sub>	81	5.4	0
13	<b>75a</b>	CH <sub>2</sub> Cl <sub>2</sub> /CH <sub>3</sub> OH	16	1.1	3 (S)
14	<b>75'a</b>	CH <sub>2</sub> Cl <sub>2</sub>	20	1.3	6 (S)
15	<b>75'a</b>	CH <sub>2</sub> Cl <sub>2</sub> /CH <sub>3</sub> OH	21	1.4	0
16	<b>76a</b>	CH <sub>2</sub> Cl <sub>2</sub>	26	1.7	13 (R)
17	<b>76a</b>	CH <sub>2</sub> Cl <sub>2</sub> /CH <sub>3</sub> OH	29	1.9	7 (R)
18	<b>76b</b>	CH <sub>2</sub> Cl <sub>2</sub>	17	1.1	6 (R)
19	<b>76b</b>	CH <sub>2</sub> Cl <sub>2</sub> /CH <sub>3</sub> OH	38	2.5	0

<sup>a</sup>Conditions: 2.5 ml, Rh: 2.5x10<sup>-6</sup> mol, Rh/substrate: 1/100, room temperature, P(H<sub>2</sub>): 10 bar.

<sup>b</sup>Conditions: 5 ml, Rh: 5x10<sup>-6</sup> mol, Rh/substrate: 1/100, room temperature, P(H<sub>2</sub>): 50 bar.

Activities were low for all the complexes tested, and a reaction time of at least 15 h was required to attain full conversion in the best cases. The most active catalytic system was the one with ligand **74c** (Table 2.13, entry 5). The enantioselectivities

were also poor, and results were also best with the catalytic system  $[\text{Rh}(\text{cod})(\mathbf{74c})]\text{BF}_4$ . Ligand **74c** has no substituents in the biphenyl moieties, and this may explain the higher activity of the catalytic system containing this ligand. The enantiomeric excesses obtained show that substitution in the biphenyl moieties has a negative effect on the enantioselectivity. This has previously been observed for related xylose derivatives with bulky diphosphites.<sup>[121]</sup>

The results depend on the solvent used, and were very different in some cases depending on whether the solvent was dichloromethane or a dichloromethane/methanol mixture. When the dichloromethane/methanol mixture was used the  $[\text{Rh}(\text{cod})(\mathbf{74c})]\text{BF}_4$  system provided the racemic mixture, while in dichloromethane the enantioselectivity was 57% (Table 2.13, entries 5, 6). A similar tendency was observed for ligand **74'b**. However, when ligand **74a** was used the enantioselectivity increased significantly in this mixture of solvents (Table 2.13, entries 1, 3). With ligands **74a**, **75a**, **75'a**, **76a** and **76b** the effect was not important or was slightly negative. However, the conversion was generally lower in dichloromethane/methanol than in dichloromethane, with the exception of  $[\text{Rh}(\text{cod})(\mathbf{74a})]\text{BF}_4$ , which may be due to the instability of the ligands in methanol. An increase in hydrogen pressure enhanced the conversion but had a little effect on the enantioselectivity (Table 2.13, entries 2 and 8 vs. 1 and 7).

As far as the influence of the substituents at positions 2 and 5 is concerned,  $[\text{Rh}(\text{cod})(\text{L})]\text{BF}_4$  complexes with ligands **74** gave better results than with ligands **75** and **76**. The major enantiomer, when the enantiomeric excesses were substantial, was always *R*.

The previously described diphosphinite ligands, with the same furanoside backbone (Figure 2.25),<sup>[107]</sup> showed very high activities (total conversion in 5 minutes at 1 bar of  $\text{H}_2$  pressure and room temperature) in the asymmetric hydrogenation of methyl acetamido acrylate, whereas the related diphosphite ligands **74-76** showed lower activities in more drastic conditions (10 bar of pressure and room temperature). This may be due to the greater steric hindrance of the diphosphite ligands (ligand **74c**, without substituents in the biphenyl moieties, showed higher activities than the rest of the related diphosphites) and also to the fact that the

diphosphite ligands are less basic than the diphosphinite ligands, since greater basicity favours the oxidative addition of hydrogen which is the rate- and enantioselective determining step of this reaction. On the other hand, in all cases the enantioselectivity of the Rh/diphosphite systems was much lower than the corresponding Rh/diphosphinite system.

### 2.3 Conclusions

New diphosphite ligands (**74-76**) with  $C_2$ -symmetry and a tetrahydrofuran backbone have been synthesised in moderate to good yields starting from D-glucosamine, D-glucitol and (2*S*,3*S*)-diethyl tartrate. Rhodium cationic complexes containing diphosphite ligands of general formula  $[\text{Rh}(\text{cod})(\text{L})]\text{BF}_4$ , (L= **74a-c**, **74'a,b**, **75a**, **75'a** and **76a-b**) were prepared by reacting  $[\text{Rh}(\text{cod})_2]\text{BF}_4$  with the respective ligands. Monocrystals of diphosphite ligand **74a** and rhodium cationic complexes  $[\text{Rh}(\text{cod})(\text{74a})]\text{BF}_4$  **90a** and  $[\text{Rh}(\text{cod})(\text{75'a})]\text{BF}_4$  **91'a**, suitable for X-ray diffraction were obtained. The structure of **74a**, **90a** and **91'a** could be proved unambiguously by single crystal X-ray diffraction.

This new family of diphosphite ligands has been applied to the rhodium-catalysed asymmetric hydroformylation of styrene and related substituted vinyl arenes. High regioselectivities to the branched aldehyde and moderate enantioselectivities were obtained. The configuration and substitution of the remote stereocenters at positions 2 and 5 of the tetrahydrofuran ring were observed to have a considerable influence on the enantioselectivity. The most significant result is that the configuration of the major isomer obtained in the hydroformylation reaction can be controlled by changing the configuration of these stereocenters.

The intermediate species in hydroformylation with diphosphite ligands **74a**, **74b**, **74'a**, **75a**, **75'a** and **76a** were studied by high pressure-NMR spectroscopy. These species were prepared *in situ* under hydroformylation conditions, observing that the formation of the hydridorhodiumcarbonyl specie was very slow. The small  $^2J_{\text{P-H}}$  coupling constants (2.0 to 9.0 Hz) and the large  $^1J_{\text{Rh-P}}$  coupling constants (230.0 to 234.1 Hz) indicate that the ligands coordinate in an equatorial-equatorial fashion in the trigonal-bypyramidal hydridorhodiumcarbonyl species. The low temperature

study of the hydridorhodiumcarbonyl species under hydroformylation conditions detected that the phosphorous atoms were non equivalent, which proved the  $C_1$ -symmetry of these complexes.

Rhodium complexes were tested in the asymmetric hydrogenation of methyl acetamidoacrylate. The conversions and the enantioselectivities were low and mainly influenced by the substitution in the biphenyl moiety and by the configuration of the remote centres at positions 2 and 5 of the tetrahydrofuran ring.

## 2.4 Experimental section

### General methods

All syntheses were performed by using standard Schlenk techniques under argon atmosphere. Solvents were purified by standard procedures. Compounds **78-80**, **82-86**, **88** and **89** <sup>[107]</sup> and phosphorochloridites <sup>[46, 114]</sup> were prepared by methods described previously. All other reagents were used as commercially available. Elemental analyses were performed on a Carlo Erba EA-1108 instrument. <sup>1</sup>H, <sup>13</sup>C{<sup>1</sup>H} and <sup>31</sup>P{<sup>1</sup>H} NMR spectra were recorded on a Varian Gemini 400 MHz spectrometer. Chemical shifts are relative to SiMe<sub>4</sub> (<sup>1</sup>H and <sup>13</sup>C) as internal standard or H<sub>3</sub>PO<sub>4</sub> (<sup>31</sup>P) as external standard. All NMR spectral assignments were determined by COSY and HSQC spectra. Gas chromatographic analyses were run on a Hewlett-Packard HP 5890A instrument (split/splitless injector, J&W Scientific, HP-5, 25 m column, internal diameter 0.25 mm, film thickness 0.33 mm, carrier gas: 150 kPa He, F.I.D. detector) equipped with a Hewlett-Packard HP3396 series II integrator. Hydroformylation reactions were carried out in a Berghof 100 ml stainless steel autoclave. Enantiomeric excesses of hydroformylation reaction were measured after oxidation of the aldehydes to the corresponding carboxylic acids on a Hewlett-Packard HP 5890A gas chromatograph (split/splitless injector, J&W Scientific, FS-Cyclodex β-I/P 50 m column, internal diameter 0.2 mm, film thickness 0.33 mm, carrier gas: 100 kPa He, F.I.D. detector). Absolute configuration was determined by comparing of retention times with optically pure (S)-(+)-2-phenylpropionic and (R)-(-)-2-phenylpropionic acids. Hydrogenation reactions were carried out in a Parr 450 ml multiple reaction vessel autoclave.



Conversion and enantiomeric excesses of the reaction crude were measured on a Hewlett-Packard HP 5890A gas chromatograph (split/splitless injector, J&W Scientific, Permabond L-Chirasil-Val, 25 m. column, internal diameter 0.25 mm., carrier gas: 100 kPa He, F.I.D. detector).

Crystal structure determination was carried out using a Bruker-Nonius diffractometer equipped with a APPEX 2 4K CCD area detector, a FR591 rotating anode with Mo<sub>K $\alpha$</sub>  radiation, Montel mirrors as monochromator and a Kryoflex low temperature device (T = 100 K). Fullsphere data collection omega and phi scans. Programs used: Data collection Apex2 V. 1.0-22 (Bruker-Nonius 2004), data reduction Saint + Version 6.22 (Bruker-Nonius 2001) and absorption correction SADABS V. 2.10 (2003). Crystal structure solution was achieved using direct methods as implemented in SHELXTL Version 6.10 (Sheldrick, Universität Göttingen (Germany), 2000) and visualized using XP program. Missing atoms were subsequently located from difference Fourier synthesis and added to the atom list. Least-squares refinement on F<sup>2</sup> using all measured intensities was carried out using the program SHELXTL Version 6.10 (Sheldrick, Universität Göttingen (Germany), 2000). All non hydrogen atoms were refined including anisotropic displacement parameters.

### **Synthesis of the ligands**

#### **General procedure for synthesizing diphosphites from the corresponding diols.** <sup>[107]</sup>

To a solution of the diol (0.5 mmol), which is previously azeotropically dried with toluene (3x1 ml), in dry and degassed toluene (5 ml) was added dry pyridine (2.0 mmol). After the mixture was cooled to 0 °C was slowly added to a solution of phosphorochloridite (2.2 mmol), synthesised *in situ* by standard procedure,<sup>[46, 114]</sup> in dry and degassed toluene (6 ml) and dry pyridine (2.2 mmol). The mixture was allowed to rise room temperature and stirred overnight. The mixture was then

filtered to eliminate the pyridine salts, and the filtrate was concentrated to dryness. The white foam was purified by chromatographic techniques.

**3,4-Bis-O-[(3,3',5,5'-tetra-*tert*-butyl-1,1'-biphenyl-2,2'-diyl)phosphite]-1,6-di-O-(*tert*-butyl-diphenylsilyl)-2,5-anhydro-D-mannitol (74a)**

The synthesis of **74a** was carried out in accordance with the general procedure from 0.3 g (0.47 mmol) of diol **80** in 5 ml of dry and degassed toluene and 0.2 ml (2.4 mmol) of dry pyridine. This solution was slowly added to a solution of 2.1 mmol of the corresponding phosphorochlorhydrite formed *in situ*, dissolved in 6 ml of toluene and 0.2 ml (2.4 mmol) of pyridine. The mixture was stirred overnight, the salts were filtered and the white foam was purified by flash column chromatography (eluent: toluene R<sub>f</sub>=0.9) to afford 0.22 g (31 %) of **74a** as a white solid.  $[\alpha]_D^{25} +76.72^\circ$  (CH<sub>2</sub>Cl<sub>2</sub>, *c* 1.005); <sup>1</sup>H NMR (CDCl<sub>3</sub>, 400 MHz)  $\delta$  7.64-7.00 (m, 28H, aromatic), 5.20 (s broad, 2H, H3), 3.96 (s broad, 2H, H2), 3.60 (m, 2H, H1), 3.38 (m, 2H, H1'), 1.43 (s, 18H, *o*-C(CH<sub>3</sub>)<sub>3</sub>), 1.37 (s, 18H, *p*-C(CH<sub>3</sub>)<sub>3</sub>'), 1.35 (s, 18H, *p*-C(CH<sub>3</sub>)<sub>3</sub>), 1.20 (s, 18H, *o*-C(CH<sub>3</sub>)<sub>3</sub>'), 0.93 (s, 18H, C(CH<sub>3</sub>)<sub>3</sub>); <sup>13</sup>C NMR (CDCl<sub>3</sub>, 100.6 MHz)  $\delta$  146.30-124.1 (aromatic), 82.5 (C2), 79.5 (broad, C3), 62.5 (C1), 35.4 (*o*-C(CH<sub>3</sub>)<sub>3</sub>), 35.3 (*o*-C(CH<sub>3</sub>)<sub>3</sub>'), 34.7 (*p*-C(CH<sub>3</sub>)<sub>3</sub>), 34.5 (*p*-C(CH<sub>3</sub>)<sub>3</sub>'), 31.6 (*o*-C(CH<sub>3</sub>)<sub>3</sub>), 31.4 (*p*-C(CH<sub>3</sub>)<sub>3</sub>), 31.3 (*o*-C(CH<sub>3</sub>)<sub>3</sub>'), 26.7 (C(CH<sub>3</sub>)<sub>3</sub>), 19.2 (C(CH<sub>3</sub>)<sub>3</sub>); <sup>31</sup>P NMR (CDCl<sub>3</sub>, 161.97 MHz)  $\delta$  143.85 (s). Anal. Calcd. for C<sub>94</sub>H<sub>126</sub>O<sub>9</sub>P<sub>2</sub>Si<sub>2</sub>: C, 74.37; H, 8.37. Found: C, 74.27; H, 9.16.

**74a. X-ray Crystallography.**

Crystals of **74a** were obtained by slow diffusion of hexane into a solution of **74a** in dichloromethane. Empirical formula: C<sub>42.40</sub> H<sub>61.60</sub> O<sub>3.80</sub> P<sub>0.80</sub> Si<sub>0.80</sub>, Formula weight: 679.36, Temperature: 100(2) K, Wavelength: 0.71073 Å, Crystal system: Monoclinic, Space group: *P*2<sub>1</sub>, Unit cell dimensions: *a*=14.6938(11) Å, *a*=90°, *b*=24.842(2) Å, *b*=109.112(2)°, *c*=15.0146(12) Å, *g*=90°, Volume: 5178.6(7) Å<sup>3</sup>, *Z*:5, Density (calculated): 1.089 Mg/m<sup>3</sup>, Absorption coefficient: 0.118 mm<sup>-1</sup>, *F*(000): 1848, Crystal size: 0.40 x 0.40 x 0.40 mm<sup>3</sup>, Theta range for data collection: 2.81 to 36.88°, Index ranges: -24 ≤ *h* ≤ 23, -41 ≤ *k* ≤ 41, -13 ≤ *l* ≤ 25,

Reflections collected: 86383, Independent reflections: 46995 [R(int) = 0.0401], Completeness to theta = 36.88°: 96.3 % , Absorption correction: SADABS (Bruker-Nonius), Refinement method: Full-matrix least-squares on F<sup>2</sup>, Data / restraints / parameters: 46995 / 1 / 1125, Goodness-of-fit on F<sup>2</sup>: 1.018, Final R indices [I > 2σ(I)]: R1 = 0.0719, wR2 = 0.2001, R indices (all data): R1 = 0.0933, wR2 = 0.2190, Absolute structure parameter: 0.16(5), Largest diff. peak and hole: 1.050 and -0.584 e.Å<sup>-3</sup>

The ligand crystallizes as a solvate with two molecules of n-hexane in the elementary cell. The measured compound crystallizes as a racemic twin (74:16). Selected bond distances and angles are given in Table 1 and 2 of the appendix.

**3,4-Bis-O-[(3,3'-di-*tert*-butyl-,5,5'-dimethoxy-1,1'-biphenyl-2,2'-diyl)phosphite]-1,6-di-O-(*tert*-butyl-diphenylsilyl)-2,5-anhydro-D-mannitol (74b)**

The synthesis of **74b** was carried out in accordance with the general procedure from 0.3 g (0.47 mmol) of diol **80** in 5 ml of dry and degassed toluene and 0.2 ml (2.4 mmol) of dry pyridine. This solution was slowly added to a solution of 2.1 mmol of the corresponding phosphorochlorhydrite formed *in situ*, dissolved in 6 ml of toluene and 0.2 ml (2.4 mmol) of pyridine. The mixture was stirred overnight, the salts were filtered and the white foam was purified by flash column chromatography (eluent: toluene R<sub>f</sub>=0.75) to afford 0.28 g (42 %) of **74b** as a white solid. [α]<sub>D</sub><sup>25</sup> +58.71° (CH<sub>2</sub>Cl<sub>2</sub>, c 0.402); <sup>1</sup>H NMR (CDCl<sub>3</sub>, 400 MHz) δ 7.65-6.58 (m, 28H, aromatic), 5.14 (broad, 2H, H3), 4.05 (m broad, 2H, H2), 3.81 (s, 6H, *p*-OCH<sub>3</sub>'), 3.74 (s, 6H, *p*-OCH<sub>3</sub>), 3.67 (m, 2H, H1), 3.53 (m, 2H, H1'), 1.42 (s, 18H, *o*-C(CH<sub>3</sub>)<sub>3</sub>'), 1.35 (s, 18H, *o*-C(CH<sub>3</sub>)<sub>3</sub>), 0.98 (s, 18H, C(CH<sub>3</sub>)<sub>3</sub>). <sup>13</sup>C NMR (CDCl<sub>3</sub>, 100.6 MHz) δ 155.5-112.6 (aromatic), 82.9 (C2), 79.6 (broad C3), 62.7 (C1), 55.5 (*p*-OCH<sub>3</sub>'), 55.4 (*p*-OCH<sub>3</sub>), 35.7 (*o*-C(CH<sub>3</sub>)<sub>3</sub>'), 35.6 (*o*-C(CH<sub>3</sub>)<sub>3</sub>), 31.5 (*o*-C(CH<sub>3</sub>)<sub>3</sub>'), 31.3 (*o*-C(CH<sub>3</sub>)<sub>3</sub>), 27.5 (C(CH<sub>3</sub>)<sub>3</sub>), 19.5 (C(CH<sub>3</sub>)<sub>3</sub>); <sup>31</sup>P NMR (CDCl<sub>3</sub>, 161.97 MHz) δ 144.54 (s). Anal. Calcd. for C<sub>82</sub>H<sub>102</sub>O<sub>13</sub>P<sub>2</sub>Si<sub>2</sub>: C, 69.66; H, 7.27. Found: C, 69.30; H, 7.96.

**3,4-Bis-O-[(1,1'-biphenyl-2,2'-diyl)phosphite]-1,6-di-O-(tert-butyl-diphenylsilyl)-2,5-anhydro-D-mannitol (74c)**

The synthesis of **74c** was carried out in accordance with the general procedure from 0.25 g (0.40 mmol) of diol **80** in 2.5 ml of dry and degassed toluene and 0.1 ml (1.6 mmol) of dry pyridine. This solution was slowly added to a solution of 1.6 mmol of the corresponding phosphorochlorhydrite formed *in situ*, dissolved in 4 ml of toluene and 0.1 ml (1.6 mmol) of pyridine. The mixture was stirred overnight, the salts were filtered and the white foam was purified by flash column chromatography (eluent: hexane/ethyl acetate 100:2 Rf=0.6) to afford 0.21 g (50 %) of **74b** as a white solid.  $[\alpha]_D^{25} +0.61^\circ$  (CH<sub>2</sub>Cl<sub>2</sub>, c 0.330); <sup>1</sup>H NMR (CDCl<sub>3</sub>, 400 MHz) δ 7.66-7.06 (m, 28H, aromatic), 5.16 (m broad, 2H, H3), 4.13 (m broad, 2H, H2), 3.76 (m, 2H, H1), 3.72 (m, 2H, H1'), 0.99 (s, 18H, C(CH<sub>3</sub>)<sub>3</sub>); <sup>13</sup>C NMR (CDCl<sub>3</sub>, 100.6 MHz) δ 146.7-121.3 (aromatic), 83.4 (C2), 79.9 (broad C3), 63.1 (C1), 27.0 (C(CH<sub>3</sub>)<sub>3</sub>), 19.5 (C(CH<sub>3</sub>)<sub>3</sub>) <sup>31</sup>P NMR (CDCl<sub>3</sub>, 161.97 MHz) δ 146.70 (s). Anal. Calcd. for C<sub>62</sub>H<sub>62</sub>O<sub>9</sub>P<sub>2</sub>Si<sub>2</sub>: C, 69.64; H, 5.84. Found: C, 69.44; H, 6.01.

**3,4-Bis-O-[(3,3',5,5'-tetra-tert-butyl-1,1'-biphenyl-2,2'-diyl)phosphite]-1,6-dideoxy-2,5-anhydro-D-mannitol (74'a)**

The synthesis of **74'a** was carried out in accordance with the general procedure from 0.15 g (1.14 mmol) of diol **80'** in 10 ml of dry and degassed toluene and 0.5 ml (5.7 mmol) of dry pyridine. This solution was slowly added to a solution of 4.6 mmol of the corresponding phosphorochlorhydrite formed *in situ*, dissolved in 12 ml of toluene and 0.5 ml (5.7 mmol) of pyridine. The mixture was stirred overnight, the salts were filtered and the white foam was purified by flash column chromatography (eluent: toluene Rf=0.9) to afford 0.84 g (72 %) of **74'a** as a white solid.  $[\alpha]_D^{25} +65.81^\circ$  (CH<sub>2</sub>Cl<sub>2</sub>, c 1.006); <sup>1</sup>H NMR (CDCl<sub>3</sub>, 400 MHz) δ 7.41 (m, 4H, aromatic), 7.15 (m, 4H, aromatic), 4.56 (m broad, 2H, H3), 4.07 (m, broad, 2H, H2), 1.46 (s, 18H, C(CH<sub>3</sub>)<sub>3</sub>'), 1.43 (s, 18H, C(CH<sub>3</sub>)<sub>3</sub>), 1.34 (s, 18H, C(CH<sub>3</sub>)<sub>3</sub>'), 1.33 (m, 18H, C(CH<sub>3</sub>)<sub>3</sub>') 1.06 (d, 6H, J<sub>1,2</sub> = 6.6 Hz, H1); <sup>13</sup>C NMR (CDCl<sub>3</sub>, 100.6 MHz) δ 146.5-124.2 (aromatic), 85.4 (broad C3), 79.5 (C2), 35.4 (o-C(CH<sub>3</sub>)<sub>3</sub>), 35.34 (o-C(CH<sub>3</sub>)<sub>3</sub>'), 34.6 (p-C(CH<sub>3</sub>)<sub>3</sub>), 34.6 (p-C(CH<sub>3</sub>)<sub>3</sub>'), 31.5 (o-C(CH<sub>3</sub>)<sub>3</sub>), 31.2 (o-

$C(\underline{C}H_3)_3$ '), 31.1 ( $p$ - $C(\underline{C}H_3)_3$ ), 18.5 ( $CH_3$ , C1)  $^{31}P$  NMR ( $CDCl_3$ , 161.97 MHz)  $\delta$  143.03 (s). Anal. Calcd. for  $C_{62}H_{90}O_7P_2$ : C, 73.78; H, 8.99. Found: C, 74.02; H, 8.98.

**3,4-Bis-O-[(3,3'-di-*tert*-butyl-,5,5'-dimethoxy-1,1'-biphenyl-2,2'-diyl)phosphite]-1,6-dideoxy-2,5-anhydro-D-mannitol (74'b)**

The synthesis of **74'b** was carried out in accordance with the general procedure from 0.15 g (1.14 mmol) of diol **80'** in 10 ml of dry and degassed toluene and 0.5 ml (5.7 mmol) of dry pyridine. This solution was slowly added to a solution of 4.6 mmol of the corresponding phosphorochlorhydrite formed *in situ*, dissolved in 12 ml of toluene and 0.5 ml (5.7 mmol) of pyridine. The mixture was stirred overnight, the salts were filtered and the white foam was purified by flash column chromatography (eluent: toluene  $R_f=0.9$ ) to afford 0.4 g (42 %) of **74'b** as a white solid.  $[\alpha]^{25}_D +20.39^\circ$  ( $CH_2Cl_2$ ,  $c$  0.466);  $^1H$  NMR ( $CDCl_3$ , 400 MHz)  $\delta$  7.08 (m, 4H, aromatic), 6.82 (m, 4, aromatic), 4.65 (m, 2H, H3), 4.31 (m, 2H, H2), 3.90 (s, 12H,  $p$ - $OCH_3$ ), 1.55 (s, 18H,  $o$ - $C(CH_3)_3$ '), 1.53 (s, 18H,  $o$ - $C(CH_3)_3$ ), 1.29 (d, 6H, ,  $J_{1,2} = 6.6$  Hz, H1);  $^{13}C$  NMR ( $CDCl_3$ , 100.6 MHz)  $\delta$  155.6-112.7 (aromatic), 85.4 (broad, C3), 79.9 (C2), 55.5 ( $p$ - $OCH_3$ '), 55.4 ( $p$ - $OCH_3$ ), 35.3 ( $o$ - $C(CH_3)_3$ ), 31.0 ( $o$ - $C(\underline{C}H_3)_3$ '), 30.8 ( $o$ - $C(\underline{C}H_3)_3$ ) 18.3 ( $CH_3$ , C1);  $^{31}P$  NMR ( $CDCl_3$ , 161.97 MHz)  $\delta$  142.45 (s). Anal. Calcd. for  $C_{50}H_{66}O_{11}P_2$ : C, 66.36; H, 7.35. Found: C, 66.49; H, 7.96.

**3,4-Bis-O-[(3,3',5,5'-tetra-*tert*-butyl-1,1'-biphenyl-2,2'-diyl)phosphite]-1,6-di-O-(*tert*-butyl-diphenylsilyl)-2,5-anhydro-L-iditol (75a)**

The synthesis of **75a** was carried out in accordance with the general procedure from 0.25 g (0.40 mmol) of diol **86** in 2.5 ml of dry and degassed toluene and 0.1 ml (1.6 mmol) of dry pyridine. This solution was slowly added to a solution of 1.6 mmol of the corresponding phosphorochlorhydrite formed *in situ*, dissolved in 4 ml of toluene and 0.1 ml (1.6 mmol) of pyridine. The mixture was stirred overnight, the salts were filtered and the white foam was purified by flash column chromatography (eluent: toluene  $R_f=0.9$ ) to afford 0.25 g (42 %) of **75a** as a white solid.  $[\alpha]^{25}_D -8.72^\circ$  ( $CH_2Cl_2$ ,  $c$  0.390);  $^1H$  NMR ( $CDCl_3$ , 400 MHz)  $\delta$  7.17-7.65 (m, 28H, aromatic), 5.07 (s broad, 2H, H3), 4.26 (m broad, 2H, H2), 3.85 (m, 2H, H1), 3.79 (m, 2H, H1'), 1.45 (s, 18H,  $o$ - $C(CH_3)_3$ ), 1.34 (s, 18H,  $o$ - $C(CH_3)_3$ ), 1.31 (s,

18H, *p*-C(CH<sub>3</sub>)<sub>3</sub>), 1.28 (s, 18H, *p*-C(CH<sub>3</sub>)<sub>3</sub>'), 0.96 (s, 18H, C(CH<sub>3</sub>)<sub>3</sub>); <sup>13</sup>C NMR (CDCl<sub>3</sub>, 100.6 MHz) δ 146.5-124.1 (aromatic), 79.7 (C2), 77.8 (broad, C3), 62.9 (C1), 35.4 (*o*-C(CH<sub>3</sub>)<sub>3</sub>'), 35.3 (*o*-C(CH<sub>3</sub>)<sub>3</sub>), 34.6 (*p*-C(CH<sub>3</sub>)<sub>3</sub>'), 34.6 (*p*-C(CH<sub>3</sub>)<sub>3</sub>), 31.5 (*o*-C(CH<sub>3</sub>)<sub>3</sub>'), 31.4 (*o*-C(CH<sub>3</sub>)<sub>3</sub>), 31.1 (*p*-C(CH<sub>3</sub>)<sub>3</sub>'), 31.1 (*p*-C(CH<sub>3</sub>)<sub>3</sub>), 26.8 (C(CH<sub>3</sub>)<sub>3</sub>), 19.2 (C(CH<sub>3</sub>)<sub>3</sub>); <sup>31</sup>P NMR (CDCl<sub>3</sub>, 161.97 MHz) δ 147.47 (s). Anal. Calcd. For C<sub>94</sub>H<sub>126</sub>O<sub>9</sub>P<sub>2</sub>Si<sub>2</sub>: C, 74.37; H, 8.37. Found: C, 74.56 ; H, 8.28.

**3,4-Bis-O-[(3,3'-di-*tert*-butyl-,5,5'-dimethoxy-1,1'-biphenyl-2,2'-diyl)phosphite]-1,6-di-O-(*tert*-butyl-diphenylsilyl)-2,5-anhydro-L-iditol (75b)**

The synthesis of **75b** was carried out in accordance with the general procedure from 0.25 g (0.40 mmol) of diol **86** in 4 ml of dry and degassed toluene and 0.1 ml (1.6 mmol) of dry pyridine. This solution was slowly added to a solution of 1.6 mmol of the corresponding phosphorochlorhydrite formed *in situ*, dissolved in 4 ml of toluene and 0.1 ml (1.6 mmol) of pyridine. The mixture was stirred overnight, the salts were filtered and the white foam was purified by flash column chromatography (eluent: toluene R<sub>f</sub>=0.6) to afford 0.18 g (32 %) of **75b** as a white solid. [α]<sub>D</sub><sup>25</sup> - 15.45° (CH<sub>2</sub>Cl<sub>2</sub>, c 1.100); <sup>1</sup>H NMR (CDCl<sub>3</sub>, 400 MHz) δ 7.83-6.85 (m, 28H, Ph), 5.14 (m broad, 2H, H3), 4.47 (m broad, 2H, H2), 4.00 (s, 6H, *p*-OCH<sub>3</sub>), 3.96 (s, 6H, *p*-OCH<sub>3</sub>'), 3.98 (m, 4H, H1, H1'), 1.62 (s, 18H, *o*-C(CH<sub>3</sub>)<sub>3</sub>), 1.50 (s, 18H, C(CH<sub>3</sub>)<sub>3</sub>'), 1.18 (s, 18H, C(CH<sub>3</sub>)<sub>3</sub>); <sup>13</sup>C NMR (CDCl<sub>3</sub>, 100.6 MHz) δ 155.9-112.9 (aromatic), 80.0 (C2), 77.7 (broad, C3), 62.7 (C1), 55.5 (*p*-OCH<sub>3</sub>), 55.4 (*p*-OCH<sub>3</sub>'), 35.3 (*o*-C(CH<sub>3</sub>)<sub>3</sub>), 35.3 (*o*-C(CH<sub>3</sub>)<sub>3</sub>'), 31.2 (*o*-C(CH<sub>3</sub>)<sub>3</sub>), 31.0 (*o*-C(CH<sub>3</sub>)<sub>3</sub>'), 26.0 (C(CH<sub>3</sub>)<sub>3</sub>), 19.2 (C(CH<sub>3</sub>)<sub>3</sub>); <sup>31</sup>P NMR (CDCl<sub>3</sub>, 161.97 MHz) δ 146.72 (s). Anal. Calcd. for C<sub>82</sub>H<sub>102</sub>O<sub>13</sub>P<sub>2</sub>Si<sub>2</sub>: C, 69.66; H, 7.27. Found: C, 69.15 ; H 7.91

**3,4-Bis-O-[(3,3',5,5'-tetra-*tert*-butyl-1,1'-biphenyl-2,2'-diyl)phosphite]-1,6-dideoxy-2,5-anhydro-L-iditol (75'a)**

The synthesis of **75'a** was carried out in accordance with the general procedure from 0.075 g (0.57 mmol) of diol **86'** in 5 ml of dry and degassed toluene and 0.25 ml (2.9 mmol) of dry pyridine. This solution was slowly added to a solution of 2.3 mmol of the corresponding phosphorochlorhydrite formed *in situ*, dissolved in 6 ml

of toluene and 0.25 ml (2.9 mmol) of pyridine. The mixture was stirred overnight, the salts were filtered and the white foam was purified by flash column chromatography (eluent: toluene Rf=0.9) to afford 0.53 g (92 %) of **75'a** as a white solid.  $[\alpha]_D^{25} -8.53^\circ$  (CH<sub>2</sub>Cl<sub>2</sub>, c 1.160); <sup>1</sup>H NMR (CDCl<sub>3</sub>, 400 MHz) δ 7.42 (m, 4H, aromatic), 7.16 (m, 4H, aromatic), 4.63 (m broad, 2H, H3), 4.12 (m, broad, 2H, H2), 1.46 (s, 18H, *o*-C(CH<sub>3</sub>)<sub>3</sub>), 1.44 (s, 18H, *o*-C(CH<sub>3</sub>)<sub>3</sub>'), 1.34 (s, 18H, *p*-C(CH<sub>3</sub>)<sub>3</sub>), 1.33 (s, 36H, *p*-C(CH<sub>3</sub>)<sub>3</sub>'), 1.09 (d, 6H, ,  $J_{1,2} = 6.2$  Hz, H1); <sup>13</sup>C NMR (CDCl<sub>3</sub>, 100.6 MHz) δ 146.5-124.1 (aromatic), 80.0 (C3  $J_{C,P} = 11.3$ ), 75.2 (broad C2), 35.4 (*o*-C(CH<sub>3</sub>)<sub>3</sub>'), 35.4 (*o*-C(CH<sub>3</sub>)<sub>3</sub>), 34.6 (*p*-C(CH<sub>3</sub>)<sub>3</sub>'), 34.6 (*p*-C(CH<sub>3</sub>)<sub>3</sub>), 31.5 (*p*-C(CH<sub>3</sub>)<sub>3</sub>'), 31.3 (*o*-C(CH<sub>3</sub>)<sub>3</sub>), 31.2 (*o*-C(CH<sub>3</sub>)<sub>3</sub>), 14.9 (CH<sub>3</sub>, C1) <sup>31</sup>P NMR (CDCl<sub>3</sub>, 161.97 MHz) δ 146.95 (s). Anal. Calcd. For C<sub>62</sub>H<sub>90</sub>O<sub>7</sub>P<sub>2</sub>: C, 73.78; H, 8.99. Found: C, 73.61 ; H, 9.43.

**3,4-Bis-O-[(3,3'-di-tert-butyl-,5,5'-dimethoxy-1,1'-biphenyl-2,2'-diyl)phosphite]-1,6-dideoxy-2,5-anhydro-L-iditol (75'b)**

The synthesis of **75'b** was carried out in accordance with the general procedure from 0.075 g (0.57 mmol) of diol **86'** in 5 ml of dry and degassed toluene and 0.25 ml (2.9 mmol) of dry pyridine. This solution was slowly added to a solution of 2.3 mmol of the corresponding phosphorochlorhydrite formed *in situ*, dissolved in 6 ml of toluene and 0.25 ml (2.9 mmol) of pyridine. The mixture was stirred overnight, the salts were filtered and the white foam was purified by flash column chromatography (eluent: toluene Rf=0.5) to afford 0.53 g (64 %) of **75'b** as a white solid.  $[\alpha]_D^{25} -47.60^\circ$  (CH<sub>2</sub>Cl<sub>2</sub>, c 0.775); <sup>1</sup>H NMR (CDCl<sub>3</sub>, 400 MHz) δ 6.96 (m, 4H, aromatic), 6.68 (m, 4,aromatic), 4.70 (m, 2H, H3), 4.26 (m, 2H, H2), 3.79 (s, 6H, *p*-OCH<sub>3</sub>'), 3.77 (s, 6H, *p*-OCH<sub>3</sub>), 1.42 (s, 18H, *o*-C(CH<sub>3</sub>)<sub>3</sub>'), 1.40 (s, 18H, *o*-C(CH<sub>3</sub>)<sub>3</sub>), 1.16 (d, 6H, ,  $J_{1,2} = 6.4$  Hz, H1); <sup>13</sup>C NMR (CDCl<sub>3</sub>, 100.6 MHz) δ 155.7-112.8 (aromatic), 80.2 (m broad, C2), 75.2 (broad C3), 55.5 (*p*-OCH<sub>3</sub>'), 55.4 (*p*-OCH<sub>3</sub>), 35.4 (*o*-C(CH<sub>3</sub>)<sub>3</sub>'), 35.3 (*o*-C(CH<sub>3</sub>)<sub>3</sub>), 31.0 (C(CH<sub>3</sub>)<sub>3</sub>'), 15.0 (CH<sub>3</sub>, C1); <sup>31</sup>P NMR (CDCl<sub>3</sub>, 161.97 MHz) δ 146.07 (s). Anal. Calcd. C<sub>50</sub>H<sub>66</sub>O<sub>11</sub>P<sub>2</sub>: C, 66.36; H, 7.35. Found: C, 66.32 ; H, 7.60 .

**(3R,4R)-(-)-3,4-Bis-O-[(3,3',5,5'-tetra-tert-butyl-1,1'-biphenyl-2,2'-diyl)phosphite]-tetrahydrofuran (76a)**

The synthesis of **76a** was carried out in accordance with the general procedure from 0.15 g (1.44 mmol) of diol **89** in 14 ml of dry and degassed toluene and 0.7 ml (5.7 mmol) of dry pyridine. This solution was slowly added to a solution of 5.7 mmol of the corresponding phosphorochlorhydrite formed *in situ*, dissolved in 15 ml of toluene and 0.7 ml (5.7 mmol) of pyridine. The mixture was stirred overnight, the salts were filtered and the white foam was purified by flash column chromatography (eluent: toluene Rf=0.9) to afford 1.00 g (75 %) of **76a** as a white solid.  $[\alpha]_D^{25}$  -51.13° (CH<sub>2</sub>Cl<sub>2</sub>, c 1.105); <sup>1</sup>H NMR (CDCl<sub>3</sub>, 400 MHz) δ 7.42 (m, 4H, aromatic), 7.16 (m, 4H, aromatic), 4.82 (m, 2H, H3), 3.84 (m, 2H, H2), 3.69 (m, 2H, H2'), 1.46 (s, 18H, *o*-C(CH<sub>3</sub>)<sub>3</sub>'), 1.41 (s, 18H, *o*-C(CH<sub>3</sub>)<sub>3</sub>), 1.35 (s, 18H, *p*-C(CH<sub>3</sub>)<sub>3</sub>'), 1.34 (s, 18H, *p*-C(CH<sub>3</sub>)<sub>3</sub>); <sup>13</sup>C NMR (CDCl<sub>3</sub>, 100.6 MHz) δ 146.6-124.2 (aromatic), 79.1 (broad, C3), 72.3 (broad, C2), 35.4 (*o*-C(CH<sub>3</sub>)<sub>3</sub>'), 35.3 (*o*-C(CH<sub>3</sub>)<sub>3</sub>), 34.6 (*p*-C(CH<sub>3</sub>)<sub>3</sub>'), 31.5 (*o*-C(CH<sub>3</sub>)<sub>3</sub>'), 31.5 (*o*-C(CH<sub>3</sub>)<sub>3</sub>), 31.2 (*p*-C(CH<sub>3</sub>)<sub>3</sub>), 31.1 (*p*-C(CH<sub>3</sub>)<sub>3</sub>), <sup>31</sup>P NMR (CDCl<sub>3</sub>, 161.97 MHz) δ 141.50 (s). Anal. Calcd. C<sub>60</sub>H<sub>86</sub>O<sub>7</sub>P<sub>2</sub>: C, 73.44; H, 8.83. Found: C, 73.21 ; H, 8.88.

**3,4-Bis-O-[(3,3'-di-tert-butyl-,5,5'-dimethoxy-1,1'-biphenyl-2,2'-diyl)phosphite] -tetrahydrofuran (76b)**

The synthesis of **76b** was carried out in accordance with the general procedure from 0.15 g (1.14 mmol) of diol **89** in 10 ml of dry and degassed toluene and 0.5 ml (5.7 mmol) of dry pyridine. This solution was slowly added to a solution of 4.6 mmol of the corresponding phosphorochlorhydrite formed *in situ*, dissolved in 12 ml of toluene and 0.5 ml (5.7 mmol) of pyridine. The mixture was stirred overnight, the salts were filtered and the white foam was purified by flash column chromatography (eluent: toluene Rf=0.9) to afford 0.3 g (29 %) of **76b** as a white solid.  $[\alpha]_D^{25}$  +19.95° (CH<sub>2</sub>Cl<sub>2</sub>, c 1.025); <sup>1</sup>H NMR (CDCl<sub>3</sub>, 400 MHz) δ 7.00 (m, 4H, aromatic), 6.74 (m, 4, aromatic), 4.85 (m, 2H, H3), 3.96 (m, 2H, H1), 3.85 (m, 2H, H1), 3.83 (s, 12H, *p*-OCH<sub>3</sub>), 1.47 (s, 18H, *o*-C(CH<sub>3</sub>)<sub>3</sub>'), 1.43 (s, 18H, *o*-C(CH<sub>3</sub>)<sub>3</sub>); <sup>13</sup>C NMR (CDCl<sub>3</sub>, 100.6 MHz) δ 155.6-112.8 (aromatic), 79.1 (m, C3),



72.3 (C2), 55.5 (*p*-OCH<sub>3</sub>), 55.5 (*p*-OCH<sub>3</sub>), 35.3 (*o*-C(CH<sub>3</sub>)<sub>3</sub>'), 35.2 (*o*-C(CH<sub>3</sub>)<sub>3</sub>), 31.0 (*o*-C(CH<sub>3</sub>)<sub>3</sub>'), 30.9 (*o*-C(CH<sub>3</sub>)<sub>3</sub>); <sup>31</sup>P NMR (CDCl<sub>3</sub>, 161.97 MHz) δ 140.97 (s). Anal. Calcd. for C<sub>48</sub>H<sub>62</sub>O<sub>11</sub>P<sub>2</sub>: C, 65.74; H, 7.13. Found: C, 64.91; H, 7.04.

### Synthesis of rhodium complexes

#### General procedure for synthesizing [Rh(cod)(L)]BF<sub>4</sub>, L=diphosphite

The complexes were prepared by adding 1.1 equivalents of diphosphinite ligand to a solution of [Rh(cod)<sub>2</sub>]BF<sub>4</sub> in the minimum volume of CH<sub>2</sub>Cl<sub>2</sub>. The mixture was then stirred for 30 min, and the solvent was removed in vacuo. The residue was washed with dry hexane first and then with dry ether in order to remove the excess diphosphite and free cyclooctadiene.

#### [Rh(cod)(74a)]BF<sub>4</sub> (90a)

Beginning with 0.015 g (0.036 mmol) of [Rh(cod)<sub>2</sub>]BF<sub>4</sub> in the minimum quantity of CH<sub>2</sub>Cl<sub>2</sub>, 0.060 g (0.040 mmol) of diphosphite **74a** and following the general procedure, 0.054 g (83%) of complex [Rh(cod)(**74a**)]BF<sub>4</sub> **90a** was obtained as a yellow solid. <sup>1</sup>H NMR (CDCl<sub>3</sub>, 400 MHz) δ 7.62-6.87 (m, 28H, aromatic), 5.88 (s broad, 2H, CH (cod)), 5.69 (s broad, 2H, H3), 4.92 (s broad, 2H, CH (cod)), 3.73 (s broad, 2H, H2), 3.52 (d, 2H, H1), 2.82 (d, 2H, H1'), 2.34 (m broad, 4H, CH<sub>2</sub> (cod)), 2.26 (m broad, 2H, CH<sub>2</sub> (cod)), 2.00 (m broad, 4H, CH<sub>2</sub> (cod)), 1.67 (s, 18H, *o*-C(CH<sub>3</sub>)<sub>3</sub>'), 1.48 (s, 18H, *p*-C(CH<sub>3</sub>)<sub>3</sub>), 1.42 (s, 18H, *p*-C(CH<sub>3</sub>)<sub>3</sub>), 1.14 (s, 18H, *o*-C(CH<sub>3</sub>)<sub>3</sub>), 0.89 (s, 18H, C(CH<sub>3</sub>)<sub>3</sub>); <sup>13</sup>C NMR (CDCl<sub>3</sub>, 100.6 MHz) δ 149.4-125.2 (aromatic), 112.9 (CH (cod)), 103.5 (CH (cod)), 78.6 (C2), 77.4 (broad, C3), 60.7 (C1), 36.0 (*o*-C(CH<sub>3</sub>)<sub>3</sub>'), 35.5 (*o*-C(CH<sub>3</sub>)<sub>3</sub>), 35.0 (*p*-C(CH<sub>3</sub>)<sub>3</sub>'), 34.6 (*p*-C(CH<sub>3</sub>)<sub>3</sub>), 32.9 (*o*-C(CH<sub>3</sub>)<sub>3</sub>'), 31.8 (*o*-C(CH<sub>3</sub>)<sub>3</sub>), 31.4 (*p*-C(CH<sub>3</sub>)<sub>3</sub>'), 31.1 (*p*-C(CH<sub>3</sub>)<sub>3</sub>), 30.6 (CH<sub>2</sub> (cod)), 29.7 (CH<sub>2</sub> (cod)), 26.8 (C(CH<sub>3</sub>)<sub>3</sub>), 19.4 (C(CH<sub>3</sub>)<sub>3</sub>); <sup>31</sup>P NMR (CDCl<sub>3</sub>, 161.97 MHz) δ 129.35 (d, J<sub>P, Rh</sub> = 254.4 Hz). Anal. Calcd. C<sub>102</sub>H<sub>138</sub>BF<sub>4</sub>O<sub>9</sub>P<sub>2</sub>RhSi<sub>2</sub>: C, 67.46; H, 7.66. Found: C, 67.49; H, 10.93. MS (Maldi) *m/z* 1727.8 [M]<sup>+</sup>, 1619.8 [M-(cod)]<sup>+</sup>; HRMS (Maldi) calcd for [C<sub>102</sub>H<sub>138</sub>O<sub>9</sub>P<sub>2</sub>RhSi<sub>2</sub>]<sup>+</sup> 1727.8410; found 1727.8404.

### [Rh(cod)(74a)]BF<sub>4</sub> (90a). X-ray Crystallography.

Crystals of [Rh(cod)(74a)]BF<sub>4</sub> (90a) were obtained by slow diffusion of hexane into a solution of [Rh(cod)(74a)]BF<sub>4</sub> (90a) in dichloromethane. Empirical formula: C<sub>103</sub>H<sub>140</sub>B Cl<sub>2</sub> F<sub>4</sub> O<sub>9.50</sub> P<sub>2</sub> Rh Si<sub>2</sub>, Formula weight: 1908.89, Temperature: 100(2) K, Wavelength: 0.71073 Å, Crystal system: Orthorhombic, Space group: *P*2<sub>1</sub>2<sub>1</sub>2<sub>1</sub>, Unit cell dimensions: a=19.512(3) Å, a=90°, b=20.172(3) Å, b=90°, c=26.249(4) Å, γ = 90°, Volume: 10332(3) Å<sup>3</sup>, Z: 4, Density (calculated): 1.227 Mg/m<sup>3</sup>, Absorption coefficient: 0.332 mm<sup>-1</sup>, F(000): 4048, Crystal size: 0.20 x 0.10 x 0.04 mm<sup>3</sup>, Theta range for data collection: 2.74 to 30.18°, Index ranges: -27 ≤ h ≤ 25, -28 ≤ k ≤ 28, -24 ≤ l ≤ 37, Reflections collected: 125396, Independent reflections: 30370 [R(int) = 0.0744], Completeness to theta = 30.18°: 99.3 %, Absorption correction: SADABS (Bruker-Nonius), Refinement method: Full-matrix least-squares on F<sup>2</sup>, Data / restraints / parameters: 30370 / 14 / 1393, Goodness-of-fit on F<sup>2</sup>: 1.013, Final R indices [I>2σ(I)]: R1 = 0.0492, wR2 = 0.1139, R indices (all data): R1 = 0.0798, wR2 = 0.1283, Absolute structure parameter: -0.022(15), Largest diff. peak and hole: 1.185 and -0.973 e.Å<sup>-3</sup>

Compound [Rh(cod)(74a)]BF<sub>4</sub> (90a) crystallizes as a cation together with a BF<sub>4</sub><sup>-</sup> anion, a disordered water molecule and two disordered positions of dichloromethane. The measured compound crystallizes in a pure chiral structure. Selected bond distances and angles are given in Tables 3 and 4 of the appendix.

### [Rh(cod)(74b)]BF<sub>4</sub> (90b)

Beginning with 0.012 g (0.030 mmol) of [Rh(cod)<sub>2</sub>]BF<sub>4</sub> in the minimum quantity of CH<sub>2</sub>Cl<sub>2</sub> and 0.046 g (0.032 mmol) of diphosphite **74b** and following the general procedure, 0.030 g (61%) of complex [Rh(cod)(74b)]BF<sub>4</sub> **90b** was obtained as a yellow solid. <sup>1</sup>H NMR (CDCl<sub>3</sub>, 400 MHz) δ 7.51-6.54 (m, 28H, aromatic), 5.81 (s broad, 2H, CH (cod)), 5.72 (s broad, 2H, H3), 4.96 (s broad, 2H, CH (cod)), 3.93 (s, 6H, *p*-OCH<sub>3</sub>'), 3.87 (dt broad, 2H, H2), 3.66 (s, 6H, *p*-OCH<sub>3</sub>), 3.59 (d, 2H, H1), 3.10 (d, 2H, H1'), 2.45 (m broad, 4H, CH<sub>2</sub> (cod)), 2.31 (m broad, 2H, CH<sub>2</sub> (cod)),

2.05 (m broad, 4H,  $\text{CH}_2$  (cod)), 1.71 (s, 18H,  $o\text{-C}(\text{CH}_3)_3$ '), 1.47 (s, 18H,  $p\text{-C}(\text{CH}_3)_3$ ), 0.89 (s, 18H,  $\text{C}(\text{CH}_3)_3$ );  $^{13}\text{C}$  NMR ( $\text{CDCl}_3$ , 100.6 MHz)  $\delta$  157.2–113.8 (aromatic), 112.8 ( $\text{CH}$  (cod)), 103.7 ( $\text{CH}$  (cod)), 76.6 (C2), 77.2 (broad, C3), 61.2 (C1), 56.0 ( $p\text{-OCH}_3$ '), 55.4 ( $p\text{-OCH}_3$ ), 36.1 ( $o\text{-C}(\text{CH}_3)_3$ '), 35.6 ( $o\text{-C}(\text{CH}_3)_3$ ), 32.9 ( $o\text{-C}(\text{CH}_3)_3$ '), 31.6 ( $o\text{-C}(\text{CH}_3)_3$ ), 31.1 ( $\text{CH}_2$  (cod)), 29.4 ( $\text{CH}_2$  (cod)), 26.7 ( $\text{C}(\text{CH}_3)_3$ ), 19.4 ( $\text{C}(\text{CH}_3)_3$ );  $^{31}\text{P}$  NMR ( $\text{CDCl}_3$ , 161.97 MHz)  $\delta$  129.85 (d,  $J_{\text{P, Rh}} = 254.8$  Hz). Anal. Calcd.  $\text{C}_{90}\text{H}_{114}\text{BF}_4\text{O}_{13}\text{P}_2\text{RhSi}_2$ : C, 63.15; H, 6.71. Found: C, 62.77; H, 6.87. MS (Maldi)  $m/z$  1623.6  $[\text{M}]^+$ , 1515.6  $[\text{M}-(\text{cod})]^+$ ; HRMS (Maldi) calcd for  $[\text{C}_{90}\text{H}_{114}\text{O}_{13}\text{P}_2\text{RhSi}_2]^+$  1623.63282; found 1623.63228.

### **[Rh(cod)(74c)]BF<sub>4</sub> (90c)**

Beginning with 0.025 g (0.061 mmol) of  $[\text{Rh}(\text{cod})_2]\text{BF}_4$  in 10 mL of  $\text{CH}_2\text{Cl}_2$  and 0.074 g (0.067 mmol) of diphosphite **74c** and following the general procedure, 0.054 g (65%) of complex  $[\text{Rh}(\text{cod})(\text{74c})]\text{BF}_4$  **90c** was obtained as a pale yellow solid.  $^1\text{H}$  NMR ( $\text{CDCl}_3$ , 400 MHz)  $\delta$  7.54–7.18 (m, 36H, aromatic), 5.68 (m broad, 4H,  $\text{CH}$  (cod)), 5.46 (s broad, 2H, H3), 4.12 (d broad, 2H, H2), 3.85 (d, 2H, H1), 3.57 (d, 2H, H1'), 2.50 (m broad, 4H,  $\text{CH}_2$  (cod)), 2.17 (m broad, 2H,  $\text{CH}_2$  (cod)), 2.09 (m broad, 2H,  $\text{CH}_2$  (cod)), 0.95 (s, 18H,  $\text{C}(\text{CH}_3)_3$ );  $^{13}\text{C}$  NMR ( $\text{CDCl}_3$ , 100.6 MHz)  $\delta$  148.0–121.4 (aromatic), 110.8 ( $\text{CH}$  (cod)), 110.1 ( $\text{CH}$  (cod)), 80.1 (broad, C3), 79.1 (C2), 62.3 (C1), 30.4 ( $\text{CH}_2$  (cod)), 29.8 ( $\text{CH}_2$  (cod)), 26.8 ( $\text{C}(\text{CH}_3)_3$ ), 19.3 ( $\text{C}(\text{CH}_3)_3$ );  $^{31}\text{P}$  NMR ( $\text{CDCl}_3$ , 161.97 MHz)  $\delta$  136.71 (d,  $J_{\text{P, Rh}} = 249.7$  Hz). MS (Maldi)  $m/z$  1279.3  $[\text{M}]^+$ , 1171.3  $[\text{M}-(\text{cod})]^+$ ; HRMS (Maldi) calcd for  $[\text{C}_{79}\text{H}_{74}\text{O}_9\text{P}_2\text{RhSi}_2]^+$  1279.3402; found 1279.3396.

### **[Rh(cod)(74'a)]BF<sub>4</sub> (90'a)**

Beginning with 0.025 g (0.062 mmol) of  $[\text{Rh}(\text{cod})_2]\text{BF}_4$  in the minimum quantity of  $\text{CH}_2\text{Cl}_2$ , 0.069 g (0.068 mmol) of diphosphite **74'a** and following the general procedure, 0.068 g (81%) of complex  $[\text{Rh}(\text{cod})(\text{74'a})]\text{BF}_4$  **90'a** was obtained as a yellow solid.  $^1\text{H}$  NMR ( $\text{CDCl}_3$ , 400 MHz)  $\delta$  7.60 (d, 2H,  $J = 1.9$  Hz, aromatic), 7.48 (d, 2H,  $J = 1.9$  Hz, aromatic), 7.19 (d, 2H,  $J = 1.9$  Hz, aromatic), 7.06 (d, 2H,  $J = 1.9$  Hz, aromatic), 5.78 (s broad, 2H, H3), 4.87 (s broad, 4H,  $\text{CH}$  (cod)), 3.85 (m broad, 2H, H2), 2.32 (m broad, 4H,  $\text{CH}_2$  (cod)), 2.20 (m broad, 2H,  $\text{CH}_2$  (cod)),

1.94 (m broad, 2H, CH<sub>2</sub> (cod)), 1.76 (s, 18H, *o*-C(CH<sub>3</sub>)<sub>3</sub>'), 1.51 (s, 18H, *p*-C(CH<sub>3</sub>)<sub>3</sub>), 1.37 (s, 18H, *p*-C(CH<sub>3</sub>)<sub>3</sub>), 1.32 (s, 18H, *o*-C(CH<sub>3</sub>)<sub>3</sub>), 0.84 (d, 6H, *J*<sub>1,2</sub> = 6.0 Hz C(CH<sub>3</sub>)<sub>3</sub>); <sup>13</sup>C NMR (CDCl<sub>3</sub>, 100.6 MHz) δ 149.4-125.4 (aromatic), 112.4 (CH (cod)), 103.6 (CH (cod)), 84.2 (C3), 72.6 (C2), 35.8 (*o*-C(CH<sub>3</sub>)<sub>3</sub>'), 35.6 (*o*-C(CH<sub>3</sub>)<sub>3</sub>), 34.9 (*p*-C(CH<sub>3</sub>)<sub>3</sub>'), 34.8 (*p*-C(CH<sub>3</sub>)<sub>3</sub>), 32.6 (*o*-C(CH<sub>3</sub>)<sub>3</sub>'), 31.8 (*o*-C(CH<sub>3</sub>)<sub>3</sub>), 31.4 (*p*-C(CH<sub>3</sub>)<sub>3</sub>'), 31.3 (*p*-C(CH<sub>3</sub>)<sub>3</sub>), 30.6 (CH<sub>2</sub> (cod)), 29.6 (CH<sub>2</sub> (cod)), 17.9 (CH<sub>3</sub>, C1); <sup>31</sup>P NMR (CDCl<sub>3</sub>, 161.97 MHz) δ 128.38 (d, *J*<sub>P, Rh</sub> = 255.0 Hz). Anal. Calcd. C<sub>70</sub>H<sub>102</sub>BF<sub>4</sub>O<sub>7</sub>P<sub>2</sub>Rh: C, 64.32; H, 7.86. Found: C, 64.41; H, 8.26. MS (Maldi) *m/z* 1219.6 [M]<sup>+</sup>, 1111.6 [M-(cod)]<sup>+</sup>; HRMS (Maldi) calcd for [C<sub>70</sub>H<sub>102</sub>O<sub>7</sub>P<sub>2</sub>Rh]<sup>+</sup> 1219.6156; found 1219.6150.

### [Rh(cod)(74'b)]BF<sub>4</sub> (90'b)

Beginning with 0.021 g (0.052 mmol) of [Rh(cod)<sub>2</sub>]BF<sub>4</sub> in the minimum quantity of CH<sub>2</sub>Cl<sub>2</sub>, 0.050 g (0.055 mmol) of diphosphite **74'b** and following the general procedure, 0.047 g (76%) of complex [Rh(cod)(74'b)]BF<sub>4</sub> **90'b** was obtained as a yellow-orange solid. <sup>1</sup>H NMR (CDCl<sub>3</sub>, 400 MHz) δ 7.22 (d, 2H, *J* = 2.5 Hz, aromatic), 7.10 (d, 2H, *J* = 2.6 Hz, aromatic), 6.84 (d, 2H, *J* = 2.5 Hz, aromatic), 6.71 (d, 2H, *J* = 2.7 Hz, aromatic), 5.85 (s broad, 2H, CH (cod)), 5.98 (s broad, 2H, H3), 5.00 (s broad, 2H, CH (cod)), 3.97 (s, 6H, *p*-OCH<sub>3</sub>'), 3.96 (m, 2H, H2), 3.92 (s, 6H, *p*-OCH<sub>3</sub>), 2.44 (m broad, 4H, CH<sub>2</sub> (cod)), 2.35 (m broad, 2H, CH<sub>2</sub> (cod)), 2.09 (m broad, 2H, CH<sub>2</sub> (cod)), 1.84 (s, 18H, *o*-C(CH<sub>3</sub>)<sub>3</sub>'), 1.57 (s, 18H, *o*-C(CH<sub>3</sub>)<sub>3</sub>), 1.03 (d, 6H, *J*<sub>1,2</sub> = 6.0 Hz C(CH<sub>3</sub>)<sub>3</sub>); <sup>13</sup>C NMR (CDCl<sub>3</sub>, 100.6 MHz) δ 157.1-114.1 (aromatic), 112.2 (CH (cod)), 103.2 (CH (cod)), 85.3 (C3), 72.6 (C2), 55.9 (*p*-OCH<sub>3</sub>'), 55.7 (*p*-OCH<sub>3</sub>), 35.8 (*o*-C(CH<sub>3</sub>)<sub>3</sub>'), 35.5 (*o*-C(CH<sub>3</sub>)<sub>3</sub>), 32.4 (*o*-C(CH<sub>3</sub>)<sub>3</sub>'), 31.5 (*o*-C(CH<sub>3</sub>)<sub>3</sub>), 30.8 (CH<sub>2</sub> (cod)), 29.6 (CH<sub>2</sub> (cod)), 18.1 (CH<sub>3</sub>, C1); <sup>31</sup>P NMR (CDCl<sub>3</sub>, 161.97 MHz) δ 128.65 (d, *J*<sub>P, Rh</sub> = 254.1 Hz). MS (Maldi) *m/z* 1115.4 [M]<sup>+</sup>, 1007.4 [M-(cod)]<sup>+</sup>; HRMS (Maldi) calcd for [C<sub>58</sub>H<sub>78</sub>O<sub>11</sub>P<sub>2</sub>Rh]<sup>+</sup> 1115.4074; found 1115.4069.

### [Rh(cod)(75a)]BF<sub>4</sub> (91a)

Beginning with 0.015 g (0.036 mmol) of [Rh(cod)<sub>2</sub>]BF<sub>4</sub> in the minimum quantity of CH<sub>2</sub>Cl<sub>2</sub>, 0.062 g (0.041 mmol) of diphosphite **75a** and following the general procedure, 0.054 g (83%) of complex [Rh(cod)(75a)]BF<sub>4</sub> **91a** was obtained as a

yellow solid.  $^1\text{H}$  NMR ( $\text{CDCl}_3$ , 400 MHz)  $\delta$  7.51-7.13 (m, 28H, aromatic), 5.67 (s broad, 2H,  $\text{CH}$  (cod)), 5.34 (s broad, 2H,  $\text{CH}$  (cod)), 4.66 (s broad, 2H, H3), 3.89 (s broad, 2H, H2), 3.44 (s broad, 4H, H1), 2.36 (m broad, 4H,  $\text{CH}_2$  (cod)), 2.23 (m broad, 2H,  $\text{CH}_2$  (cod)), 2.05 (m broad, 4H,  $\text{CH}_2$  (cod)), 1.51 (s, 18H,  $o\text{-C}(\text{CH}_3)_3$ '), 1.35 (s, 18H,  $p\text{-C}(\text{CH}_3)_3$ ), 1.33 (s, 18H,  $p\text{-C}(\text{CH}_3)_3$ ), 1.25 (s, 18H,  $o\text{-C}(\text{CH}_3)_3$ ), 0.96 (s, 18H,  $\text{C}(\text{CH}_3)_3$ );  $^{13}\text{C}$  NMR ( $\text{CDCl}_3$ , 100.6 MHz)  $\delta$  149.6-125.4 (aromatic), 112.8 (broad,  $\text{CH}$  (cod)), 103.4 (broad,  $\text{CH}$  (cod)), 80.9 (C2), 74.7 (broad, C3), 63.1 (broad, C1), 35.6 ( $o\text{-C}(\text{CH}_3)_3$ '), 35.3 ( $o\text{-C}(\text{CH}_3)_3$ ), 34.8 ( $p\text{-C}(\text{CH}_3)_3$ ), 32.3 ( $o\text{-C}(\text{CH}_3)_3$ ), 31.4 ( $p\text{-C}(\text{CH}_3)_3$ ), 30.3 ( $\text{CH}_2$  (cod)), 29.7 ( $\text{CH}_2$  (cod)), 26.8 ( $\text{C}(\text{CH}_3)_3$ ), 19.2 ( $\text{C}(\text{CH}_3)_3$ );  $^{31}\text{P}$  NMR ( $\text{CDCl}_3$ , 161.97 MHz)  $\delta$  126.62 (d,  $J_{\text{P, Rh}} = 258.7$  Hz). MS (Maldi)  $m/z$  1727.8  $[\text{M}]^+$ , 1619.8  $[\text{M}(\text{cod})]^+$ ; HRMS (Maldi) calcd for  $[\text{C}_{102}\text{H}_{138}\text{O}_9\text{P}_2\text{RhSi}_2]^+$  1727.8410; found 1727.8404.

### **[Rh(cod)(75'a)]BF<sub>4</sub> (91'a)**

Beginning with 0.025 g (0.062 mmol) of  $[\text{Rh}(\text{cod})_2]\text{BF}_4$  in the minimum quantity of  $\text{CH}_2\text{Cl}_2$ , 0.069 g (0.068 mmol) of diphosphite **75'a** and following the general procedure, 0.068 g (81%) of complex  $[\text{Rh}(\text{cod})(\mathbf{75'a})]\text{BF}_4$  **91'a** was obtained as a yellow solid.  $^1\text{H}$  NMR ( $\text{CDCl}_3$ , 400 MHz)  $\delta$  7.58 (d, 2H,  $J = 1.9$  Hz, aromatic), 7.48 (d, 2H,  $J = 1.9$  Hz, aromatic), 7.15 (d, 2H,  $J = 1.9$  Hz, aromatic), 7.09 (d, 2H,  $J = 1.9$  Hz, aromatic), 5.85 (s broad, 2H,  $\text{CH}$  (cod)), 5.49 (s broad, 2H, H3), 5.00 (s broad, 2H,  $\text{CH}$  (cod)), 4.13 (m broad, 2H, H2), 2.34 (m broad, 4H,  $\text{CH}_2$  (cod)), 2.10 (m broad, 2H,  $\text{CH}_2$  (cod)), 2.01 (m broad, 2H,  $\text{CH}_2$  (cod)), 1.73 (s, 18H,  $o\text{-C}(\text{CH}_3)_3$ '), 1.54 (s, 18H,  $p\text{-C}(\text{CH}_3)_3$ ), 1.36 (s, 18H,  $p\text{-C}(\text{CH}_3)_3$ ), 1.34 (s, 18H,  $o\text{-C}(\text{CH}_3)_3$ ), 0.86 (d, 6H,  $J_{1,2} = 6.5$  Hz  $\text{C}(\text{CH}_3)_3$ );  $^{13}\text{C}$  NMR ( $\text{CDCl}_3$ , 100.6 MHz)  $\delta$  149.2-125.3 (aromatic), 111.8 ( $\text{CH}$  (cod)), 104.2 ( $\text{CH}$  (cod)), 81.5 (C3), 71.0 (C2), 35.8 ( $o\text{-C}(\text{CH}_3)_3$ '), 35.4 ( $o\text{-C}(\text{CH}_3)_3$ ), 34.8 ( $p\text{-C}(\text{CH}_3)_3$ '), 34.7 ( $p\text{-C}(\text{CH}_3)_3$ ), 32.4 ( $o\text{-C}(\text{CH}_3)_3$ '), 31.6 ( $o\text{-C}(\text{CH}_3)_3$ ), 31.3 ( $p\text{-C}(\text{CH}_3)_3$ '), 31.3 ( $p\text{-C}(\text{CH}_3)_3$ ), 30.1 ( $\text{CH}_2$  (cod)), 29.6 ( $\text{CH}_2$  (cod)), 16.1 ( $\text{CH}_3$ , C1);  $^{31}\text{P}$  NMR ( $\text{CDCl}_3$ , 161.97 MHz)  $\delta$  127.97 (d,  $J_{\text{P, Rh}} = 253.9$  Hz). Anal. Calcd.  $\text{C}_{70}\text{H}_{102}\text{BF}_4\text{O}_7\text{P}_2\text{Rh}$ : C, 64.32; H, 7.86. MS (Maldi)  $m/z$  1219.6  $[\text{M}]^+$ , 1111.6  $[\text{M}(\text{cod})]^+$ ; HRMS (Maldi) calcd for  $[\text{C}_{70}\text{H}_{102}\text{O}_7\text{P}_2\text{Rh}]^+$  1219.6156; found 1219.6150.

### **[Rh(cod)(75'a)]BF<sub>4</sub> (91'a). X-ray Crystallography.**

Crystals of [Rh(cod)(75'a)]BF<sub>4</sub> (91'a) were obtained by slow diffusion of hexane into a solution of [Rh(cod)(75'a)]BF<sub>4</sub> (91'a) in dichloromethane. Empirical formula: C<sub>142.83</sub> H<sub>209.35</sub> B<sub>2</sub> Cl<sub>5.67</sub> F<sub>8</sub> O<sub>14</sub> P<sub>4</sub> Rh<sub>2</sub>, Formula weight: 2854.67, Temperature: 100(2) K, Wavelength: 0.71073 Å, Crystal system: Orthorhombic, Space group: *P*<sub>2</sub><sub>1</sub><sub>2</sub><sub>1</sub><sub>2</sub><sub>1</sub>, Unit cell dimensions: a=19.1067(15) Å, a=90°, b=26.855(2) Å, b=90°, c=30.828(3) Å, γ = 90°, Volume: 15818(2) Å<sup>3</sup>, Z:4, Density (calculated):1.199 Mg/m<sup>3</sup>, Absorption coefficient: 0.408 mm<sup>-1</sup>, F(000): 6027, Crystal size: 0.20 x 0.04 x 0.02 mm<sup>3</sup>, Theta range for data collection: 2.50 to 30.73°, Index ranges: -27 ≤ h ≤ 27, -37 ≤ k ≤ 38, -44 ≤ l ≤ 40, Reflections collected: 209015, Independent reflections: 48854 [R(int) = 0.0598], Completeness to theta = 30.73°: 99.3 %, Absorption correction: SADABS (Bruker-Nonius), Max. and min. transmission: 0.9919 and 0.9229, Refinement method: Full-matrix least-squares on F<sup>2</sup>, Data / restraints / parameters: 48854 / 0 / 1644, Goodness-of-fit on F<sup>2</sup>: 1.065, Final R indices [I>2σ(I)]: R1 = 0.0674, wR2 = 0.1837, R indices (all data): R1 = 0.0880, wR2 = 0.1984, Absolute structure parameter: 0.000(18), Largest diff. peak and hole: 1.788 and -1.045 e.Å<sup>-3</sup>

Compound [Rh(cod)(75'a)]BF<sub>4</sub> (91'a) crystallizes with two independent cations in the elementary cell. The crystal cell also contains two BF<sub>4</sub> anions and four disordered positions of dichloromethane molecules. The independently obtained cationic structures have different conformations. The measured compound crystallizes in a pure chiral structure. Selected bond distances and angles are given in Tables 5 and 6 of the appendix.

### **[Rh(cod)(76a)]BF<sub>4</sub> (92a)**

Beginning with 0.025 g (0.062 mmol) of [Rh(cod)<sub>2</sub>]BF<sub>4</sub> in the minimum quantity of CH<sub>2</sub>Cl<sub>2</sub>, 0.068 g (0.068 mmol) of diphosphite **74a** and following the general procedure, 0.059 g (75%) of complex [Rh(cod)(74a)]BF<sub>4</sub> **92a** was obtained as a yellow-orange solid. <sup>1</sup>H NMR (CDCl<sub>3</sub>, 400 MHz) δ 7.61 (d, 2H, J= 1.9 Hz, aromatic),

7.50 (d, 2H,  $J = 1.9$  Hz, aromatic), 7.21 (d, 2H,  $J = 1.9$  Hz, aromatic), 7.08 (d, 2H,  $J = 1.9$  Hz, aromatic), 5.51 (s broad, 2H, H<sub>3</sub>), 4.65 (s broad, 4H, CH (cod)), 4.13 (m, 2H, H<sub>2</sub>), 3.72 (t, 2H, H<sub>2</sub>'), 2.21 (m broad, 4H, CH<sub>2</sub> (cod)), 2.18 (m broad, 2H, CH<sub>2</sub> (cod)), 2.07 (m broad, 2H, CH<sub>2</sub> (cod)), 1.75 (s, 18H, *o*-C(CH<sub>3</sub>)<sub>3</sub>'), 1.53 (s, 18H, *p*-C(CH<sub>3</sub>)<sub>3</sub>), 1.38 (s, 18H, *p*-C(CH<sub>3</sub>)<sub>3</sub>), 1.36 (s, 18H, *o*-C(CH<sub>3</sub>)<sub>3</sub>); <sup>13</sup>C NMR (CDCl<sub>3</sub>, 100.6 MHz)  $\delta$  149.6-125.6 (aromatic), 112.6 (CH (cod)), 103.2 (CH (cod)), 80.1 (C<sub>3</sub>), 67.9 (C<sub>2</sub>), 35.8 (*o*-C(CH<sub>3</sub>)<sub>3</sub>'), 35.4 (*o*-C(CH<sub>3</sub>)<sub>3</sub>), 34.9 (*p*-C(CH<sub>3</sub>)<sub>3</sub>'), 34.7 (*p*-C(CH<sub>3</sub>)<sub>3</sub>), 32.7 (*o*-C(CH<sub>3</sub>)<sub>3</sub>), 31.4 (*p*-C(CH<sub>3</sub>)<sub>3</sub>'), 31.3 (*p*-C(CH<sub>3</sub>)<sub>3</sub>), 30.5 (CH<sub>2</sub> (cod)), 29.5 (CH<sub>2</sub> (cod)); <sup>31</sup>P NMR (CDCl<sub>3</sub>, 161.97 MHz)  $\delta$  127.85 (d,  $J_{P, Rh} = 253.5$  Hz). MS (Maldi)  $m/z$  1191.6 [M]<sup>+</sup>, 1083.6 [M-(cod)]<sup>+</sup>; HRMS (Maldi) calcd for [C<sub>68</sub>H<sub>98</sub>O<sub>7</sub>P<sub>2</sub>Rh]<sup>+</sup> 1191.5843; found 1191.5837.

### [Rh(cod)(76b)]BF<sub>4</sub> (92a)

Beginning with 0.025 g (0.062 mmol) of [Rh(cod)<sub>2</sub>]BF<sub>4</sub> in the minimum quantity of CH<sub>2</sub>Cl<sub>2</sub>, 0.061 g (0.068 mmol) of diphosphite **74b** and following the general procedure, 0.054 g (79%) of complex [Rh(cod)(**74b**)]BF<sub>4</sub> **92a** was obtained as a yellow-orange solid. <sup>1</sup>H NMR (CDCl<sub>3</sub>, 400 MHz)  $\delta$  7.13 (d, 2H,  $J = 2.9$  Hz, aromatic), 7.01 (d, 2H,  $J = 2.9$  Hz, aromatic), 6.75 (d, 2H,  $J = 2.9$  Hz, aromatic), 6.62 (d, 2H,  $J = 2.9$  Hz, aromatic), 5.64 (s broad, 2H, CH (cod)), 5.43 (s broad, 2H, H<sub>3</sub>), 4.80 (s broad, 2H, CH (cod)), 4.07 (m, 2H, H<sub>2</sub>), 3.87 (s, 6H, *p*-OCH<sub>3</sub>'), 3.83 (s, 6H, *p*-OCH<sub>3</sub>), 3.66 (t, 2H, H<sub>2</sub>'), 2.26 (m broad, 4H, CH<sub>2</sub> (cod)), 2.15 (m broad, 2H, CH<sub>2</sub> (cod)), 1.82 (m broad, 2H, CH<sub>2</sub> (cod)), 1.71 (s, 18H, *o*-C(CH<sub>3</sub>)<sub>3</sub>'), 1.48 (s, 18H, *o*-C(CH<sub>3</sub>)<sub>3</sub>); <sup>13</sup>C NMR (CDCl<sub>3</sub>, 100.6 MHz)  $\delta$  157.3 -114.2 (aromatic), 113.6 (CH (cod)), 103.8 (CH (cod)), 80.3 (C<sub>3</sub>), 68.1 (C<sub>2</sub>), 56.2 (*p*-OCH<sub>3</sub>'), 55.3 (*p*-OCH<sub>3</sub>), 36.1 (*o*-C(CH<sub>3</sub>)<sub>3</sub>'), 35.7 (*o*-C(CH<sub>3</sub>)<sub>3</sub>), 32.7 (*o*-C(CH<sub>3</sub>)<sub>3</sub>), 31.6 (*o*-C(CH<sub>3</sub>)<sub>3</sub>'), 30.8 (CH<sub>2</sub> (cod)), 30.1 (CH<sub>2</sub> (cod)); <sup>31</sup>P NMR (CDCl<sub>3</sub>, 161.97 MHz)  $\delta$  129.36 (d,  $J_{P, Rh} = 256.0$  Hz). MS (Maldi)  $m/z$  1087.4 [M]<sup>+</sup>, 979.4 [M-(cod)]<sup>+</sup>; HRMS (Maldi) calcd for [C<sub>56</sub>H<sub>74</sub>O<sub>11</sub>P<sub>2</sub>Rh]<sup>+</sup> 1087.3761; found 1087.3756.

### Hydroformylation experiments

In a typical experiment, the autoclave was purged three times with CO. The solution was formed from [Rh(acac)(CO)<sub>2</sub>] (0.013 mmol), diphosphite (0.015

mmol) and styrene (13 mmol) in toluene (15 ml). After the desired reaction time, the autoclave was cooled to room temperature and depressurised. The reaction mixture was analysed by gas chromatography. The aldehydes obtained from the hydroformylation were oxidised to carboxylic acids to determine the enantiomeric excess.

### ***In situ HP-NMR hydroformylation experiments***

In a typical experiment, a sapphire tube ( $\varnothing$ 10 mm) was filled under argon with a solution of  $[\text{Rh}(\text{acac})(\text{CO})_2]$  ( $2 \cdot 10^{-2}$  M) and ligand (molar ratio PP/Rh=1.1) in  $[\text{D}_8]$ toluene (2 ml). The solution was analysed and then the HP-NMR tube was purged three times with CO and pressurized to the appropriate pressure of CO/H<sub>2</sub>. After a reaction time of 15 hours during which the solution was shaken at 80°C of temperature, the solution was analysed.

#### **[Rh(acac)(74a)]**

<sup>1</sup>H NMR ( $\text{C}_6\text{D}_8$ , 300 MHz)  $\delta$  7.72-6.92 (m, 28H, aromatic), 5.61 (broad, 2H, H<sub>3</sub>), 5.15 (s, 1H,  $\text{CH}$ ), 3.92 (m broad, 2H, H<sub>2</sub>), 3.61 (d, 2H, H<sub>1</sub>), 3.28 (d, 2H, H<sub>1'</sub>), 1.96 (s, 18H, *o*-C(CH<sub>3</sub>)<sub>3</sub>'), 1.80 (s, 18H, *p*-C(CH<sub>3</sub>)<sub>3</sub>), 1.32 (s, 6H,  $\text{CH}_3$ ), 1.32 (s, 18H, *p*-C(CH<sub>3</sub>)<sub>3</sub>), 1.20 (s, 18H, *o*-C(CH<sub>3</sub>)<sub>3</sub>), 1.09 (s, 18H, C(CH<sub>3</sub>)<sub>3</sub>); <sup>31</sup>P NMR ( $\text{C}_6\text{D}_8$ , 121.47 MHz)  $\delta$  140.77 (d,  $J_{\text{Rh}, \text{P}} = 301.4$  Hz.).

#### **[RhH(CO)<sub>2</sub>(74a)]**

<sup>1</sup>H NMR ( $\text{C}_6\text{D}_8$ , 300 MHz)  $\delta$  7.81-6.99 (m, 28H, aromatic), 5.40 (broad, 2H,  $J = 8.5$  Hz, H<sub>3</sub>), 4.04 (broad, 2H, H<sub>2</sub>), 3.58 (dd, 2H, H<sub>1</sub>), 3.58 (dd, 2H, H<sub>1'</sub>), 1.67 (s, 18H, *o*-C(CH<sub>3</sub>)<sub>3</sub>'), 1.63 (s, 18H, *p*-C(CH<sub>3</sub>)<sub>3</sub>), 1.29 (s, 18H, *p*-C(CH<sub>3</sub>)<sub>3</sub>), 1.21 (s, 18H, *o*-C(CH<sub>3</sub>)<sub>3</sub>), 1.16 (s, 18H, C(CH<sub>3</sub>)<sub>3</sub>), -9.93 (t, 1H,  $J_{\text{H}, \text{Rh}} = 2.0$  Hz,  $J_{\text{H}, \text{P}} = 2.0$  Hz); <sup>31</sup>P NMR ( $\text{C}_6\text{D}_8$ , 121.47 MHz)  $\delta$  152.70 (d,  $J_{\text{Rh}, \text{P}} = 231.9$  Hz.).



**[Rh(acac)(74b)]**

$^1\text{H}$  NMR ( $\text{C}_6\text{D}_8$ , 300 MHz)  $\delta$  7.73-6.78 (m, 28H, aromatic), 5.61 (s broad, 2H, H3), 5.15 (s, 1H, CH), 4.00 (s broad, 2H, H2), 3.61 (d, 2H, H1), 3.42 (d, 2H, H1'), 3.39 (s, 6H, OCH<sub>3</sub>'), 3.35 (s, 6H, OCH<sub>3</sub>), 1.94 (s, 18H, *o*-C(CH<sub>3</sub>)<sub>3</sub>'), 1.72 (s, 18H, *o*-C(CH<sub>3</sub>)<sub>3</sub>), 1.43 (s, 6H, CH<sub>3</sub>), 1.11 (s, 18H, C(CH<sub>3</sub>)<sub>3</sub>);  $^{31}\text{P}$  NMR ( $\text{C}_6\text{D}_8$ , 121.47 MHz)  $\delta$  141.29 (d,  $J_{\text{Rh}, \text{P}} = 300.4$  Hz.).

**[RhH(CO)<sub>2</sub>(74b)]**

$^1\text{H}$  NMR ( $\text{C}_6\text{D}_8$ , 300 MHz)  $\delta$  7.79 - 6.64 (m, 28H, aromatic), 5.38 (m broad, 2H,  $J = 9.9$  Hz, H3), 4.17 (broad, 2H, H2), 3.84 (dd, 2H, H1), 3.67 (dd, 2H, H1'), 3.32 (s, 6H, OCH<sub>3</sub>'), 3.29 (s, 6H, OCH<sub>3</sub>), 1.62 (s, 18H, *o*-C(CH<sub>3</sub>)<sub>3</sub>'), 1.57 (s, 18H, *o*-C(CH<sub>3</sub>)<sub>3</sub>), 1.17 (s, 18H, C(CH<sub>3</sub>)<sub>3</sub>), -9.91 (q, 1H,  $J_{\text{H}, \text{Rh}} = 3.4$  Hz,  $J_{\text{H}, \text{P}} = 3.9$  Hz);  $^{31}\text{P}$  NMR ( $\text{C}_6\text{D}_8$ , 121.47 MHz)  $\delta$  155.33 (d,  $J_{\text{Rh}, \text{P}} = 230.0$  Hz.).

**[Rh(acac)(74'a)]**

$^1\text{H}$  NMR ( $\text{C}_6\text{D}_8$ , 300 MHz)  $\delta$  7.58 (m, 4H, aromatic), 7.34 (m, 4H, aromatic), , 5.10 (s, 1H, CH), 4.83 (broad, 2H, H3), 3.88 (m broad, 2H, H2), 1.93 (s, 18H, *o*-C(CH<sub>3</sub>)<sub>3</sub>'), 1.77 (s, 18H, *o*-C(CH<sub>3</sub>)<sub>3</sub>), 1.56 (s, 6H, CH<sub>3</sub>), 1.28 (s, 18H, *p*-C(CH<sub>3</sub>)<sub>3</sub>), 1.27 (s, 18H, *p*-C(CH<sub>3</sub>)<sub>3</sub>), 0.97 (d, 6H,  $J_{1,2} = 6.2$  Hz, H1);  $^{31}\text{P}$  NMR ( $\text{C}_6\text{D}_8$ , 121.47 MHz)  $\delta$  141.13 (d,  $J_{\text{Rh}, \text{P}} = 299.4$  Hz.).

**[RhH(CO)<sub>2</sub>(74'a)]**

$^1\text{H}$  NMR ( $\text{C}_6\text{D}_8$ , 300 MHz)  $\delta$  7.60 (m, 4H, aromatic), 7.32 (m, 4H, aromatic), , 4.95 (m, 2H, H3), 4.11 (m, 2H, H2), 1.69 (s, 18H, *o*-C(CH<sub>3</sub>)<sub>3</sub>'), 1.63 (s, 18H, *o*-C(CH<sub>3</sub>)<sub>3</sub>), 1.26 (s, 36H, *p*-C(CH<sub>3</sub>)<sub>3</sub>), 1.16 (d, 6H,  $J_{1,2} = 6.2$  Hz, H1), -10.14 (q broad, 1H,  $J_{\text{H}, \text{Rh}} = 2.7$  Hz,  $J_{\text{H}, \text{P}} = 3.8$  Hz);  $^{31}\text{P}$  NMR ( $\text{C}_6\text{D}_8$ , 121.47 MHz)  $\delta$  155.43 (d,  $J_{\text{Rh}, \text{P}} = 231.6$  Hz.).

**[RhH(CO)<sub>2</sub>(75a)]**

<sup>1</sup>H NMR (C<sub>6</sub>D<sub>8</sub>, 300 MHz) δ 7.81-6.96 (m, 28H, aromatic), 5.59 (dd, 2H, H<sub>3</sub>), 4.67 (m broad, 2H, H<sub>2</sub>), 3.95 (dd, 2H, H<sub>1</sub>), 3.63 (dd, 2H, H<sub>1</sub>'), 1.64 (s, 18H, *o*-C(CH<sub>3</sub>)<sub>3</sub>'), 1.60 (s, 18H, *p*-C(CH<sub>3</sub>)<sub>3</sub>), 1.31 (s, 18H, *p*-C(CH<sub>3</sub>)<sub>3</sub>), 1.16 (s, 18H, *o*-C(CH<sub>3</sub>)<sub>3</sub>), 1.13 (s, 18H, C(CH<sub>3</sub>)<sub>3</sub>), -9.85 (q, 1H, J<sub>H, Rh</sub> = 2.9 Hz, J<sub>H, P</sub> = 3.1 Hz); <sup>31</sup>P NMR (C<sub>6</sub>D<sub>8</sub>, 121.47 MHz) δ 158.09 (d, J<sub>Rh, P</sub> = 233.6 Hz.).

**[Rh(acac)(75'a)]**

<sup>1</sup>H NMR (C<sub>6</sub>D<sub>8</sub>, 300 MHz) δ 7.61 (m, 4H, aromatic), 7.33 (m, 4H, aromatic), 5.25 (s broad, 2H, H<sub>3</sub>), 5.13 (s, 1H, CH), 3.92 (m broad, 2H, J<sub>2,1</sub> = 6.2 Hz, H<sub>2</sub>), 1.92 (s, 18H, *o*-C(CH<sub>3</sub>)<sub>3</sub>'), 1.81 (s, 18H, *o*-C(CH<sub>3</sub>)<sub>3</sub>), 1.56 (s, 6H, CH<sub>3</sub>), 1.30 (s, 18H, *p*-C(CH<sub>3</sub>)<sub>3</sub>), 1.27 (s, 18H, *p*-C(CH<sub>3</sub>)<sub>3</sub>), 0.80 (d, 6H, J<sub>1,2</sub> = 6.2 Hz, H<sub>1</sub>); <sup>31</sup>P NMR (C<sub>6</sub>D<sub>8</sub>, 121.47 MHz) δ 141.55 (d, J<sub>Rh, P</sub> = 300.1 Hz.).

**[RhH(CO)<sub>2</sub>(75'a)]**

<sup>1</sup>H NMR (C<sub>6</sub>D<sub>8</sub>, 300 MHz) δ 7.58 (m, 4H, aromatic), 7.32 (m, 4H, aromatic), 5.18 (m, 2H, H<sub>3</sub>), 4.16 (m, 2H, H<sub>2</sub>), 1.69 (s, 18H, *o*-C(CH<sub>3</sub>)<sub>3</sub>'), 1.62 (s, 18H, *o*-C(CH<sub>3</sub>)<sub>3</sub>), 1.27 (s, 36H, *p*-C(CH<sub>3</sub>)<sub>3</sub>), 0.83 (d, 6H, J<sub>1,2</sub> = 6.5 Hz, H<sub>1</sub>), -10.05 (q, 1H, J<sub>H, Rh</sub> = 3.9 Hz, J<sub>H, P</sub> = 4.3 Hz); <sup>31</sup>P NMR (C<sub>6</sub>D<sub>8</sub>, 121.47 MHz) δ 155.27 (d, J<sub>Rh, P</sub> = 234.1 Hz.).

**[RhH(CO)<sub>2</sub>(76a)]**

<sup>1</sup>H NMR (C<sub>6</sub>D<sub>8</sub>, 300 MHz) δ 7.61 (d, 2H, J = 2.3 Hz, aromatic), 7.59 (d, 2H, J = 2.3 Hz, aromatic), 7.30 (d, 2H, J = 2.3 Hz, aromatic), 7.28 (d, 2H, J = 2.3 Hz, aromatic), 5.35 (m, 2H, H<sub>3</sub>), 3.86 (dd, 2H, H<sub>2</sub>), 3.60 (dd, 2H, H<sub>1</sub>') 1.69 (s, 18H, *o*-C(CH<sub>3</sub>)<sub>3</sub>'), 1.60 (s, 18H, *o*-C(CH<sub>3</sub>)<sub>3</sub>), 1.25 (s, 36H, *p*-C(CH<sub>3</sub>)<sub>3</sub>), -10.24 (q, 1H, J<sub>H, Rh</sub> = 3.8 Hz, J<sub>H, P</sub> = 3.9 Hz); <sup>31</sup>P NMR (C<sub>6</sub>D<sub>8</sub>, 121.47 MHz) δ 156.40 (d, J<sub>Rh, P</sub> = 232.1 Hz.).

### Hydrogenation experiments

The experiments were prepared in a multiple reaction vessel autoclave in a glovebox. After the addition of the substrate to a solution of [Rh(cod)(L)]BF<sub>4</sub> (2.5x10<sup>-3</sup> mmol) in the corresponding solvent (2.5 ml) the autoclave was pressurised to the desired pressure with hydrogen. After the desired reaction time the autoclave was depressurised. The reaction mixture was analysed by gas chromatography.

### 2.5 References

- [1] R. I. Hollingsworth, G. Wang, *Chem. Rev.* **2000**, *100*, 4267.
- [2] D. Steinborn, H. Junicke, *Chem. Rev.* **2000**, *100*, 4283.
- [3] T. V. RajanBabu, A. L. Casalnuovo, T. A. Ayers, in *Advances in Catalytic Processes, Vol. 2* (Ed.: M. P. Doyle), Ed.; JAI Press: Greenwich, CT, **1998**, pp. 1.
- [4] S. Castellón, C. Claver, Y. Díaz, *Chem. Soc. Rev.* **2005**, *34*, 702.
- [5] M. Dieguez, O. Pàmies, A. Ruiz, Y. Diaz, S. Castillon, C. Claver, *Coord. Chem. Rev.* **2004**, *248*, 2165.
- [6] M. Dieguez, O. Pàmies, C. Claver, *Chem. Rev.* **2004**, *104*, 3189.
- [7] G. Descotes, D. Lafont, D. Sinou, *J. Organomet. Chem.* **1978**, *150*, C14.
- [8] W. R. Cullen, Y. Sugi, *Tetrahedron Lett.* **1978**, *19*, 1635.
- [9] R. Jackson, D. J. Thompson, *J. Organomet. Chem.* **1978**, *159*.
- [10] M. Beller, B. Cornils, C. D. Frohning, C. W. Kohlpaintner, *J. Mol. Catal. A: Chem.* **1995**, *104*, 17.
- [11] F. Agbossou, J. F. Carpentier, A. Mortreux, *Chem. Rev.* **1995**, *95*, 2485.
- [12] S. Gladiali, J. C. Bayon, C. Claver, *Tetrahedron: Asymmetry* **1995**, *6*, 1453.
- [13] K. Nozaki, in *Comprehensive Asymmetric Catalysis. Chapter 11, Vol. 1*, Jacobsen, E.N., Pfaltz, A., Yamamoto, H. ed., Springer-Verlag, Berlin, **1999**.
- [14] P. W. N. M. van Leeuwen, Claver, C., *Rhodium Catalyzed Hydroformylation, Vol. 22*, Kluwer Academic Press., Dordrecht, **2000**.
- [15] P. W. N. M. van Leeuwen, in *Homogeneous Catalysis: Understanding the art, Vol. 8*, Kluwer Academic Publishers, Dordrecht, **2004**, p. 139.
- [16] M. Dieguez, O. Pàmies, C. Claver, *Tetrahedron: Asymmetry* **2004**, *15*, 2113.
- [17] A. J. Chalk, in *Flavors and Fragrances: A World Perspective* (Ed.: B. M. Lawrence, Mookherjee, B. D. and Willis, B. J.), Elsevier Science, Amsterdam, **1988**.

- [18] C. Botteghi, M. Marchetti, S. Paganelli, in *Transition Metal for Organic Synthesis. Building Blocks and Fine Chemicals, Vol. 1* (Eds.: M. Beller, C. Bolm), Wiley-WCH, Weinheim, **1998**.
- [19] R. F. Heck, D. S. Breslow, *J. Am. Chem. Soc.* **1961**, *83*, 4023.
- [20] R. F. Heck, D. S. Breslow, *J. Am. Chem. Soc.* **1962**, *84*, 2499.
- [21] R. F. Heck, *Acc. Chem. Res.* **1969**, *2*, 10.
- [22] D. Evans, G. Yagupsky, Wilkinso.G, *J. Chem. Soc. A* **1968**, 2660.
- [23] D. Evans, J. A. Osborn, Wilkinso.G, *J. Chem. Soc. A* **1968**, 3133.
- [24] C. K. Brown, Wilkinso.G, *J. Chem. Soc. A* **1970**, 2753.
- [25] P. W. N. M. van Leeuwen, C. P. Casey, G. T. Whiteker, in *Chapter 4. Rhodium Catalyzed Hydroformylation, Vol. 22* (Ed.: P. W. N. M. van Leeuwen, Claver, C.), Kluwer Academic Press., Dordrecht, **2000**, p. 296.
- [26] A. Castellanos-Paez, S. Castellón, C. Claver, P. W. N. M. van Leeuwen, W. G. J. de Lange, *Organometallics* **1998**, *17*, 2543.
- [27] O. Roelen, *US 2327066* **1943**.
- [28] B. Cornils, in *New Syntheses with Carbon Monoxide* (Ed.: J. Falbe), Springer-Verlag, Berlin, **1980**, pp. 1.
- [29] J. K. Stille, H. Su, P. Brechot, G. Parrinello, L. S. Hegedus, *Organometallics* **1991**, *10*, 1183.
- [30] G. Consiglio, S. C. A. Nefkens, A. Borer, *Organometallics* **1991**, *10*, 2046.
- [31] M. Diéguez, M. M. Pereira, A. M. Masdeu Bultó, C. Claver, J. C. Bayón, *J Mol. Catal. A: Chem.* **1999**, 143.
- [32] J. E. Babin, G. T. Whiteker, [Chem. Abs. 1993, 119, P159 872 h], (Union Carbide Chem. Plastics Techn. Co.)WO 93/03839, **1993**.
- [33] G. J. H. Buisman, L. A. van Der Veen, A. Klootwijk, W. G. J. De Lange, P. C. J. Kamer, P. W. N. M. van Leeuwen, D. Vogt, *Organometallics* **1997**, *16*, 2929.
- [34] M. Diéguez, O. Pàmies, A. Ruiz, S. Castellón, C. Claver, *Chem. Commun.* **2000**, 1607.
- [35] M. Diéguez, O. Pàmies, A. Ruiz, C. Claver, *New J. Chem.* **2002**, *26*, 827.
- [36] M. Diéguez, O. Pàmies, A. Ruiz, C. Claver, S. Castellón, *Chem. Eur. J.* **2001**, *7*, 3086.
- [37] C. J. Copley, K. Gardner, J. Klosin, C. Praquin, C. Hill, G. T. Whiteker, A. Zanotti-Gerosa, J. L. Petersen, K. A. Abboud, *J. Org. Chem.* **2004**, *69*, 4031.
- [38] C. J. Copley, J. Klosin, C. Qin, G. T. Whiteker, *Org. Lett.* **2004**, *6*, 3277.
- [39] K. Nozaki, N. Sakai, T. Nanno, T. Higashijima, S. Mano, T. Horiuchi, H. Takaya, *J. Am. Chem. Soc.* **1997**, *119*, 4413.
- [40] G. Franciò, W. Leitner, *Chem. Commun.* **1999**, 1663.
- [41] G. J. Clarkson, J. R. Ansell, D. J. Cole-Hamilton, P. J. Pogorzelec, J. Whittell, M. Wills, *Tetrahedron: Asymmetry* **2004**, *15*, 1787.

- [42] S. Breeden, M. Wills, *J. Org. Chem.* **1999**, *64*, 9735.
- [43] A. T. Axtell, C. J. Cobley, J. Klosin, G. T. Whiteker, A. Zanotti-Gerosa, K. A. Abboud, *Angew. Chem. Int. Ed.* **2005**, *44*, 5834.
- [44] D. J. Wink, T. J. Kwok, A. Yee, *Inorg. Chem.* **1990**, *29*, 5006.
- [45] N. Sakai, K. Nozaki, K. Mashima, H. Takaya, *Tetrahedron: Asymmetry* **1992**, *3*, 581.
- [46] G. J. H. Buisman, P. C. J. Kamer, P. W. N. M. van Leeuwen, *Tetrahedron: Asymmetry* **1993**, *4*, 1625.
- [47] G. J. H. Buisman, E. J. Vos, P. C. J. Kamer, P. W. N. M. van Leeuwen, *J. Chem. Soc., Dalton Trans.* **1995**, 409.
- [48] G. J. H. Buisman, L. A. van der Veen, P. C. J. Kamer, P. van Leeuwen, *Organometallics* **1997**, *16*, 5681.
- [49] S. Cserépi-Szucs, I. Tóth, J. Bakos, L. Párkányi, *Tetrahedron: Asymmetry* **1998**, *9*, 3135.
- [50] S. Cserépi-Szucs, G. Huttner, L. Zsolnai, J. Bakos, *J. Organomet. Chem.* **1999**, *586*, 70.
- [51] S. Cserépi-Szucs, G. Huttner, L. Zsolnai, A. Szölosy, C. Hegedüs, J. Bakos, *Inorg. Chim. Acta* **1999**, *296*, 222.
- [52] Y. Jiang, S. Xue, Z. Li, J. Deng, A. Mi, A. S. C. Chan, *Tetrahedron: Asymmetry* **1998**, *9*, 3185.
- [53] Z. Freixa, J. C. Bayón, *J. Chem. Soc., Dalton Trans.* **2001**, 2067.
- [54] G. J. H. Buisman, M. E. Martin, E. J. Vos, A. Klootwijk, P. C. J. Kamer, P. W. N. M. van Leeuwen, *Tetrahedron: Asymmetry* **1995**, *6*, 719.
- [55] R. Kadyrov, D. Heller, R. Selke, *Tetrahedron: Asymmetry* **1998**, *9*, 329.
- [56] O. Pàmies, G. Net, A. Ruiz, C. Claver, *Tetrahedron: Asymmetry* **2000**, *11*, 1097.
- [57] M. Dieguez, O. Pàmies, C. Claver, *Chem. Commun.* **2005**, 1221.
- [58] N. Sakai, S. Mano, K. Nozaki, H. Takaya, *J. Am. Chem. Soc.* **1993**, *115*, 7033.
- [59] K. Nozaki, T. Matsuo, F. Shibahara, T. Hiyama, *Adv. Syn. Catal.* **2001**, *343*, 61.
- [60] K. Nozaki, Y. Itoi, F. Shibahara, E. Shirakawa, T. Ohta, H. Takaya, T. Hiyama, *J. Am. Chem. Soc.* **1998**, *120*, 4051.
- [61] K. Nozaki, F. Shibahara, Y. Itoi, E. Shirakawa, T. Ohta, H. Takaya, T. Hiyama, *Bull. Chem. Soc. Jpn.* **1999**, *72*, 1911.
- [62] A. Kless, J. Holz, D. Heller, R. Kadyrov, R. Selke, C. Fischer, A. Börner, *Tetrahedron: Asymmetry* **1996**, *7*, 33.
- [63] S. Deerenberg, P. C. J. Kamer, P. W. N. M. van Leeuwen, *Organometallics* **2000**, *19*, 2065.
- [64] M. Diéguez, O. Pàmies, G. Net, A. Ruiz, C. Claver, *Tetrahedron: Asymmetry* **2001**, *12*, 3441.
- [65] P. Meakin, J. P. Jesson, F. N. Tebbe, M. El., *J. Am. Chem. Soc.* **1971**, *93*, 1797.

- [66] P. Meakin, J. P. Jesson, Muettter, *J. Am. Chem. Soc.* **1972**, *94*, 5271.
- [67] K. Nozaki, T. Matsuo, F. Shibahara, T. Hiyama, *Organometallics* **2003**, *22*, 594.
- [68] R. Noyori, in *Asymmetric Catalysis in Organic Synthesis*, Wiley, New York, **1994**.
- [69] I. Ojima, in *Catalytic Asymmetric Synthesis*, Wiley, New York, **1993**.
- [70] C. R. Landis, J. Halpern, *J. Am. Chem. Soc.* **1987**, *109*, 1746.
- [71] W. J. Tang, X. M. Zhang, *Chem. Rev.* **2003**, *103*, 3029.
- [72] W. S. Knowles, M. J. Sabacky, *Chem. Commun.* **1968**, 1445.
- [73] L. Horner, H. Siegel, H. Buthe, *Angew. Chem. Int. Ed.* **1968**, *7*, 942.
- [74] J. A. Osborn, F. H. Jardine, J. F. Young, Wilkinso, G., *J. Chem. Soc. A* **1966**, 1711.
- [75] H. B. Kagan, T. P. Dang, *J. Am. Chem. Soc.* **1972**, *94*, 6429.
- [76] W. S. Knowles, B. D. Vineyard, M. J. Sabacky, *J. Chem. Soc. Chem. Commun.* **1972**, 10.
- [77] W. S. Knowles, *J. Chem. Educ.* **1986**, *63*, 222.
- [78] W. S. Knowles, *Angew. Chem. Int. Ed.* **2002**, *41*, 1999.
- [79] A. Miyashita, A. Yasuda, H. Takaya, K. Toriumi, T. Ito, T. Souchi, R. Noyori, *J. Am. Chem. Soc.* **1980**, *102*, 7932.
- [80] R. Noyori, *Science* **1990**, *248*, 1194.
- [81] W. A. Nugent, T. V. Rajanbabu, M. J. Burk, *Science* **1993**, *259*, 479.
- [82] M. J. Burk, *Acc. Chem. Res.* **2000**, *33*, 363.
- [83] Y. Y. Yan, T. V. RajanBabu, *Org. Lett.* **2000**, *2*, 4137.
- [84] W. Li, X. Zhang, *J. Org. Chem.* **2000**, *65*, 5871.
- [85] X. Zhang, *U.S. Patent WO 01/34612 A2* **2001**.
- [86] W. Li, J. P. Waldkirch, X. Zhang, *J. Org. Chem.* **2002**, *67*, 7618.
- [87] J. Holz, M. Quirnbach, U. Schmidt, D. Heller, R. Stürmer, A. Börner, *J. Org. Chem.* **1998**, *63*, 8031.
- [88] W. Li, Z. Zhang, D. Xiao, X. Zhang, *J. Org. Chem.* **2000**, *65*, 3489.
- [89] D. Liu, W. Li, X. Zhang, *Org. Lett.* **2002**, *4*, 4471.
- [90] X. Zhang, *WO Patent 03/040149 A2* **2003**.
- [91] A. Bayer, P. Murszat, U. Thewalt, B. Rieger, *Eur. J. Inorg. Chem.* **2002**, 2614.
- [92] J. Holz, U. Schmidt, H.-J. Drexler, D. Heller, A. Börner, R. Stürmer, H.-P. Krimmer, *Eur. J. Org. Chem.* **2001**, 4615.
- [93] D. Carmichael, H. Doucet, J. M. Brown, *Chem. Commun.* **1999**, 261.
- [94] M. Diéguez, O. Pàmies, A. Ruiz, S. Castellón, C. Claver, *Tetrahedron: Asymmetry* **2000**, *11*, 4701.
- [95] R. Selke, *React. Kinet. Catal. Lett.* **1979**, *10*, 135.
- [96] D. Sinou, G. Descotes, *React. Kinet. Catal. Lett.* **1980**, *14*, 463.
- [97] R. Selke, H. Pracejus, *J. Mol. Catal.* **1986**, *37*, 213.
- [98] R. Selke, *J. Organomet. Chem.* **1989**, *370*, 249.

- [99] R. Selke, M. Schwarze, H. Baudisch, I. Grassert, M. Michalik, G. Oehme, N. Stoll, B. Costisella, *J. Mol. Catal.* **1993**, *84*, 223.
- [100] T. V. RajanBabu, T. A. Ayers, A. L. Casalnuovo, *J. Am. Chem. Soc.* **1994**, *116*, 4101.
- [101] T. A. Ayers, T. V. RajanBabu, *U.S. Patent 5510507* **1996**.
- [102] T. V. RajanBabu, T. A. Ayers, G. A. Halliday, K. K. You, J. C. Calabrese, *J. Org. Chem.* **1997**, *62*, 6012.
- [103] E. Guimet, M. Diéguez, A. Ruiz, C. Claver, *Tetrahedron: Asymmetry* **2004**, *15*, 2247.
- [104] E. Guimet, J. Parada, M. Diéguez, A. Ruiz, C. Claver, *Appl. Catal. A* **2005**, *282*, 215.
- [105] E. Guimet, M. Diéguez, A. Ruiz, C. Claver, *Tetrahedron: Asymmetry* **2005**, *16*, 2161.
- [106] E. Guimet, M. Diéguez, A. Ruiz, C. Claver, *Inorg. Chim. Acta* **2005**, *358*, 3824.
- [107] M. Aghmiz, A. Aghmiz, Y. Diaz, A. Masdeu-Bulto, C. Claver, S. Castillón, *J. Org. Chem.* **2004**, *69*, 7502.
- [108] M. T. Reetz, T. Neugebauer, *Angew. Chem. Int. Ed.* **1999**, *38*, 179.
- [109] M. Diéguez, A. Ruiz, C. Claver, *J. Org. Chem.* **2002**, *67*, 3796.
- [110] D. Horton, K. D. Philips, *Methods Carbohydr. Chem* **1976**, *7*, 68.
- [111] D. A. Otero, R. Simpson, *Carbohydr. Res.* **1984**, *128*, 79.
- [112] S. Clautre, F. Bringaud, L. Azema, R. Baron, J. Perie, M. Willson, *Carbohydr. Res.* **1999**, *315*, 339.
- [113] R. D. Guthrie, I. D. Jenkins, J. J. Watters, M. W. Wright, R. Yamasaki, *Aust. J. Chem.* **1982**, *35*, 2169.
- [114] T. Jongsma, M. Fossen, G. Challa, P. W. N. M. van Leeuwen, *J. Mol. Catal.* **1993**, *83*, 17.
- [115] R. J. Rafka, B. J. Morton, *Carbohydr. Res.* **1994**, *260*, 155.
- [116] S. Cassel, C. Debaig, T. Benvegna, P. Chaimbault, M. Lafosse, D. Plusquellec, P. Rollin, *Eur. J. Org. Chem.* **2001**, 875.
- [117] A. Terfort, *Synthesis-Stuttgart* **1992**, 951.
- [118] P. Uriz, E. Fernandez, N. Ruiz, C. Claver, *Inorg. Chem. Commun.* **2000**, *3*, 515.
- [119] M. Dieguez, O. Pàmies, G. Net, A. Ruiz, C. Claver, *Tetrahedron: Asymmetry* **2001**, *12*, 651.
- [120] C. Claver, P. W. N. M. van Leeuwen, in *Chapter 5. Rhodium Catalyzed Hydroformylation, Vol. 22* (Ed.: P. W. N. M. van Leeuwen, Claver, C.), Kluwer Academic Press., Dordrecht, **2000**, p. 296.
- [121] O. Pamies, G. Net, A. Ruiz, C. Claver, *Tetrahedron: Asymmetry* **2000**, *11*, 1097.